VENTILATION IN MINIBUS TAXIS AS A MEANS OF AIRBORNE INFECTION CONTROL

A thesis submitted to the Faculty of Health Sciences, University of Cape Town, in full fulfilment of the requirements for the degree of Master of Science in Medicine (Biomedical Engineering)

By:

Munyaradzi. T. Matose

MTSMUN003

Department of Human Biology

University of Cape Town

Supervisor:

Mladen Poluta

Department of Human Biology: Division of Biomedical Engineering

Co-supervisor:

Prof Tania Douglas

South African Research Chair in Biomedical Engineering & Innovation

PLAGIARISM DECLARATION

1. I know that plagiarism is wrong. Plagiarism is to use another's work and pretend that it is one's own.
2. I have used the Harvard convention for citation and referencing. Each contribution to, and quotation in, this dissertation from the work(s) of other people, has been attributed and has been cited and referenced.
3. This dissertation is my own work.
4. I have not allowed, and will not allow, anyone to copy my work with the intention of passing it off as their own work or part thereof.

Name: **Munyaradzi. T. Matose**

Signature: Signed by candidate **Date:** 01 August 2018

ACKNOWLEDGEMENTS

Thanks to my supervisors Prof Tania Douglas and Mladen Poluta for providing a wealth of knowledge, resources and support that maintained and steered the completion of this project.

Thanks to Dr Grant Theron and the research group at the University of Cape Town Lung Infection and Immunity Unit, for all the advice and weekly meetings in which my understanding of TB and its impact in Cape Town were cemented.

Thanks to Dr Reshma Kassanjee of the University of Cape Town Statistical Consulting Service, Department of Statistical Sciences for providing insight into data interpretation and contributions to the statistical analyses.

To my colleagues in the Division of Biomedical Engineering, particularly Madelein Dreyer and Quik Kung, thank you for all the daily discussions.

Thanks to Charles Harris, the Department of Human Biology mechanical workshop staff and the Smiths for the vital efforts put in implementation and execution of the experiments.

To my parents Frank and Tamsanqa Matose, your encouragement throughout kept me going.

To my partner Tracy, thank you for the love, understanding and drive to complete this thesis.

Finally, I'll thank God for placing the right people in my path, I am eternally grateful.

ABSTRACT

Airborne infection control (AIC) measures are used extensively in healthcare settings to curtail the spread of airborne infectious diseases; these measures include administrative, architectural, engineering (e.g. ventilation) and personal protective interventions, serving either to reduce the concentration of airborne infectious particles or to protect individuals from direct exposure to airborne infection. Few such measures are applied in public congregate spaces outside of health facilities, such as those associated with public transport. Limited literature is available on existing AIC measures in the context of public transport modalities. This study explores the role of ventilation as an AIC measure in minibus taxis in Cape Town, South Africa, to determine its potential role in reducing airborne infectious disease transmission.

The minibus taxi model chosen for the study was the Toyota Quantum Ses'fikile, which is commonly used in the Cape Town metropole. The Ses'fikile taxi has 6 windows, 2 at the front, 2 in line with the main passenger door and 2 towards the rear of the taxi. Ultrasonic anemometers were placed at key positions throughout the taxi-interior to measure and log airflow patterns, under different window-open/close configurations and at different taxi speeds. To determine ventilation rates, the configurations were tested in an occupied taxi, with occupants comprising the driver, a researcher, and 14 volunteer participants. This study analysed TB transmission risk using the Issarow equation, a dose-response model.

Airflows created by different window configurations produced patterns in airflow direction and velocity. A linear regression model fit to the ventilation data revealed that increasing taxi speed increased ventilation. Ventilation rates were found to depend on interior airflow as a result of the window configuration, as well as on the number of open windows, although the ventilation rate was not highest with the highest number of open windows. The best ventilation rates were found with four open windows, which included the front windows on both sides of the vehicle, and either the middle windows on both sides or the rear windows on both sides. The ventilation rates produced by these configurations at all tested taxi speeds (40 km/h, 80 km/h and 100 km/h) ranged from 108 to 316 L/s and exceeded the World Health Organization recommendation for new healthcare facilities, airborne precaution rooms, and general wards and outpatient departments. TB transmission probabilities in a taxi were dependent on ventilation, occupancy, number of infectors and duration of exposure. The risk of transmission was shown to increase substantially when ventilation rates fell below 50 L/s.

In conclusion, minibus taxis were found to provide an effective range of ventilation rates that reduce the risk of TB transmission at varying speeds, however when natural ventilation is not used and with typical high occupancies, the risk posed to all occupants is high. Alternative AIC interventions may have to be considered.

TABLE OF CONTENTS

LIST OF ABBREVIATIONS

ACH – Air changes per hour (unit of ventilation)

AIC- Airborne Infection Control

ASHRAE - The American Society of Heating, Refrigerating and Air-Conditioning Engineers

CDC - Centre for Disease Control and Prevention

CFD - Computational fluid dynamics

CI - Confidence interval

EP-TB - Extrapulmonary TB

HEPA - High efficiency particulate air (concerning filters)

HIV - Human immunodeficiency virus

L/s/p - Litres per second per person (unit of ventilation)

MDR-TB - Multiple drug-resistant TB

PPM - Parts per million (unit of quantity/concentration)

REHVA - The Federation of European Heating, Ventilation and Air Conditioning Associations

TB - Tuberculosis

UVGI - Ultraviolet germicidal irradiation using UV-C light

WHO - World Health Organisation

XDR-TB - Extensively drug-resistant TB

LIST OF FIGURES

LIST OF TABLES

1 INTRODUCTION

1.1 Background to Project

1.1.1 TB-related Infection

Tuberculosis (TB) is an airborne disease caused by Mycobacterium tuberculosis and is one of the leading causes of death globally. It causes serious human or animal disease with high mortality if untreated and can be readily transmitted from an infectious individual to a susceptible recipient. South Africa ranks within the top 5 countries in the world with the highest numbers of diagnosed TB patients and those diagnosed with drug-resistant strains of TB. Africa has a very high HIV and TB co-infection rate, accounting for 75% of the global count for HIV-infected TB patients. In a study conducted in South Africa, 64% of tested TB patients were HIV positive (World Health Organization, 2013). HIV-positive people are not only more susceptible to pulmonary TB, but also to extra-pulmonary TB (EP-TB). EP-TB results when TB infection occurs in any organ in the body outside the lungs, notably lymph nodes, pleura, and osteoarticular areas (Golden & Vikram, 2005). Worldwide, 10-25% of TB infections occur in extra pulmonary sites, however more than 50% of TB infected HIV-positive patients develop EP-TB. A 2011 autopsy study reviewed in the 2013 global TB report stated that in South Africa, undiagnosed TB was the leading cause of death in HIV-positive people (World Health Organization, 2013).

TB is spread through minute airborne droplets known as droplet nuclei that each contain 1-10 bacilli. The droplets are released through coughing, sneezing, talking, singing and any other lung exhalation, including bronchoscopic procedures. The nuclei range in size from 1um to 100um with the smaller droplets able to remain suspended in the air for hours; if some infectious individual coughs in a space and moves away, the bacteria might still be present in the area long after that person has left. Droplet nuclei containing the TB bacteria can cause infection when inhaled and become attached to the alveolar surfaces deep in the lungs. This infection does not normally lead to immediate active pulmonary TB in healthy individuals, but can remain dormant (latent infection), until the infected individual's resistance falls and is overwhelmed by the virulence of the bacilli. Even healthy individuals can incur infection through repeated exposure to and inhalation of the airborne bacilli.

It is typically understood that the people who are at highest risk to TB infection and disease are the healthcare workers who spend long periods with infected individuals, HIV positive patients who have a compromised immune system, and other susceptible people who spend prolonged periods in confined spaces (miners, for example). The spread of TB within healthcare facilities (nosocomial transmission) is a topic that is continuously under discussion, with several methods available to reduce the risk of transmission (described

in the next chapter). Several guidelines have been published that address healthcare-associated spread of TB.

From an infection control perspective, the most dangerous individuals are those undiagnosed and not receiving any treatment, and therefore highly contagious. Many of these individuals never enter healthcare facilities. Furthermore, by the time most infectious individuals present to healthcare facilities, they may have already caused a substantial amount of transmission of TB. Undiagnosed and untreated smear positive pulmonary TB patients have been estimated to infect from 10 to 15 people annually. Furthermore, the cost of treating normal drug-resistant (DR) forms of TB far exceeds that of normal strains of TB, despite there being fewer patients with either multiple drug-resistant (MDR) or extensively drug-resistant (XDR) (MSF, 2011). A study in 2010 showed that the costs of treating the combined multiple drug-resistant cases are disproportionately higher, where 2.2% (MDR-TB and XDR-TB cases) of the total cases consumed 45% of the budget (Pooran, et al., 2013). An important point to consider is that DR-TB is now considered to be mostly transmitted from person to person; DR-TB was mainly thought of as a complication arising in TB patients acquiring resistance to drugs over time, but now first-time TB patients are acquiring DR-TB without ever having contracted normal TB (Shah, et al., 2017).

1.1.2 Infection Settings

To properly address the TB-related burden in South Africa, it becomes essential to consider congregate settings other than health facilities as hotspots of transmission. Given that many health workers and patients make use of public transport, it is only natural that these settings are addressed next (Cobelens, et al., 2000). In active case finding of TB, it is believed that household and close contacts to patients have higher risks of infection, although a low proportion of contacts sharing a household with infected individuals were found to have the same strain as the source case in a 2004 study (Verver, et al., 2004). The transmission of TB outside the households of infected individuals has been estimated to contribute significantly to the spread of the disease as seen in a high incidence township in Cape Town amongst residents of low socio-economic status (Wood, et al., 2012). The Wood study focussed on the time spent and the number of contacts met in indoor locations, with risk of transmission increasing with the number of social contacts. It noted that further studies on environmental conditions such as those in public transport are potentially important for ongoing TB infection control. A study conducted on the main public transport modes in Cape Town concluded that minibus taxi commuters had the highest risk of TB infection based on CO_2 measurement and transmission risk assessment using the Wells-Riley equation (Andrews, et al., 2013). This finding closely matched conclusions made in a study on TB transmission in minibus taxis in Lima Peru (Zamudio, et al., 2015). A study on TB transmission in public settings in Tanzania quantified that after prisons, public transport (commuter buses) carried the highest annual risk (Hella, et al., 2017).

Urban public transport in South Africa is divided mainly into three forms: buses, trains and minibus-taxis. Of the three forms, the last-mentioned accounted for 68% of public transport commutes to work with over 3.65 million daily public transport trips nationally, in 2013 (Statistics South Africa, 2014). This was an increase of 4.5% from the national average minibus taxi usage in 2003 (Department of Transport, 2003).

In the Western Cape, public transport was found to account for 38% of all work trips with minibus taxis being the main mode of transport (39%), followed by trains (34%) and buses (18%) (Statistics South Africa, 2014). In 2013 the Department of Transport showed that in informal settlings in Cape Town, where the vulnerability of people to infectious diseases such as TB is reported as high, minibus taxis are used extensively by people of lower economic standing (2014).

Minibus taxis in common use come in a range from 15 to 22seater models, however during peak operation taxis are often filled to over-capacity. This results in overcrowding in the limited interior space. A report on passenger transport trends in South Africa showed that in the Western Cape, 54% of all minibus-taxi users surveyed were dissatisfied with the levels of overcrowding (Lombard, et al., 2007).

Ventilation in minibus taxis is achieved mainly through the passenger door (entering and exiting) and windows, though the opening of windows is left to the discretion of the passengers. Poor ventilation increases risk to passengers as conditions within the minibus taxi allow for transmission of airborne diseases. The national average taxi commute to work in South Africa was 50 minutes in 2013 (Statistics South Africa, 2014).

Given that taxis may contain infectious spreaders (drivers, conductors or passengers), and are used most frequently by people of a lower socioeconomic status (in which the incidence of TB is higher), it would be worthwhile to evaluate (and quantify where possible) the likely risk of exposure and infection with respect to time spent in the taxi, relative positioning of occupants, and the degree and nature of air movement (leading to dilution of infectious airborne particles). These issues are the focus of this study.

1.2 Aims and Objectives of the Project

The aim of this research project is to characterise the risk of transmission of TB in the minibus taxi environment through direct observation, experimental methods and numerical models, and based on the insights gained, to recommend AIC measures that decrease the concentration of the airborne contaminants. To meet these aims the following objectives were set:

1. To observe commuter concentration, seating and movement, and associated ventilation scenarios (closing and opening of doors and windows) on selected minibus taxi routes in the Cape Town area.

2. To characterise minibus taxi occupancy, air movement and ventilation for various active operating conditions and scenarios.
3. To estimate the effect on cross-infection risk (using TB-transmission models) of current ventilation scenarios.

Limited research has been conducted in modelling of TB-related infection risk in public transport systems in South Africa. Few measures have been taken to address infection control within such congregate settings as the focus has been on reducing transmission risk within healthcare facilities (Bock, et al., 2007) and congregate settings such as prisons (Johnstone-Robertson, et al., 2011). The high incidence rates of TB and continued prevalence despite national efforts to curb transmission in healthcare facilities show that active measures are required within other public congregate settings in the battle against TB (Johnstone-Robertson, 2012). This project provides a platform for evidence-based AIC interventions in minibus taxis as well as other public transport settings.

1.3 Plan of Development

Chapter 2 reviews methods of reducing airborne infections and methods to track and model potential transmission. Chapter 3 describes the preliminary investigation, observations within operational minibus taxis along their journeys, which was used to inform the methodology used in the project. Chapter 4 explores the materials and configurations used in the project. Chapter 5 presents the methodology for the air flow visualisation, airflow characterisation and ventilation experiments in a minibus taxi. Chapter 6 presents and discusses the results of the experiments. Finally, conclusions and recommendations for further studies are made in Chapter 7.

2 REVIEW OF MEASURES AGAINST SPREAD OF TB

In this chapter, measures used against the spread of TB are reviewed. The measures include administrative solutions in healthcare settings, treatment of infected persons, measures to control the contaminant levels in the congregated environments, as well as personal protective measures.

The spread of TB in South Africa is closely associated with poverty. Khayelitsha, a peri-urban township outside Cape Town, is a primary example of the high correlation between poverty, crowding and high levels of both HIV and TB prevalence (Cox, et al., 2010). However, although poverty is noted by the WHO as a core determinant of health, its alleviation is not explicitly stated as a response to control tuberculosis (Benatar & Upshur, 2010). Thus, poverty and accompanying socio-economic problems such as overcrowding in households, although an immediate concern in the spread of disease, cannot be dealt with easily and fast enough to reduce TB transmission.

2.1 Administrative Measures in Healthcare Facilities

The greatest threat of TB transmission comes from undiagnosed infectious individuals. Infection control guidelines suggest that workplace administrative procedures are critical in impacting the transmission of TB within facilities (Bock, et al., 2007). These measures ensure that infectious patients are monitored, placed in secluded areas with people with the same type of TB, and that the rooms they occupy have measures to reduce any possibility of disease spread. Staff education, especially addressing gaps in knowledge of infectious disease transmission, is a necessary step before developing any prevention strategies. The difficulty with administrative measures is in managing the level of adherence (Cardo, et al., 2010).

2.2 TB Treatment

Medication is the most common measure taken globally to reduce the spread of TB, as the disease can be cured and individuals suffering from tuberculosis who are put on the correct medication cease to be infectious (WHO, 2013). The TB drugs isoniazid and rifampicin are the first-line drugs that effectively decrease the emission of live bacilli from infected individuals (NTCP, 2007). The limitations of TB medication have been displayed through the emergence of multiple-drug resistant TB (MDR-TB) and extensively drug resistant TB (XDR-TB) caused by of the mutation of the bacilli, facilitated by inadequate drug treatments (where treatments are either not completed by the patients, the medication runs out before the patients complete the treatment plan, or the delivery of quality medication to the patients is compromised) (MSF, 2011). In the past, most DR-TB cases were

endogenously acquired (through treatment default, for example), recent data from South Africa show that nearly 50% of XDR-TB strains detected in the Western Cape were likely originating from the Eastern Cape (Chihota, et al., 2012). This underscores the importance of disrupting person-to-person transmission.

2.3 Environmental Control Measures (Ventilation, Filtration, UVGI)

Basic infection control measures could be achieved through policies that address a host of factors such as infectious agents and their prevalence, mortalities caused by the disease, identification of risk factors, and identification of groups susceptible to the disease. To realise basic infection control, measures to i) identify the disease and infectious spreaders, ii) enrol infectious individuals in treatment, iii) reduce transmission and iv) protect those susceptible from infection, are necessary (Raza, et al., 2004).

In a room/closed space occupied by an infectious individual, contaminants are constantly introduced into the airspace through talking, sneezing, coughing and breathing. To reduce the concentration of contaminants in the air, dilution by means of introduction of clean air into the space and extraction of contaminated air can be achieved either naturally or mechanically.
Possible environmental controls include:

- Ventilation (natural or mechanical)
- Air filtration
- Air purification

2.3.1 Ventilation

Ventilation can be used to achieve various desired effects, the most significant of which are dilution and removal of contaminated air. Natural ventilation is often described as the most economic, energy efficient solution in providing air movement to reduce the number of infectious particles within indoor spaces, but it is not without its disadvantages (Atkinson, et al., 2009). It is subject to minute-to-minute changes in the environment and alone would not provide the consistent air changes per hour required to dilute the concentration of the airborne droplet nuclei (Nardell , et al., 1991). Also, a study on the relationship of indoor and outdoor parameters such as temperature and humidity concluded that if there are marked differences in the indoor and outdoor environments when using outdoor ventilation, indoor occupants' health could be compromised (Nguyen, et al., 2014); this is important to note when suggesting solutions to ventilation of the indoor occupant space.

Measures such as mechanical (forced) ventilation can be used to supply clean air into a room as well as extract contaminated air to dilute and reduce the contaminant concentration.

In 2009 the WHO produced a paper regarding natural ventilation requirements for health-care facilities to help prevent airborne infections (WHO, 2009). Their recommendations were as follows:

1) 160 L/s/patient (hourly average) for airborne precaution rooms, with a minimum of 80 L/s/patient, for new health-care facilities and major renovations
2) 60 L/s/patient in general wards and outpatient departments
3) 2.5 L/s/patient in corridors and other transient spaces with changing patient numbers, but 1) applies when patient care is undertaken in those transient spaces.

where L/s denotes the ventilation rate in litres per second

A study by Andrews et.al (2013) in minibus taxis noted that CO_2 concentration (used to determine ventilation) in an active taxi environment does not stabilise due to varying internal conditions, however during peak travel times, when the occupancy rates are highest the concentration levels are expected to be at their maximum. In the taxi environment, natural ventilation can be achieved when windows are opened in specific configurations. The ventilation achieved/achievable would depend on factors such as:

- the degree of window opening;
- air movement within the taxi;
- speed of the taxi;
- passenger/occupant position.

Some vehicles might have operational air supply diffusers installed that blow air downwards from the ceiling, but their effectiveness in providing the minimum required air changes per hour would need to be quantified. The diffusers would need to supply external air and not simply recirculate indoor air (as this could result in air mixing and increased contaminant spread). In a study where they estimated the probability of infection in an occupied space by measuring the CO_2 levels, Rudnick and Milton (2003) concluded that although increasing outdoor air supply in a confined space can prevent transmission of some common respiratory infections and influenza, the effects are reduced when aimed at highly contagious diseases.

2.3.2 Filtration

Further reduction of contaminants can be achieved by employing high-efficiency particulate arrestor (HEPA) filters in conjunction with mechanical ventilation systems. HEPA filters are applicable and frequently recommended as additional measures in hospital guidelines. Portable HEPA filtration units are recommended by the CDC (CDC, 2005)in health-care facilities to increase equivalent ACH however an effective ventilation system is required as well.

The CDC noted that HEPA filtration can be used in emergency transport vehicles in conjunction with existing mechanical ventilation, placement of the patient would have to be considered as well (CDC, 2005). The closer the infected individual is to the exhaust end of the air distribution the less likely the infectious particles are mixed with the internal air. In the case of public transport settings such as taxis where internal air supply diffusers are the only available option for mechanical ventilation, this solution could be inefficient. Due to initial purchase and maintenance needs, filters would be a costly and high maintenance solution for AIC in minibus taxis, despite their effectiveness in reducing concentration of airborne contaminants when used properly (Kujundzic, et al., 2007). Furthermore, the installation of filters into ventilation systems is not simple; the installations would have to be properly designed, installed and tested to ensure effectiveness (REHVA, 2004). Whether this measure could be implemented well in minibus taxis is unknown.

2.3.3 Air Purification

The use of ultraviolet light for sterilisation has been documented since the early 1900s (Reed, 2010). The use of artificially generated UV-C as a means of disinfection by inactivating contaminants (bacteria, fungi, spores) is known as ultraviolet germicidal irradiation (UVGI). UV-C ranges from 100nm-280nm and peak bactericidal action is achieved at wavelengths close to 265nm. Low pressure mercury vapour lamps have a near monochromic output at 254nm, thus making them cost-effective options for UVGI.

UVGI technology – when applied to air disinfection - is implemented through several methods, with standalone fixtures, fan-cabinet fixtures, in-duct fixtures and upper room fixtures being the most common. In healthcare settings the upper room modality (Ko, et al., 2002) shows the greatest promise in terms of general applicability in public sector facilities, especially those at the primary level of care where the bulk of patient contacts occur and other engineering interventions may not be feasible or cannot be relied on for continuous efficacy (Coker, et al., 2007) (Granich, et al., 1999). The use of UVGI

has been documented in healthcare facilities, laboratories and industrial settings such as water purification as well as in home air purification.

In the literature studied, UVGI was not suggested as an air purification measure in transport systems. The only current practical implementation of UVGI in public transport would be using adapted fan-cabinet fixtures, which facilitate air mixing within the occupied space and do not expose the public to any UV-C radiation, which Nardell noted as harmful to room occupants if they are exposed to excessive doses (2008).

2.4 Personal Protective Measures (Respirators)

In general, respirators may be powered or non-powered and may have particulate filters, gas and vapour filters, or a combination of the types. The filters can be embedded, making the respirator disposable, or modular, allowing the filter component to be replaced and the respirator to be reused. The respirators used by healthcare workers, patients and occasionally visitors within health facilities are non-powered and disposable. For the respirators to be effective in terms of infection control the following are needed:

- User specific face-fit testing (the respirator-skin interface must be air-tight to protect the user from contaminants in the environment);
- Leakage monitoring;
- Training on donning and doffing;
- Maintenance/replacement, depending on the type of respirator used.

However, the respirators are costly and usually require personal fitting, making them impractical in many if not most healthcare environments (Gammaitoni & Nucci, 1997). In addition, the respirators – especially if available to health workers and not to patients – present a socio-cultural barrier in terms of the associated stigma (implied illness), are uncomfortable to wear for extended periods, and interfere with communication between patients and their care-takers.

A study done in an MDR-TB ward in South Africa showed that when infectious individuals are wearing surgical masks, risk of infection is reduced significantly (56% reduction) but not eliminated (Dharmadhikari, et al., 2012). The main benefit is derived from that fact that fewer infectious droplets are released into the air.

The introduction of respirators and even surgical masks for users of public transport would be impractical and prohibitively expensive, besides experiencing high levels of resistance due to the stigma against wearing of masks and respirators in public spaces (at least in the South African context).

2.5 AIC-related Investigations in Literature

Approaches used and reported on include both experimental and mathematical methods. The methods reviewed below have been used in healthcare, public transport and public congregate contexts that were applicable or relevant to this study.

It must be noted that although guidelines provided for healthcare settings could be applied in minibus taxis, their implementation would require adaptation to the taxi environments. The occupation densities in the minibus taxis are usually much higher than those in healthcare facilities. High occupant densities are also seen in prisons, where overcrowding and lack of ventilation are commonly noted as factors increasing disease transmission. Air changes per hour (ACH) levels exceeding minimum international prison levels (3 ACH) were revealed to be effective in a study on ventilation efficacy in overcrowded prisons in South Africa (where 8 ACH and the optimal 12 ACH, modelled in conjunction with reduction in occupant density and enclosure time, resulted in 30% and 50% transmission reduction respectively) (Johnstone-Robertson, et al., 2011). The annual TB transmission risk of 90% reported in the study at Pollsmoor prison (2011) was calculated using the Wells-Riley equation and probability analyses of contact between prisoners. It showed that increasing the ventilation from 1ACH to 12ACH could reduce the risk of infection over days from 80% to 20%. Parameters recorded in the calculations included cell dimensions, occupancy, lock-up time, TB incidence and treatment delays, some of which could be applicable in a minibus taxi context.

The American Society of Heating, Refrigerating and Air-Conditioning Engineers (ASHRAE) gave recommendations for vehicle ventilation to acceptable indoor air quality as 8L/s/person for 150 people per 100m^2 (ASHRAE, 2004). These recommendations could be modified to calculate minimum ACH for sufficient dilution of contaminated air (ASHRAE, 2004) in minibus taxis. These values can be used to assess whether current ventilation seen in public transport is adequate or inadequate.

2.5.1 Experimental Methods

The methods related to ventilation testing in specific public congregate interior spaces such as health-care facilities, various public transport modes, prisons and schools are reviewed below. Experimental methods are usually time-consuming and can amass large amounts of data requiring extensive

analysis. The data collected from experimental methods is often used to support the numerical models mentioned in the following section.

Airflow Measurement and Visualisation Techniques

Visualisation of airflow is usually carried about with visible particles released into the airspace, using for example, incense sticks, smoke generators or more recently, helium gas bubble-generators (Kale, et al., 2007) (Zhang, et al., 2009) (Cao, et al., 2014). Common to most of the published airflow studies is the use of anemometers to measure the airflow speeds within the study environment and at the boundary edges. The anemometers used include ultrasonic, optical and hot-wire types, depending on the level of accuracy required and the parameters being measured (Zhang, et al., 2009).

A study conducted in India on airflow within a non-air-conditioned bus used a Perspex scale model immersed in a water channel to derive airflow patterns circulating within and outside the bus (Kale, et al., 2007). In another study, on visualising the volume of air movements in a hospital room due to door motions, the water scale-model technique was used to visualise airflow patterns (Eames, et al., 2009).

A method employed in an airplane cabin study used an array of anemometers placed on an equipment rig, which could be manually repositioned to allow measurements at different points on air diffusers in the cabin (Zhang, et al., 2009).

Tracer Gas Techniques

For studies relating to infection control in airplanes, reconstructed cabin areas and full-scale models have been used (Zhang, et al., 2009). Tracer gas techniques have been used in studies of both health facility and airliner cabin settings. The tracer gases and particulate contaminants such as sulphur hexafluoride and non-evaporative monodispersed di-ethyl-hexyl sebacat particles in conjunction with gas-samplers were used to simulate transport of gaseous and particulate contaminants within the airliner cabin model environment (Zhang, et al., 2009) (Hewlett, et al., 2013).

CO_2 dispersion and measurement are used in interior airspace studies to such a degree that the WHO mandated monitoring CO_2 for indoor air quality monitoring in European schools (WHO, 2011). CO_2 dispersion involves release of a known quantity of CO_2 in the indoor environment and measuring the reduction in concentration over a known period. CO_2 concentration in the occupied space is dependent on internal factors such as size of the interior space, passenger occupancy, how long the

space has been occupied and the supply of fresh air. CO_2 monitoring is widely used in congregate settings; in some cases, the concentration levels are linked to ventilation systems, i.e. with increased ventilation, there is less accumulation of CO_2 (Persily, 1997). The concentration decay curve of carbon dioxide in a monitored environment can be used to calculate the ventilation rate by taking slope of the natural logarithm of a CO_2 concentration curve and multiplying it with a volume conversion as shown in Equation 2.5.1-1 below derived from that used in (Persily, 1997):

$$I = \frac{ln(C_0) - ln(C_1)}{t_1 - t_0} \times \frac{V}{3.6}$$

Equation 2.5.1-1 Ventilation rate equation

Where:

I is the air change rate (L/s)

t is time (hr)

C_0 is the CO_2 concentration at $t = 0$ (ppm)

V is the volume of the space (m^3)

A study on indoor airborne bacterial communities indicated that both ventilation and occupant movements play a key in understanding microbial dynamics (Meadow, et al., 2014). Heated boxes representing people have been used in previous certain airliner studies as they similarly generate the warm plumes of air that influence overall airflow (Zhang, et al., 2009).

2.5.2 Numerical Models

Numerical models to estimate airborne transmission and infection probabilities, particle movement and tracking of TB are reviewed below.

Wells-Riley Deterministic Approach

The Wells-Riley equation (Equation 2.5.2-1) is a widely used probabilistic numerical model that estimates the number of newly infected individuals exposed to an infectious source for a known period (Johnstone-Robertson, et al., 2011) (Noakes & Sleigh, 2008).

$$C = S\left(1 - e^{-\frac{Iqpt}{Q}}\right)$$

Equation 2.5.2-1 Wells-Riley equation

Where*:*

C is the number of new cases over total exposure time *t* (s)

Q is the outdoor ventilation supplied at a constant rate ($m^3.s^{-1}$)

S represents the number of susceptible persons

I is the number of infectious people

p is the pulmonary ventilation rate ($m^3.s^{-1}$) of *S*

q is the unit of infection 'quantum' (the generation rate of an infectious person).

Quantum *q* varies depending on the state of infectiousness of *I*, whereby people with laryngeal TB are regarded as having higher quanta than non-infectious individuals (Johnstone-Robertson, et al., 2011). One limitation of this model in that assuming that air is fully mixed was questioned by Noakes and Sleigh (2008) who showed that significant underestimations could be translated into the risk assessments of airborne transmission when using the model.

In calculating the quanta generation rate, which requires backward calculation from an outbreak, implicit errors result from the many factors influencing the outbreak (Sze To & Chao, 2009). In the comparative study by Sze To and Chao, the quanta generation rates were noted to be widely varying across studies.

Modified Wells-Riley

Rudnick and Milton assessed the use of carbon dioxide concentration as a measure of risk of infection. They noted that Equation 2.5.2-1 was derived based on assumptions that the airspace being investigated is well-mixed and that there are steady state conditions (quantum concentration and outdoor air supply rate are constant). When the outdoor air supply rate is small or inconsistent (as may be found in minibus taxi scenarios) steady-state cannot be assumed. Equation 2.5.2-2 is valid regardless of whether steady state has been achieved and is used in the derivation of Equation 2.5.1-1. Equation 2.5.2-3 is a carbon dioxide based risk equation that also assumes that the airspace is well-mixed; however, it 'has general applicability when the outdoor air supply rate is not constant (varies with time) and for both steady-state and non-steady state conditions' (Rudnick & Milton, 2003). It however assumes that the reduction of infectious particles in the airspace due to interventions other than ventilation, such as filtration, is comparatively small. Equation 2.5.2-3 can be employed for infection risk assessment, and knowing the average CO_2 and occupancy rate, the likelihood for an infection to reproduce can be calculated.

$$f = \frac{C - C_0}{C_a}$$

Equation 2.5.2-2 Rebreathed air equation

Where:

f is the fraction of indoor air that is exhaled air, which is also the rebreathed fraction

C is the volume fraction of CO_2 in indoor air

C_0 is volume fraction of CO_2 in outdoor air

C_a is the volume fraction of CO_2 added to exhaled air during breathing

$$P = \frac{C}{S} = \left(1 - e^{-\frac{\not{f} I q t}{n}}\right)$$

Equation 2.5.2-3 Rudnick-Milton modified Wells-Riley equation

Where:

P is the probability of infection for susceptible persons

$\not{f}$ is the average fraction of indoor air (from Equation 2.5.2-2) that is exhaled breath

n is number of people in the ventilated space.

A 2014 ventilation study was the first publication to use the Rudnick-Milton equation to provide ventilation recommendations under non-steady state conditions in schools to reduce TB transmission risk (Richardson, et al.). A later study by Taylor et al (2016) also used the Rudnick-Milton equation to estimate the risk of TB infection in congregate settings within a high risk rural community in KwaZulu-Natal in South Africa.

Exhaled Air Dose Response Approach

Issarow et al (2015) devised an equation to predict the risk of airborne infection of TB in a non-steady state environment using the rates at which air is re-breathed. The measurements of the CO_2 in the occupied space along with the ventilation rates and estimates of the deposition fraction (rate at which infectious particles are deposited successfully in a susceptible individual's lungs) can be used in the infectious risk estimation. This differs slightly from the Rudnick-Milton modified equation in that it can consider the total possible reduction of infectious particles due to ventilation and other quantified measures. This equation also relies on the deposition fraction as opposed to the infectious quanta used in both the Wells-Riley and Rudnick-Milton equations. The deposition fraction used in the equation however was based on tests done on guinea pigs, and there is a lack of detail on the deposition fraction in susceptible human lungs. The deposition fraction of TB in humans for varying scenarios was explained through simulated models and experimental data by Miller et al (2012) and Majid et al (2011) .

$$P = 1 - e^{-\lambda},$$

$$\lambda = \frac{I(\beta - \mu)\Theta pnt}{Q}\left[1 - \frac{V}{QT}\left(1 - e^{-(QT/V)}\right)\right]$$

Equation 2.5.2-4 Issarow equation

Where:

P is the probability of TB-transmission risk for susceptible individuals occupying an enclosed space with infectious individuals.

I is the number of infectious individuals

β is the generation rate of airborne infectious particles based on exhaled CO_2 levels (particles/s)

μ is the elimination rate of the airborne infectious particles (particles/s)

β - *μ* is the survival rate of infectious particles reaching infection site in susceptible lungs (particles/s)

Θ is the deposition fraction of the infectious particles in the susceptible individual's lungs

p is the breathing rate of susceptible individuals (L/hr)

n is the number of people in the occupied space

Q is the ventilation rate (L/hr)

V is the volume of the occupied space (m^3)

t is the time in which the susceptible individuals are in the occupied space and can be exposed the infectious particles (hr)

T is the total exposure time of the susceptible individuals to the infectious particles (hr) (when the infectious people are in the occupied space)

This non-steady state dose response equation using rebreathed air (CO_2) was used for the risk assessment.

CFD Modelling

Computational fluid dynamics (CFD) modelling has been used to simulate airflow and contaminant transport (particle trajectories) in enclosed spaces. The dispersion of contaminants within the defined space can be accurately modelled for varying configurations. CFD models are increasingly being used in various indoor studies, especially within healthcare facilities (Gammaitoni & Nucci, 1997) (Hewlett, et al., 2013).

Numerical simulations are sensitive to boundary conditions, as performance of CFD models showed in airline cabin studies (Zhang, et al., 2009) (Yan, et al., 2017). In the studies reviewed that modelled health facility spaces, airplane cabins and bus interiors, the software package commonly used was the commercial FLUENT CFD software package (ANSYS, 2014). The mathematical equations defining

airflow consisted mainly of Navier-Stokes equations (some adopted the Reynolds-averaged Navier-Stokes equations) with renormalizing group k-ε (RNG k-ε) turbulence model used to predict temperature and contaminants in airflow (Zhang , et al., 2007). The Lagrangian method predicts discrete droplet nuclei dispersion in the air and was used in airliner cabin and room studies. (Hathway, et al., 2011) (Zhang, et al., 2009).

The use of CFD models to simulate minibus taxi environments is unlikely to yield practically useful insights, given the complex and dynamic nature of these environments and the many different scenarios that would have to be considered.

2.6 Minibus Taxi Studies

In this section, two studies that explored TB transmission in minibus taxis in South Africa are reviewed (Johnstone-Robertson, 2012) (Andrews, et al., 2013). Although similar studies on TB transmission were conducted in other countries (Zamudio, et al., 2015) (Hella, et al., 2017), the details on models of vehicles and scopes of the studies differed from what was required in this study.

In studies involving airborne disease transmission in occupied minibus taxis, CO_2 was used as the tracer gas (Johnstone-Robertson, 2012) (Andrews, et al., 2013) (Hella, et al., 2017). In the Johnstone-Robertson study (2012), a combination of window openings was used to produce ventilation scenarios, whilst in other studies (Andrews, et al., 2013) (Hella, et al., 2017) ventilation was recorded without monitoring window configurations.

In airborne disease transmission studies in public transport, the Wells-Riley equation (and its modified versions) are commonly applied (Johnstone-Robertson, 2012) (Andrews, et al., 2013) (Hella, et al., 2017).

2.6.1 Calculating the Risk of Infection of Mycobacterium tuberculosis in Endemic Settings

Johnstone-Robertson (2012) investigated the risk of TB transmission in minibus taxis. They hypothesised that conditions within minibus taxis could pose significant TB transmission risk. The study performed initial preliminary surveys in minibus taxis during normal operating hours, where CO_2 was monitored. Ventilation characteristics for varying conditions were explored in a stationary taxi. The South African national smear-positive notification rate for adults was used to determine the

probability of an infectious passenger being present in a taxi journey. The Wells-Riley equation was used to determine transmission probabilities for the explored ventilation scenarios.

Their preliminary survey, made during 22 journeys in October (spring), found that windows were closed or partially open in over 60% of the trips. CO_2 was over 1000ppm for over 80% of the trips and reached a maximum recording of 5866ppm.

Ventilation flow rate measurements were carried out in a stationary taxi using repeated CO_2 tracer gas tests, where the sampling occurred at every 5 – 10 seconds. Four ventilation scenarios with 3 window configurations were tested: i) closed window and no fan (0.51 air changes per hour (ACH)) ii) Single driver-window open and no fan (4.29ACH) iii) closed windows with fresh-air fan (9.17ACH) iv) 2 windows opened, driver and passenger (9.7ACH).

The risk of transmission to passengers and drivers respectively from a year of commuting ranged from 28.7% and 73.9% at the lowest ventilation rate (0.51ACH), to 1.9% and 7.5% at the highest ventilation rate (9.7ACH). The study highlighted the increased risk posed to drivers due to their longer exposure and the need for improved ventilation during journeys (Johnstone-Robertson, 2012). The risk increased risk posed to drivers was also noted in the study by Hella, et. al (2017) on commuter buses in Tanzania.

2.6.2 Modelling the role of public transport in sustaining TB transmission in South Africa

The Andrews et. al study (2013) investigated the role of 3 public transport modes in sustaining TB transmission in South Africa. They placed importance on the density of respiratory contacts as an important contributor to transmission in high risk settings. Minibus taxis in Cape Town were explored on 9 – 10 trips, whilst CO_2 was sampled continuously at 5-second intervals during the journeys.

Minibus taxis were found to have the highest mean CO_2 concentrations of 1880ppm in journeys and carried the highest risk of transmission, surpassing busses and trains. Regular users of buses/minibuses in a study by Zamudio, et. al (2015) in Peru were found to be 12 times more likely to have TB than non-users

The risk of infection, calculated using a modified Wells-Riley equation with 1 infectious passenger, was between 3.5 – 5% for individuals taking 400 one-way trips annually.

They noted that one of the major conditions driving transmission was over-crowding and poor ventilation. They highlighted that even with increased TB detection and treatment successes, the high-risk congregate settings seen in public transport must be addressed with improved ventilation standards and possibly using air purification techniques such as filters or UVGI.

Although the average CO_2 concentration levels were stated in the studies (Andrews, et al., 2013) (Hella, et al., 2017), the conditions in which the data were recorded were not given, such as vehicle models used, passenger occupancy, ventilation scenarios and open window configurations. The lack of context in which the data were collected, affects the interpretation of the transmission risk analyses.

2.7 Summary of the Literature and Considerations for Public Transport

This chapter has reviewed the measures against the spread of TB in public spaces including healthcare facilities, prisons and public transport systems. Methods applied in public transport systems to reduce airborne infection were environmental control measures such as ventilation and air filtration. In the studies reviewed ventilation was noted as an important factor in reducing the risk of TB transmission. Experimental methods used to quantify airflows in test spaces included airflow visualisation and airflow characterisation in both full-scale and fractional models. Numerical models were used in airflow and airborne particle visualisation, as well as in transmission risk analyses.

Public transport studies used combinations of experimental and numerical methods to determine transmission probabilities and provide risk-reducing recommendations. The experimental methods used in public transport were airflow measurement, visualisation and tracer gas techniques. In minibus taxi studies, CO_2 was used in occupied vehicles to determine ventilation flow rates. Airborne infection transmission studies in public transportation used numerical models like CFD models (common in airline cabin studies) and probabilistic models such as Wells-Riley (common in minibus studies).

From the literature reviewed, the main elements of experimental and numerical methods used to determine the transmission of airborne diseases in public transport are:

1) Transport survey
2) Airflow visualisation
3) Airflow characterisation
4) Tracer gas tests

5) Particle tracking
6) Ventilation assessment
7) Transmission risk assessment

The review has revealed gaps in the literature with respect to ventilation in minibus taxis, namely: 1) airflow visualisation and airflow pattern tests had not been conducted in minibus taxis ii) ventilation scenarios tested for in minibus taxis were limited iii) TB transmission analyses in minibus taxis only used either the Wells-Riley or the modified Well-Riley equations.

As a dose-response model, the Issarow equation (2015) monitors the exhaled air from infectors carrying airborne diseases and tracks the quantity of pathogens, as opposed to the infectious quanta used in the Wells-Riley equation (Sze To & Chao, 2009). The infectious quanta evaluation differs from the quantity of pathogens as it is based on i) outbreak case data (in the study location) ii) ventilation data iii) contact period in the infectious space, whilst excluding the impact of proximity to infectors (Noakes & Sleigh, 2008). The infectious quanta were noted as a difficult parameter to estimate in a minibus taxi study by Andrews, et. al (2013).The Issarow equation is a flexible model applicable in both steady state and non-steady state conditions as would be found in minibus taxis, whereas the Wells-Riley assumes well-mixed steady-state conditions. These factors make the Issarow equation more suitable for TB transmission analysis in a minibus taxi.

2.8 Hypotheses

Based on the review of the literature, the following was anticipated regarding ventilation in minibus taxis:

1) There would be a relationship between window openings, taxi speeds and ventilation rates; however, at higher speeds increasing window openings would not increase overall ventilation.
2) Airflow patterns would emerge from window configurations that are consistent at differing taxi speeds or at differing heights within the taxi.
3) Ventilation produced by certain window configurations would not provide adequate risk reduction for TB transmission.

The chapters that follow describe experiments to test these hypotheses.

3 PRELIMINARY INVESTIGATIONS

Preliminary investigations were carried out prior to formulating the experimental procedures for the project. As stated in the literature review, limited information was available on ventilation in operational minibus taxis along their journeys. Journeys were taken by the author in operational taxis along multiple routes within Cape Town using multiple models of minibus taxis available.

In a taxi, internal temperature is recordable, but the external temperature changes with location. Another concern was that only upper air openings (windows) are present in a taxi and hence a vertical pressure differential might not be created. It was acknowledged however that internal air temperature is guaranteed to be higher in winter, thus the air is expected to rise and exit the windows from the upper half. In summer, the external temperature could exceed the internal temperature and reverse the flow.

3.1 Direct Observation

Direct observation was used to gather preliminary data on which to base the methodology, particularly data collection and configuration of equipment. Taxis operating from the Cape Town station were entered at different times of the day (between peak morning rush hours and afternoon hours). Both passenger and driver behaviour were observed without engaging with these parties and introducing bias to observed parameters. Journeys were taken between the Cape Town central business district (CBD) and township suburbs of Khayelitsha and Gugulethu. Intra-city routes were selected as opposed to intercity routes, as these were the most frequently used routes in daily commuting.

The following parameters were observed during the preliminary journeys:

1. Combinations of open windows, frequency of opening and closing of windows, duration of opening, instances at which windows were opened and degree of window opening.
2. Door opening and closing frequency, duration of opening and instances at which the door was opened in the journey.
3. Passenger occupancy which included number of passengers seated in the taxi as well as their positions within the taxi.
4. Taxi average and maximum speeds on highways and main roads.
5. Routes taken by the taxi to reach the destinations.

The taxi speeds were observed both on the vehicle's odometer from a passenger seat and on a mobile GPS tracking application. Precise times of door and window opening/shutting were recorded as they occurred, in relation to the journey time. Parameters such as passenger cough etiquette, passenger-demographics, age and gender were not recorded. Journaled observations were exported into an excel spreadsheet on completion of the observations for further exploratory analysis.

3.2 Results

A total of 23 trips were taken during the Cape Town winter season. Routes travelled in the preliminary journeys were split primarily between short trips along main roads to and from the CBD, and longer trips that occurred between the CDB and township suburbs that reported the highest TB cases in their local TB clinics. These areas as alluded to in the literature Chapter 1.1.2 coincided mainly with the poorer township communities. In 2013 these areas had the highest usage of public transport, especially taxis and trains as they are historically areas furthest from the city centre (Statistics South Africa, 2014).

The short journeys ranged between 5 and 10km to and from the CBD along a main and heavily signalled road; to trips longer than 10km to and from townships that primarily used highways. The short trips were characterised by frequent stops, high passenger seating position shifting, high occupancy changes, and relatively lower average speeds below 60 km/h. The long trips were characterised by low passenger seat position shifting, higher average speeds above 80 km/h, and lower passenger occupancy fluctuations.

3.2.1 Window Openings and Configurations

Throughout the journeys taken the windows that were most frequently opened were the driver and conductor windows, the conductor window was on the main door that most passengers use to enter and exit the taxi. Passengers generally chose to open windows primarily when the air inside the taxi was humid and warm. However, deviations from this general pattern occurred in instances when the external temperature was relatively low, it was raining, and the taxi was moving at high speeds above 80 km/h; in these conditions, passengers refrained from opening windows. Window openings ranged from partial to full depending on preference. Of the 23 preliminary journeys taken, none of the vehicles used the air diffusers either in the front of the vehicle or those above the passenger cabin (when available). Doors were only open when the taxi was moving at speeds below 10 km/h either when offloading passengers or departing after loading passengers.

3.2.2 Average Taxi Speeds, Stopping Frequency and Passenger Occupancy

For all journeys that started from the minibus taxi stations, vehicles departed only when fully loaded. The passenger loading capacity was usually determined by the maximum seating capacity of the vehicle; however, overloading was seen were 14-seater taxis carried up to 16 passengers, and 16 seater taxis carried up to 18 passengers depending on seat arrangements. Below-capacity passenger occupancy coincided with the taxi stopping and passengers disembarking and entering the taxi.

A difference was observed between passengers loading on long journeys as opposed to short journeys. Long journeys used the highways where there were fewer places to safely offload passengers whilst short journeys used main non-highway roads with greater opportunities for passenger offloading even at non-designated drop-off areas. On long journeys out of the CBD, the frequency of passenger stops and pickups was lower than that observed on all short journeys, with little to no passenger seating changes along the journey. Along all journeys to and from the CBD the taxi would stop when on-board passengers requested to be dropped and when the taxi capacity was below maximum and potential passengers were seen by the driver. Every stop did not necessarily result in increased passenger numbers.

Long journeys into the CBD involved both highway and main road routes therefore resulting in more frequent stops as passengers disembarked on points on the way after exiting the highways and joining the main roads. In those instances, when the taxi stopped, there were also points at which new passengers would potentially enter the taxi and the passenger seating order changed.

On the long routes speeds up to 115 km/h were recorded with total average moving speeds above 70 km/h in 11 journeys. For all short journeys taken, the average moving speed was below 50 km/h and the frequency of passenger/taxi stops was higher than observed in the long journeys, this resulted in more seating changes and less predictable occupancy rates along the journeys.

3.3 Conclusions

For the purposes of the study, three speeds of 40 km/h, 80 km/h and 100 km/h were selected as representative of the varying speeds observed in the journeys. Each of the speeds was selected for testing along routes on main roads and highways.

When considering whether door openings could be used in the experiments, it was assumed that doors were only opened when the taxi was moving at speeds below 10 km/h either when offloading

or loading passengers. This was not considered an adequate parameter either in terms of practicality or safety to test for airflow characterisation or ventilation implications in the taxi experiments.

Based on observations made in the preliminary journeys, 10 window configurations were selected for the experimental phases. These configurations represented both the observed and possible configurations that could be used in operational vehicles for ventilation. For the chosen configurations in the experiments, the windows were fully opened.

4 MATERIALS AND EXPERIMENTAL CONFIGURATION

This chapter gives an overview of the equipment and support structures used in the project.

4.1 Minibus Taxi Selection

Based on literature reviewed and preliminary direct observations, the minibus taxi model chosen for the experiments in the study was the Toyota Quantum Ses'fikile, one of the most commonly used taxis within the Cape Town metropole (Johnstone-Robertson, 2012). The taxi model is a 16-seater vehicle which has a 15-passenger seating arrangement. Observations revealed that even in the same taxi model varying internal seat arrangements could be found however the maximum passenger loading was maintained, and in the final selected taxi, the seating capacity required was 16 without a need for a specific seat arrangement in the passenger cabin. The Ses'fikile taxi has 6 windows, 2 at the front, 2 in line with the main passenger door and 2 towards the rear of the taxi. Each of the 3 sets of windows has different area openings. The main passenger door along with the front row, centre row and back row windows have the following respective area openings: 1.75m^2, 0.37m^2, 0.13m^2 and 0.14m^2. The estimated interior volume of the taxi was 11.85m^3, derived from interior wall and floor measurements discounting the space taken by seats. The front windows were roll-down windows, whereas the main cab windows at the passenger seats were sliding windows that would open sideways.

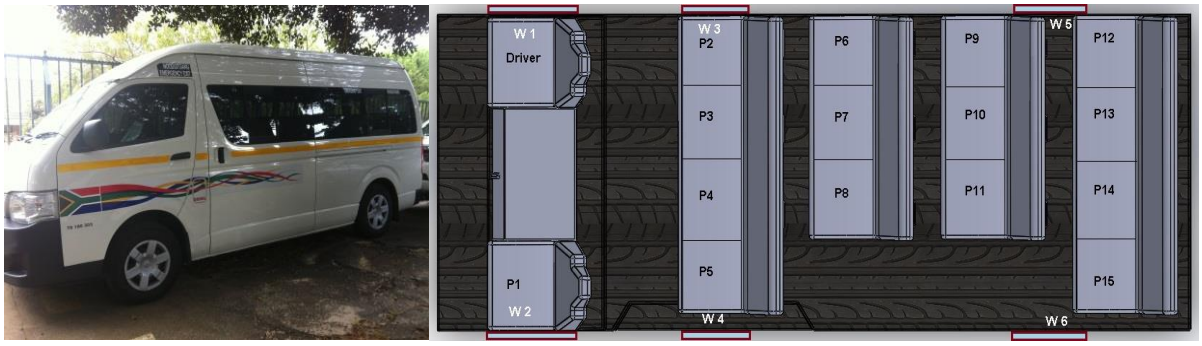

Figure 4.1-1 Toyota Quantum Ses'fikile 2014 model and seat arrangement, P denotes a passenger seat whilst W denotes a window.

A university-certified minibus Ses'fikile taxi was hired for the tests (the owner was a registered university-vendor and driver of student transport vehicles). An agreement was made on hiring that any equipment loaded on the vehicle would be removed at the end of the testing day (hence it would need to be re-loaded on the following testing day).

4.2 Equipment

An arrangement of hotwire anemometers had initially been envisioned as the primary method to track the flow of air within the minibus taxi as was employed in the aircraft cabin study reviewed in Chapter 2.5.1. However, the limited space and nature of the experiments (mobile tests at varying speeds and manual movement of anemometers) required a more adaptable approach to the airflow measurements. Multiple anemometers at key positions throughout the taxi-interior were required to measure and log airflow patterns. The anemometers needed to measure both wind speed and direction in either 2D or 3D. Ultrasonic anemometers were selected for this application. These meters work by measuring when airflow interrupts the pulses of sound that are continuously sent in-between sensor nodes. Due to space limitations within the taxi passenger cabin a 3D anemometer could not be installed for airflow measurements, despite having the best resolution, accuracy and range of measurement. WindSonic ultrasonic 2D anemometers were used for measuring airflow inside the taxi. The meters were small and could be easily mounted allowing for fixed placement and manual repositioning in the taxi. The meters were also robust during mobile experiments and their measurements were not affected by vibrations of the taxi. WindSonic anemometers were used as they allowed manual repositioning and multidirectional recordings, similar to the airline cabin anemometers reviewed in Chapter 2.5.1. A Garmin 18x 5Hz GPS unit was used to record travel data. A WIKA® TR60-A RTD thermometer was used during the experiments to record internal temperature fluctuations resulting from the window configurations.

The dataTaker DT80-3 data logger was used to collect the readings from the sensors and save them internally on a 124mb drive or to a connected memory stick depending on preference.

Readily available rechargeable 12V 7.6Ahlead-acid batteries were used in the experiments to power the sensors, and this complied with the requirement for easy removal of instrumentation from the taxi after each test.

4.2.1 Anemometer Specifications

Besides the ultrasonic anemometers, a wide diameter vane anemometer was also used to test the reliability of the measurements by the ultrasonic anemometers.

Ultrasonic Anemometer

Three WindSonic anemometers were used to record internal airflow, with manufacturer reported wind speed resolution of 0.01m/s, accuracy ± 2% (at 12 m/s) and range of 0-60m/s, and wind direction

resolution of 1°, accuracy of ± 3° (at 12m/s) and range of 0-359°. The anemometers were set to analogue output (4-20mA) which allowed it to connect directly to the data logger, sampling at frequencies of 1Hz (the maximum the data logger would permit).

Large Vane Thermo-Anemometer

The Extech®AN700 thermo-anemometer was used to verify measurements made by the WindSonic anemometers in the experiments. It was reported to have a resolution of 0.01m/s, accuracy of ± (1.5% reading +0.3m/s and a range of 0.2-30m/s.

4.2.2 Resistance Temperature Detectors

Measurements involving airflow are often accompanied by temperature sensors to see the effect of changing airflow on the measured interior space (Zhang, et al., 2009). A WIKA TR60-A resistance temperature detector (RTD), with a platinum wire-wound glass measuring resistor, specifically designed to measure ambient air temperature was used in the experiments. The RTD measures temperatures between -40°C to +80°C continuously, whilst encased in a perforated stainless-steel probe making it suitable for fast response time measurements and high vibration resistance. The sampling rate for the RTD was set to 0.1Hz.

4.2.3 Position and Speed Tracking

Due to the nature of the on-road tests, the ideal speeds (40 km/h, 80 km/h and 100 km/h) set for the experiments could not be maintained therefore speed was recorded continuously. A Garmin GPS 18x 5Hz was used to record continuous taxi speed and routes taken during experiments. A dataTaker CANgate Controller Area Network (CAN) to ASCII gateway converted GPS data to serial data. The CANgate was used to connect the GPS unit to the data logger for both data collection and operating power supply.

4.2.4 Data logging

A multichannel dataTaker DT80-3 data logger was used to record information from the multiple sensors used concurrently in the experiments. During all airflow experiments, the following sensors were all used: the 3 ultrasonic anemometers, 1 GPS unit a, 1 CANgate adapter and 1 RTD thermometer. The data logger required a 12v power supply which was provided through a rechargeable lead acid battery, all other sensors were powered by the battery connected to the data logger.

The DT80-3 was programmed through deLogger a graphical and text software for dataTaker data loggers with a DBD output format that could be read through dataTaker Dplot graphical software and

exported as CSV files for processing in Excel and R. The DT80-3 was programmed to separate logged data into 3 sections: GPS data, temperature data and airflow data (from all 3 anemometers).

4.2.5 Tracer Gas Sensor

The Extech®SD800 CO_2 humidity/temperature data logger was used to measure the interior CO_2 levels during all the tracer gas phases of the experiments. The SD800 used a dual wavelength NDIR CO_2 sensor with a resolution of 1ppm, accuracy of ±40ppm (<1000ppm); ±5% reading (>1000ppm) and range of 0-4000ppm. The humidity sensor had a resolution of 0.1%, accuracy of ±4% RH and range of 10-90%RH. The temperature sensor had a resolution of 0.1°C, accuracy of ±0.8°C and range of 0-50 °C. The internal data logger had a 2 GB SD memory card and data were recorded in CSV format at a sampling frequency of 0.2Hz. A 9V output converter was built to allow the SD800 to be powered by the 12V battery connect to the DT80-3 data logger.

4.2.6 Smoke Machine

The BeamZ S700-JB was used to generate smoke during all the airflow visualisation experiments. This machine could be operated within a taxi as it was 2.3kg (hand operable), required 700W and had a warm up time of 5minutes. This unit was powered with 12V to 240V inverter with a 1000W rating connected to two 12V lead acid batteries and allowed the visualisation tests to be carried out on any selected route. The flow rate of the smoke was 75m^3 per minute and was pulse-controlled with a remote-control.

4.2.7 Equipment Performance

Ultrasonic Anemometers

Early testing of the WindSonic anemometers revealed that data recordings below 0.05m/s were unreliable, some negative values were also noted and assumed to be fluctuations of the signals entering the data logger. The anemometer manual suggested that values below the lower threshold of data recordings be set to 0.1m/s. The wind speed data analysed excluded measurements below 0.1m/s.

GPS unit

It was observed that when moving at low speeds a slower sampling rate would not affect the data collected yet when moving at higher speeds above 60 km/h, the sampling rate needed to be increased proportionately to avoid errors due to GPS drift. The highest sampling rate of 1 Hz was used.

Data logger

Initially during the tests, the data logged would reach 100 MB in a 4-hr testing period, a mere 28 MB shy of the 128 MB internal storage capacity. The frequency of the measurements from the connected sensors determined how much the logged data size would be. As a result, the logger was set to save the data on an external 2 GB flash-drive, thus enabling longer testing periods and removing the risk of overwritten data.

4.3 Measurement Rig and Mounting Cylinders

The mechanical workshop of the Department of Human Biology constructed a framework onto which all the instrumentation for the experiments could be attached. The frame material requirements were vibration stability during driving tests and robustness for multiple usage and equipment loading. The frame had to be removed daily as the vehicle used in the tests was hired only for the testing hours. All the daily installation and dismantling was done by the mechanical workshop technician. A wooden frame was used (other choices included aluminium, plastic and Perspex) as it provided ample support for sensors and was built to allow speedy assembly and dismantling prior to and after the experiments (Figure 4.3-1).

Mounting holes were drilled on several points along the horizontal planks of the frame (Figure 4.3-1). This allowed the anemometers to be placed at points that corresponded with likely passenger seating positions. To attach the 3 ultrasonic anemometers in a line to the equipment frame, separate solid aluminium mounting tubes were made that had enough weight to stabilise the anemometers while the taxi was in motion (excess oscillations could affect air velocity measurements). In addition to the mounting cylinders, height-adjustable hollow-aluminium mounting tubes were made, that allowed mounting of the anemometers on the support frame to measure airflow at different specific heights, namely lower middle and upper heights as show in Figure 4.3-2, Figure 4.3-3,Figure 4.3-4, Figure 4.3-5 and Figure 4.3-6. The lower height corresponded to the seated head-height of a passenger, the middle and upper heights were set at 20cm and 30cm above the lower height. This is shown in Figure 4.3-2 and Figure 4.3-6.

Figure 4.3-1 Equipment rig installed in taxi

Figure 4.3-2 shows the wooden equipment frame with anemometers mounted along all the length of the passenger cabin.

Figure 4.3-2 Equipment frame with mounted anemometers

Figure 4.3-3 shows the placement of the anemometers in the front row of the passenger cabin at both the bottom and middle heights.

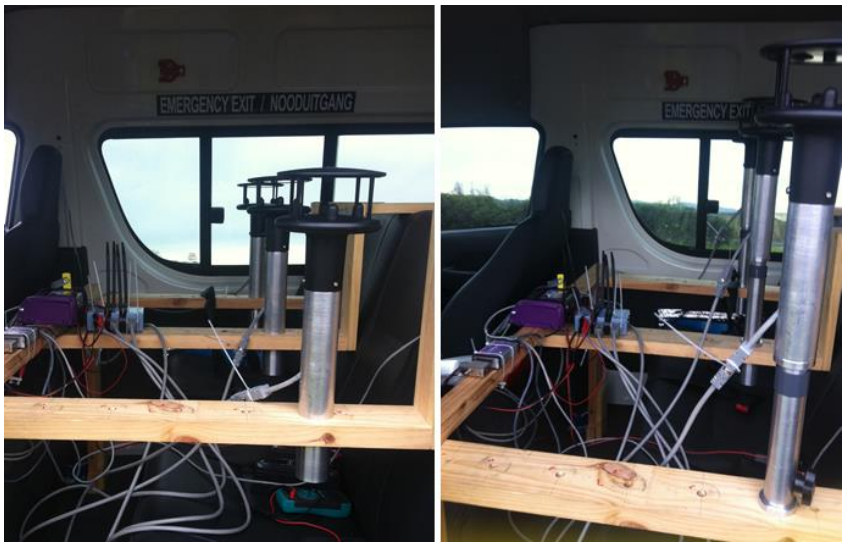

Figure 4.3-3 Anemometers at adjustable heights

Figure 4.3-4 Anemometer and mounting cylinders

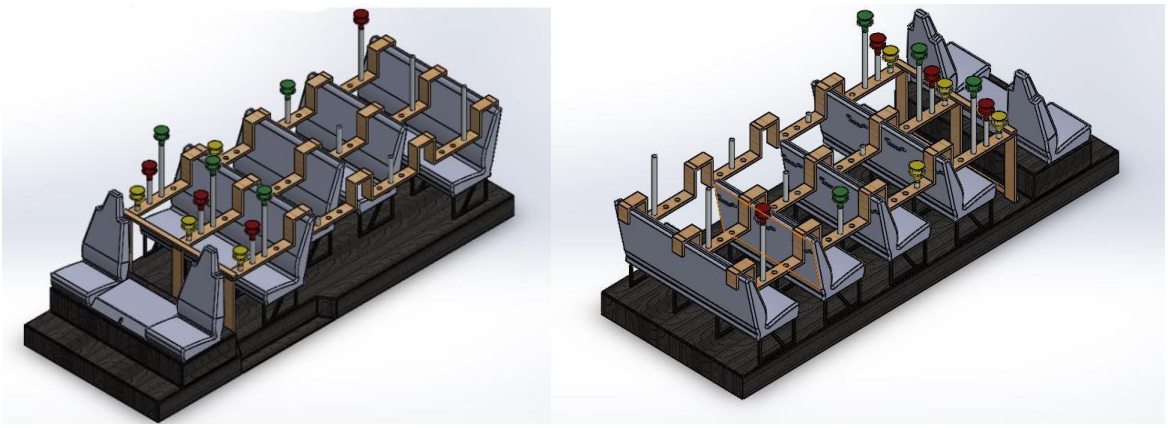

Figure 4.3-5 Model of equipment rig with mounted anemometers

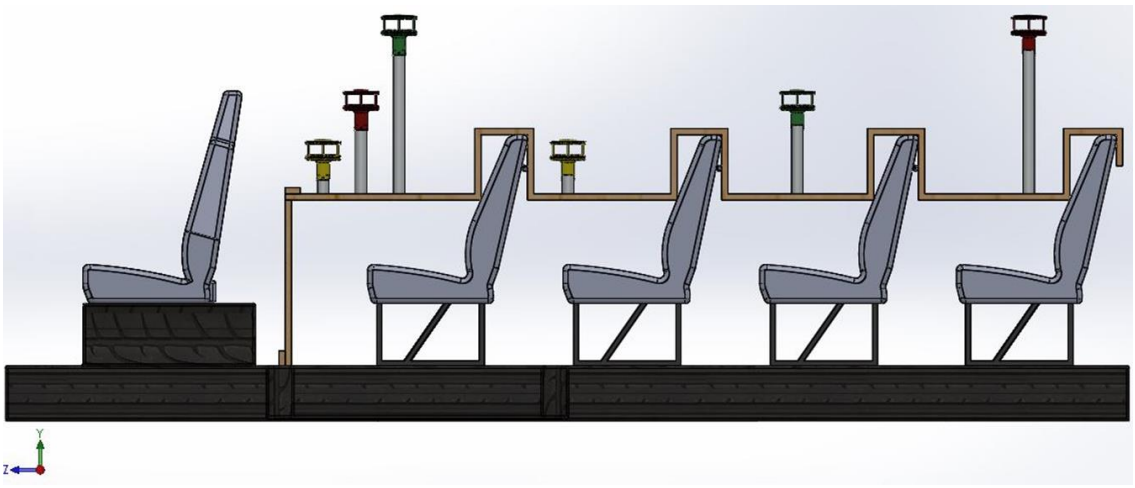

Figure 4.3-6 Side view of anemometers at test heights

4.4 Experimental Configurations

4.4.1 Window Configurations

There were 6 windows available in the selected experiment taxi model as shown in Figure 4.4.1-1. The 10 configurations referred to in Chapter 3.3 are as follows:

- 3 configurations with a single window opened (B, D, F) along the longitudinal plane of the taxi were used in the experiment
- 7 symmetrical window configurations along the longitudinal plane of the as shown below in Table 4.4.1-1

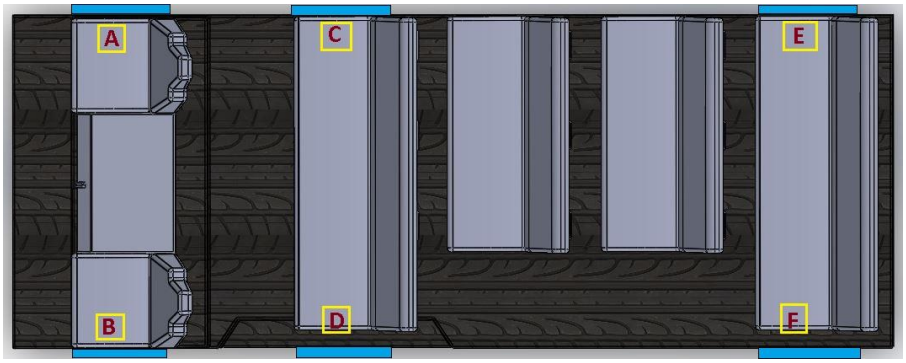

Figure 4.4.1-1 Window seat positions in minibus taxi

Table 4.4.1-1 Window configuration for road tests

Window Configurations	1	2	3	4	5	6	7	8	9	10
Windows Open	F	D	B	A & B	C & D	E & F	A, B, E & F	A, B, C & D	C, D, E & F	A - F

The single window configurations 1 -3 with windows F, D and B were chosen as they allowed for smoother transitions between window configuration changes during tests as opposed to windows C & E.

4.4.2 Sensor Placement

The anemometer placement in the experiments was based on aircraft cabin experiments that placed the sensors in the flow stream as indicated in Chapter 2.5.1. Thirty-six positions were used for the anemometer placements:

- 4 sensor-arrangements, 3 longitudinal and 1 lateral arrangement as shown in Figure 4.4.2-1. For each sensor placement, the anemometers are divided into the front, centre and back positions.
- 3 height levels where the sensors were positioned within the breathing zone (lower, middle and upper) as shown in Figure 4.3-6
- A total of 12 sensor positions at three height levels, for a total of 36 positions.
- Four seat rows were used where anemometer arrangements on the frame-grid aligned with passenger seating positions. Twelve measuring frame-grid positions were used because of the airflow visualisation. These positions were set at 15cm forward from seat-backs and 30cm away from interior walls

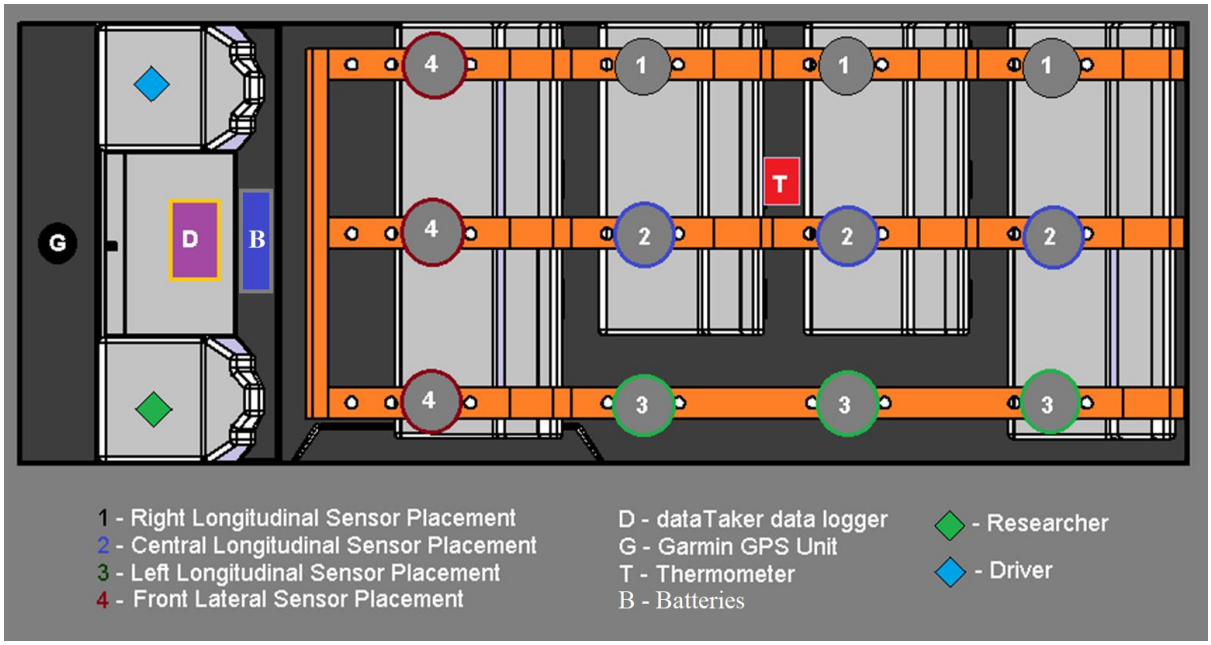

Figure 4.4.2-1 Equipment placement

As stated in Section 4.2.6, the smoke machine was handheld and plugged to the batteries shown in Figure 4.4.2-1. The smoke machine was lifted to aim the smoke to the back seats and the front seat. Its position was not stationary, rather the smoke volume released was constant, thus its position is not shown in the figure above.

5 METHODOLOGY

This chapter covers the methodology used to collect data in the air flow visualisation, airflow characterisation and ventilation experiments. The methods used for the project were derived from the airborne infection control literature covered in Chapter 2.5. In instances were literature was not available, published guidelines were used to construct methods suitable for the taxi environment.

5.1 Airflow Visualisation Procedure

Prior to measuring interior air speeds whilst the taxi was in motion, critical points of measurement had to be identified. Airflow patterns in the breathing zone (taken from the chest height of a seated adult passenger to the ceiling of the taxi) were explored to locate the required critical points, hence smoke generation was used to visualise airflow similar to experiments reviewed in Chapter 2.5.1.
Direct observation was used to record the movement of smoke within the breathing zone in the taxi during tests. The smoke was too fine to record with a camera. Two observers were present during all the visualisation tests, and the smoke movements were noted.

Testing procedures for both the airflow characterisation and ventilation testing phases were based on guidelines set in the REHVA Guidebook (REHVA, 2004), but adapted for use in a minibus taxi.

The testing procedure during airflow characterisation tests were as follows:

1. All taxi windows and doors were closed.
2. Smoke machine was heated up.
3. Smoke was generated into the clear taxi environment for 30-60s and allowed to fill the cabin until a visibly recordable amount was suspended in the breathing zone.
4. Window configuration (Chapter 4.4.1) being tested was opened fully and airflow was recorded until the smoke had either dissipated or a constant (non-recordable) haze was suspended in the breathing zone.
5. Stop recording.
6. Clear remaining smoke.
7. The test was repeated before changing the window configuration.

In the mobile tests, the taxi was travelling at the predetermined steady speeds (40, 80, 100 km/h). The 10 configurations were tested for at a single speed (including repeats) before the speed was altered and the procedure repeated.

The GPS unit and data logger were used in the tests to record the taxi speed and route taken. Each configuration test was repeated three times at 100 km/h and twice at 40 km/h and 80 km/h, and the results were averaged for each speed. The smoke was regenerated for each test.

5.2 Airflow Pattern Testing

The method employed was based on the airplane cabin study (Zhang, et al., 2009) explored in Chapter 2.5.1. Ultrasonic anemometers were placed on a wooden frame rig and were manually repositioned to allow measurements at 12 different points and 3 height levels within the breathing zone (36 total measuring points). At each measuring point, the anemometers were set to record airflow for each of the window configurations at the specified taxi speed (the anemometers were moved manually after each data collection set (all 10 window configurations).

The procedure was carried as follows:

1. Anemometers were placed in the frame-grid arrangement (3 sensors) and the GPS unit (front of taxi), temperature sensor (centre of taxi in line with the top of the passenger seat) and data logger were placed in their positions.
2. Taxi doors were closed, and the window configuration opened.
3. Taxi maintained testing speed and the airflow was recorded for 5 minutes.
4. Taxi stopped, and window configuration was changed, and recording resumed when the testing speed was achieved.
5. Airflow was recorded for all 10 window configurations.
6. The grid-arrangement was changed (height maintained) and the airflow measurement procedure was repeated.
7. When all the 12 grid-position airflows were recorded for each of the 10 window configurations, the height of the sensors was then increased.
8. The 12 grid-position measurements were repeated at the new height.
9. When all 36 measurements were carried out for each of the 10 window configurations, the tests where repeated.

The collected data from the tests showed the airflow patterns within the taxi at differing heights within the breathing zone. This data were then processed through the dataTaker software for visual analysis and exported as .csv files for further analysis in Excel and MATLAB.

The directions of the airflow would be determined to the closest secondary intercardinal direction (16 compass points), where each direction has a 22.5° range of values (e.g. NNE is between 11.25°-33.75° as shown below in Figure 5.2-1). Directions N, S, E, and W refer to the front, back, right side and left side of the taxi.

For the purposes of this study, partial density-based cluster analysis (Tan, et al., 2005) was conducted visually on the data collected. When high cluster cohesion exists between data points, the airflow was classified as distinct airflow. Airflow was noted as having a distinct direction when data clusters fell within 35° of a direction. A range of 35° is roughly 1.5 times the range used to determine a singular direction and was chosen as a suitable range for distinct airflows. When cluster separation existed between data points, within a 35° - 67.5° range around an average direction, the airflow was assigned a mixed airflow classification. A range of 35 - 67.5° is 1.5 - 3 times the range used to determine a direction and would represent airflow fluctuating within 4 adjacent directions (e.g. between E, ESE, SE and SSE). A non-distinct airflow classification was given to data points that were well separated, where majority of points lay outside 67.5° of any average direction.

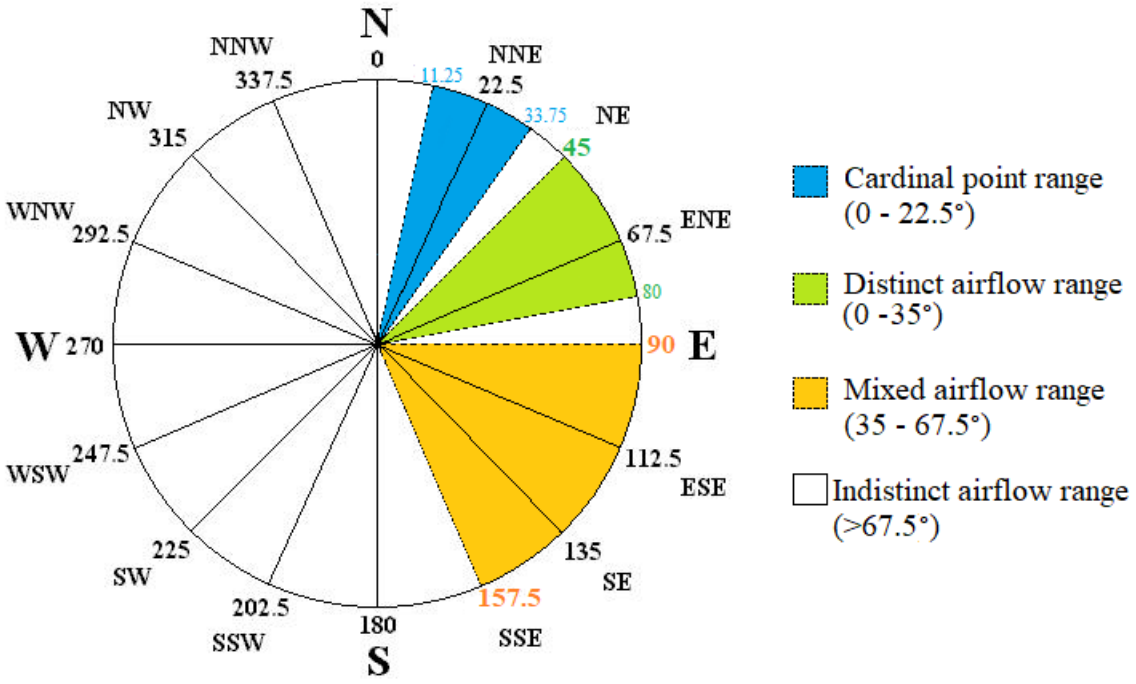

Figure 5.2-1 Cardinal directions and corresponding angles for distinct, mixed and indistinct airflows. The locations of the airflow patterns with regard to the cardinal directions are for illustration.

5.3 Ventilation Testing

5.3.1 Study Participants

The study participants were students recruited from the University of Cape Town Faculty of Health Sciences. The selection criteria allowed for any healthy participants aged 18 - 50 years of age to participate/volunteer as research taxi passengers. All participants in the study were required to answer a TB screening and risk assessment questionnaire that checked whether the participants were recently ill or at the time receiving treatment. This was to safeguard all participants against exposure to potential (undiagnosed) carriers of respiratory infectious diseases during the study. The total number of people in the taxi during the tests was 16 and consisted of the UCT transport personnel (driver), the researcher and the 14 participants.

This phase of the study was approved by the University of Cape Town Human Research Ethics Committee and access to students for the study was granted by the Department of Student Affairs. All participants in the study were insured under the UCT No Fault Compensation Policy during their time in the minibus taxi. The insurance cover was limited to 50 participants. Written participant consent was provided for each of the tests.

5.3.2 Stationary Unoccupied CO_2 Decay Tests

To establish baseline ventilation rates in a stationary taxi, tests were performed using CO_2 decay tracer gas techniques. The procedure could be summarised as follows:

1. All taxi windows and doors were closed.
2. The CO_2 datalogger, thermometer and dataTaker datalogger were mounted in the centre of the taxi, then switched on (the CO_2 sensor recorded every 5s and the thermometer logged every 10s).
3. The background CO_2 concentration and temperature in the centre of the taxi were measured and logged.
4. The taxi was vacated.
5. The electric fan was activated, and CO_2 was released (from a medical grade CO_2 cylinder) until a concentration above 3500ppm was achieved.
6. The electric fan was switched off after 60s of air mixing (for uniform distribution of the tracer gas).

7. The window configuration was opened, and the gas was then left to dissipate to a concentration within 50ppm of baseline concentration levels (<550ppm).
8. The taxi windows were then closed and CO_2 re-distributed into the taxi.
9. The processed was repeated for all window configurations.

The rate of decay of the known concentration of CO_2 in a known interior volume was used to calculate the stationary ventilation in a taxi for the different window configurations. The sampling position was kept constant throughout the experiment at the breathing-level position of the central passenger seats. The experiment was repeated twice for each window configuration, and results were averaged.

5.3.3 Occupied Mobile CO_2 Decay Tests

The CO_2 measurements were used to determine whether the ventilation in the taxis could meet health care settings standards for rooms with infectious individuals and to identify instances, coinciding with certain window configurations, when ventilation is suboptimal. The mobile tests were conducted for an hour from 13:00 – 14:00 during the lunch hours for participating students.

The testing procedure was carried out as follows:

1. The CO_2 datalogger, thermometer, GPS unit and dataTaker datalogger were mounted in the taxi, then switched on (the CO_2 sensor recorded every 5s and the thermometer logged every 10s).
2. The background CO_2 concentration and temperature in the centre of the taxi were measured and logged.
3. All participants entered the taxi and windows and doors were closed.
4. Taxi achieved and maintained testing speed whilst hand fans were used by half of the participants to facilitate uniform CO_2 distribution for 5 minutes until a concentration above 2000ppm was achieved.
5. The participants stopped fanning the air.
6. The window configuration was opened, and the gas was then allowed to decay for 5minutes or until concentration to decreased to within 200ppm of baseline concentration levels (<700ppm).
7. The taxi windows were then closed, and the CO_2 concentration could rise again.
8. The processed was repeated for varying window configurations.

The taxi departure point was outside the Anatomy building on the Faculty of Health Sciences at the University of Cape Town. All participants were informed of the CO_2 and temperature recordings conducted during the journeys as well as the window opening configurations required of the participants on window-seats. Given the time constrained nature of the experiments, full stability was not achieved in accumulation of CO_2 when windows were closed. Only 6 configurations were tested in each 1hr testing period. The taxi travelled on routes that allowed movement at the predetermined speeds, 40 km/h off the highway and both 80 km/h and 100 km/h on the highway.

The CO_2 data gathered was used to calculate the risk of infection posed on taxi commuters.

5.3.4 Regression Analysis

CO_2 decay data collected in the ventilation tests was used to determine the ventilation rates for each of the tested window configurations at the three taxi speeds. R-Studio was used to preform linear regression analysis on the resultant ventilation rates. A fitted model was used to identify if a relationship could be found between increase in speed and increase in ventilation, as well as between increase in window openings and increase in ventilation.

5.3.5 Transmission Risk Analysis

The ventilation data were used in the Issarow Equation 2.5.2-4 to calculate the risk of airborne TB infection in susceptible individuals for the tested window configurations and speeds.

The simulation mirrored that of the source study (Issarow, et al., 2015), to observe the effect of the attributing factors to the probability of transmission risk; non-contributing parameters were assigned constant values:

- (B - μ), which describes the survival rate of infectious particles from the infector to the target site of infection, was based on the concentration of CO_2 in the test environment. In the Issarow study, (B - μ) was set as 13 and 32 particles/hr. In this study, (B - μ) was set as 15 particles/hr.
- The deposition fraction (Θ), which must be greater than 0 for infection to occur, was based on findings made in the study by Majid et. al (2011) [0.02].
- The breathing rate of passengers (p), was obtained by converting the lowest average breathing rate of 12 breaths per min to the volume per hour equivalent (Grossman, 1983) [360 L/hr].
- The interior volume of the taxi (V) was estimated using internal measurements made in the taxi model used [11.85 m^3].

The probability of TB-transmission (*P*) was simulated for scenarios in which the number of infectious individuals (*I*) and the ventilation rate (*Q*) [L/hr] varied.

6 RESULTS

Outlined in this chapter are the results of the experiments carried out using the methodology explained in the previous chapter. The chapter addresses the characterisation of air movement and ventilation in a taxi under varying operating conditions. It shows the varying ventilation rates in a taxi and connects those to the cross-infection risk as outlined in the objectives of the project.

6.1 Airflow Visualisation

On-road smoke visualisation was carried out for each of the 10 window configurations described in

Table 4.4.1-1, for three different taxi speeds (40 km/h, 80 km/h, 100 km/h).

In each experiment set with 10 window configurations, the observed airflow varied so that instances of distinct, mixed (with some patterns observed) and non-distinct (highly mixed directions with no clear patterns) airflows were measured. Table 6.1-1 below shows the airflow types observed in the experiment as non-distinct (ND), mixed (M) and distinct (D). In the table, YES denotes that a full exchange of air resulted in all the smoke being cleared in the taxi during the 5-minute experimental timeframe outlined in Chapter 5.1. When distinct airflow occurred, the smoke was always cleared within the testing period, whereas mixed and non-distinct flows could leave smoke lingering.

Table 6.1-1 Summary of airflow visualisation at different speeds

Speed	Window configuration	1	2	3	4	5	6	7	8	9	10
40 km/h	Airflow type	ND	ND	M	M	ND	ND	D	D	M	M
	Full air change	NO	NO	NO	YES	YES	NO	YES	YES	YES	YES
	Smoke clearance time [minutes]	n/a	n/a	n/a	1	3	n/a	0.5	0.5	1.5	0.5
80 km/h	Airflow type	M	ND	D	D	M	M	D	D	M	D
	Full air change	NO	NO	YES	YES	NO	NO	YES	YES	YES	YES
	Smoke clearance time [minutes]	n/a	n/a	1.5	0.5	n/a	2	0.2	0.2	1	0.2
100 km/h	Airflow type	M	ND	M	D	D	D	D	M	M	M
	Full air change	NO	NO	YES	YES	YES	YES	YES	YES	YES	YES
	Smoke clearance time [minutes]	n/a	n/a	0.5	0.25	1	1	0.2	0.25	1	0.1

The results of the experiments are reported below for the following configurations: single window (configurations 1-3 in

Table 4.4.1-1), double window (4-6) and stacked-double window (7-10); stacked-double window refers to more than one window pair being open. The main differences observed for airflow at different speeds for the same configuration, were the smoke dissipation times.

6.1.1 Single Sided Window Configurations

In configuration 1, mixed airflow was observed at 80 and 100 km/h as smoke was pulled out slowly from the open window and fresh air pushed towards the opposite side, as shown in Figure 6.1.1-1. Smoke did not fully clear in the front rows at all the speeds within 3 minutes.

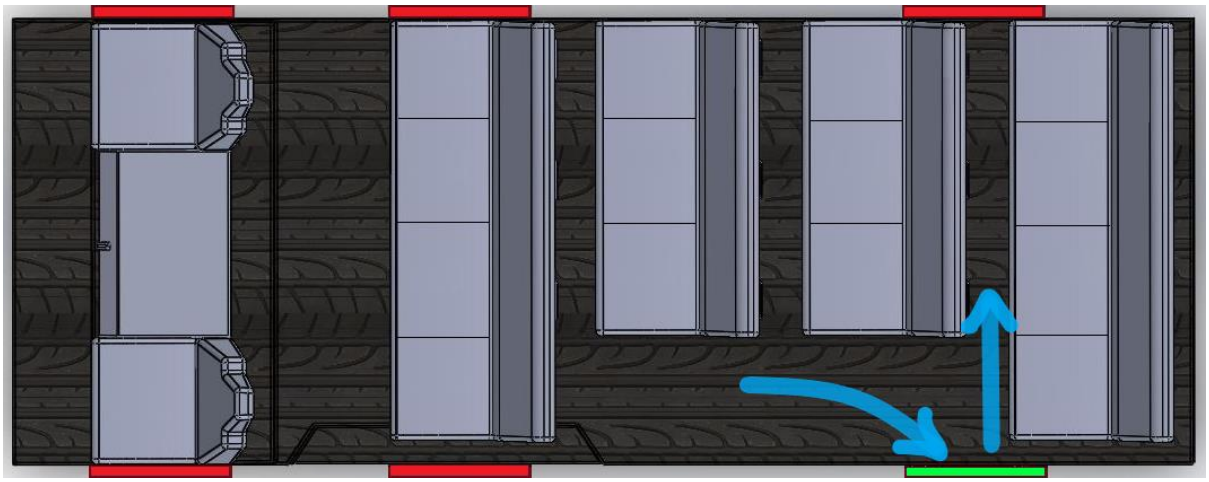

Figure 6.1.1-1 Airflow visualisation for configuration 1

In configuration 2, as shown in Figure 6.1.1-2 below, apart from slight backward pushing on air from the open window, no distinct airflow pattern was observed in other areas of the taxi at all speeds. Smoke lingered above both front and rear seats, taking 3 minutes to clear at 100 km/h and not clearing at both 40 km/h and 80 km/h in 3 minutes.

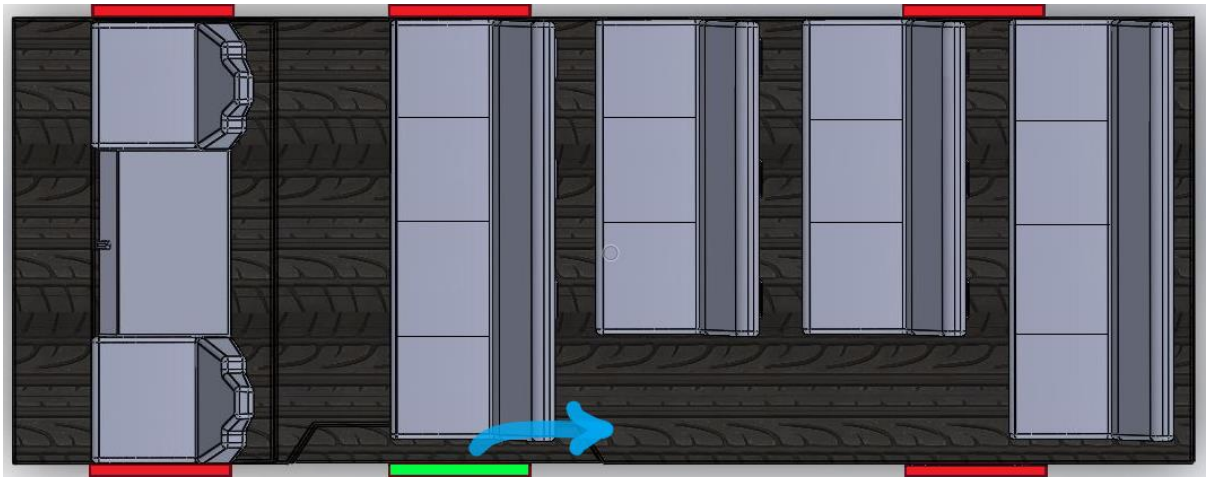

Figure 6.1.1-2 Airflow visualisation for configuration 2

In configuration 3, smoke lingered in the rear of the taxi, but cleared in the front 2 rows. At both 40 and 100 km/h mixed airflow patterns were observed, however at 80 km/h air was pushed back along the left side and pulled through the centre (creating an anticlockwise swirl in the centre of the taxi shown in Figure 6.1.1-3). At 40 km/h smoke was not fully cleared from the taxi in 3 minutes, at 80 km/h full clearing was achieved in 2 min and at 100 km/h this occurred in 30 seconds.

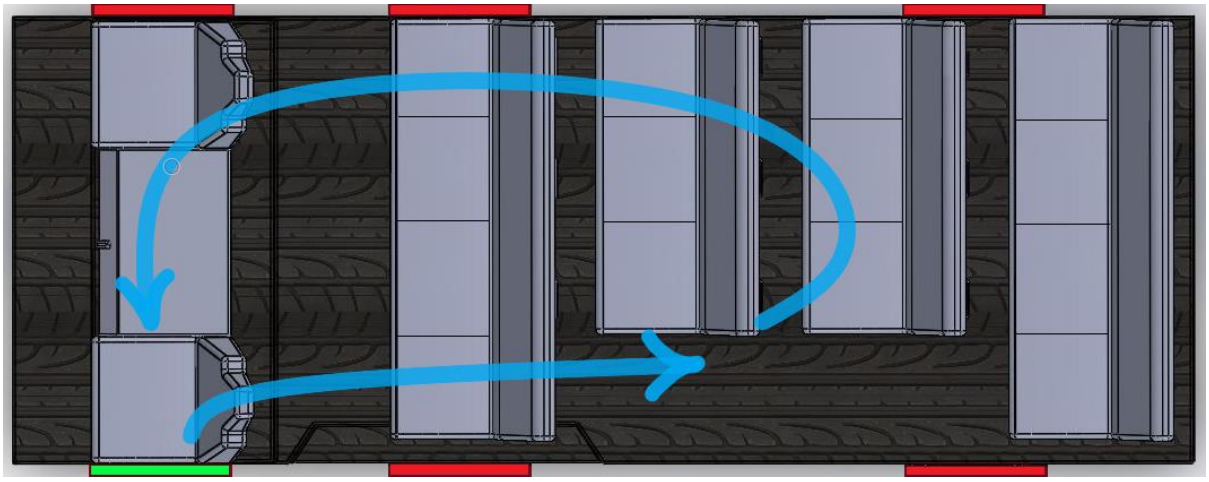

Figure 6.1.1-3 Airflow visualisation for configuration 3, 80 km/h

6.1.2 Double Sided Window Configurations

In configuration 4, air flowed backwards along the sides of the taxi and forwards through the centre of the taxi. This airflow pattern, shown in Figure 6.1.2-1, was discernible at all speeds and, in addition, vortices were observed in the front of the taxi at the 2 lower speeds. Smoke dispersed completely in under 1 minute at 40 km/h, and under 30 seconds at 80 km/h and 100 km/h.

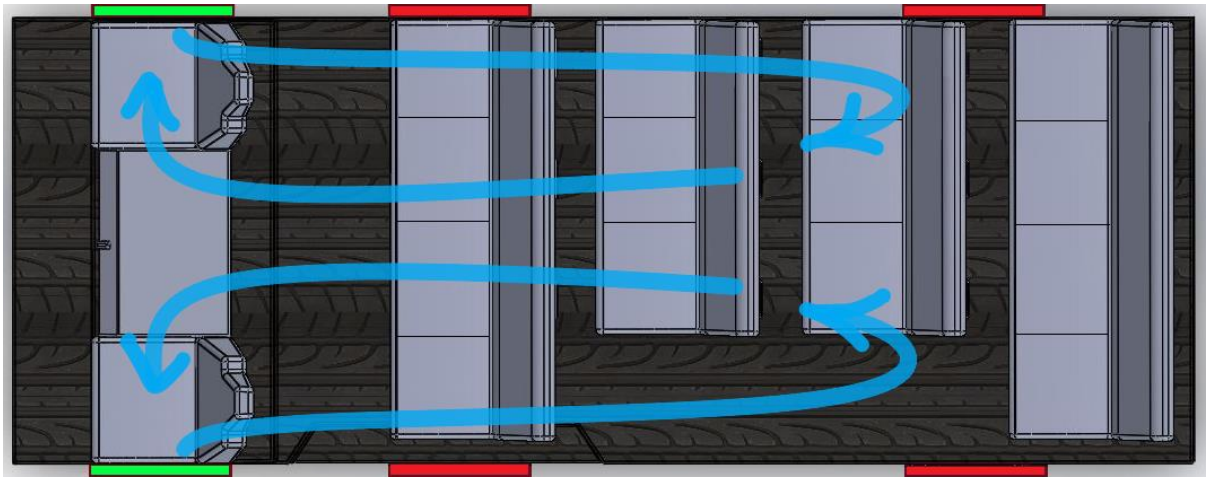

Figure 6.1.2-1 Airflow visualisation for configuration 4

In configuration 5 at 40 km/h no distinct airflow pattern was observed, and air was drawn out from both windows. Smoke cleared within 3 minutes at 40 km/h, 2 minutes at 80 km/h and 1 minute at 100 km/h where a clear vortex was formed as shown in Figure 6.1.2-2.

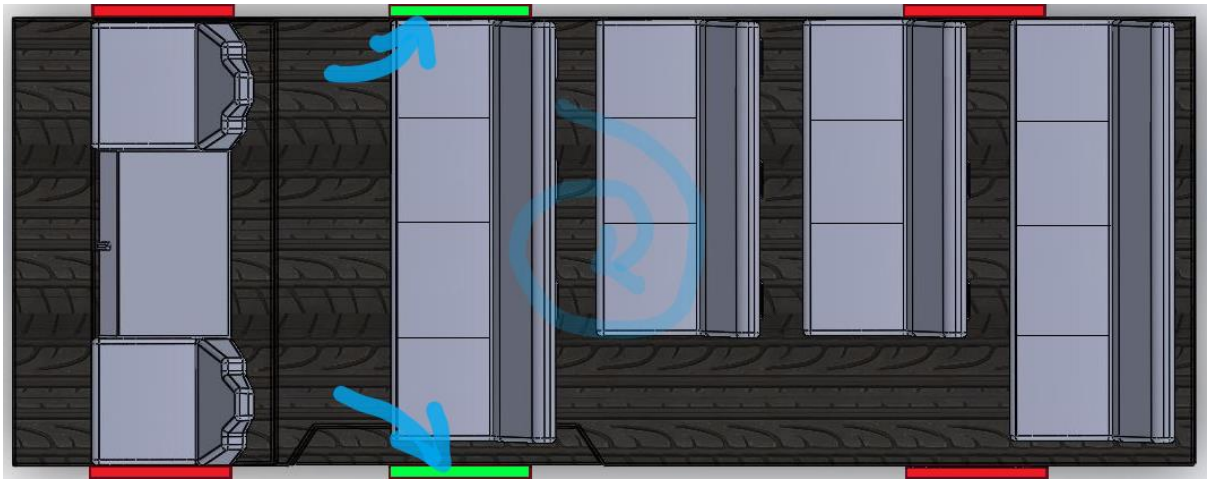

Figure 6.1.2-2 Airflow visualisation for configuration 5. The vortex in the centre was formed at 100 km/h.

In configuration 6, air was clearly observed moving from the front of the cabin to the rear as shown in Figure 6.1.2-3, at both 80 km/h and 100 km/h. At all speeds the smoke cleared, but clearing time varied from 3 minutes at 40 km/h to 1 minute at 100 km/h.

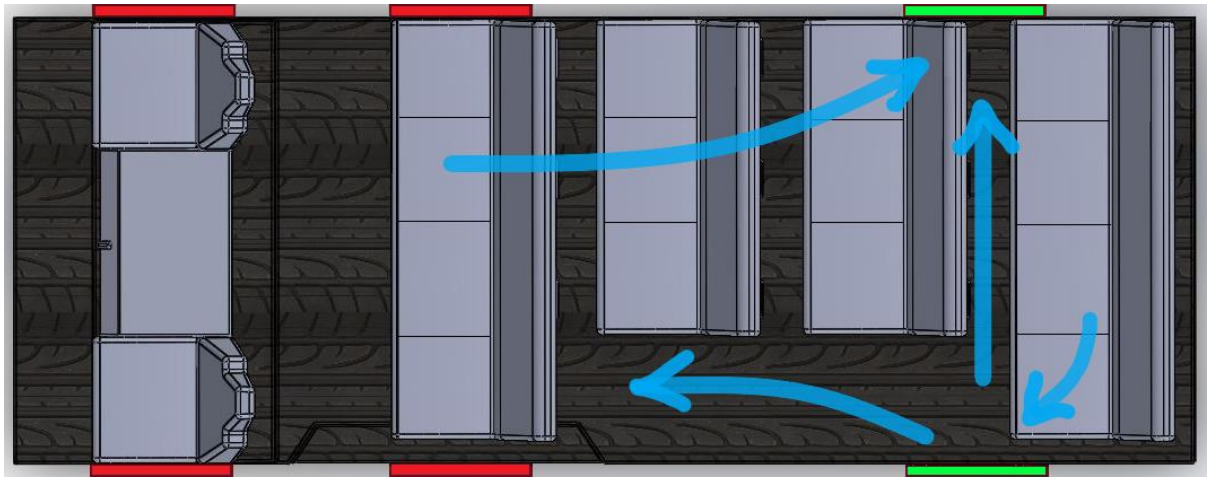

Figure 6.1.2-3 Airflow visualisation for configuration 6, 80 km/h and 100 km/h

6.1.3 Stacked-double Sided Window Configurations

In configuration 7, shown below in Figure 6.1.3-1, air flowed towards the front of the taxi through the centre (primarily in the front half of the taxi), and cleared through the front windows but also cleared from the rear windows (with mixing flows observed in the rear). Smoke dissipated completely in less than 30 seconds at all speeds.

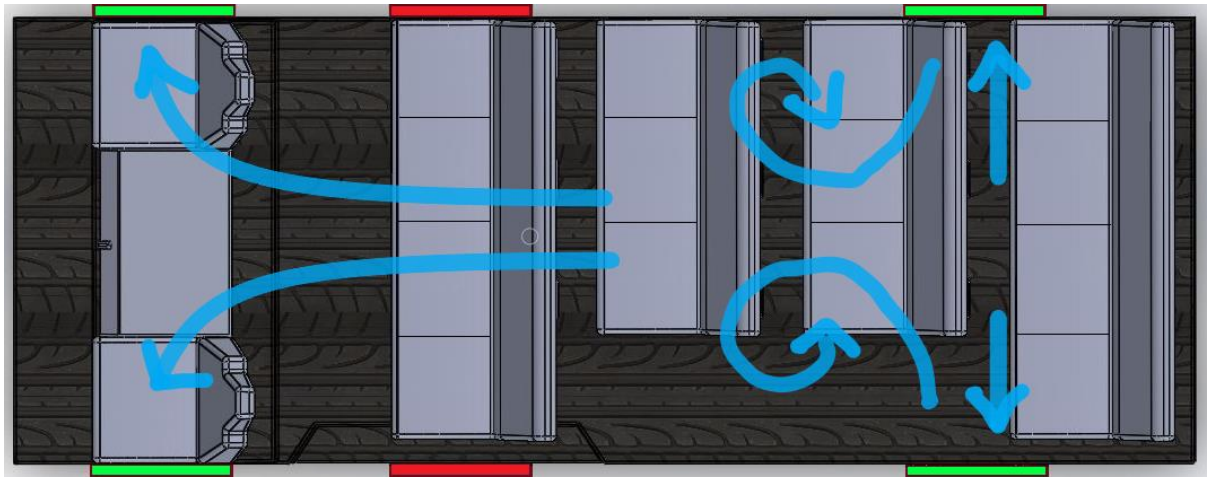

Figure 6.1.3-1 Airflow visualisation for configuration 7

In configuration 8, air flowed through the front windows (with clear forward flow in the front central half of the taxi, shown in Figure 6.1.3-2), however mixing resulted in the rear from air being drawn in through the left and out the right windows. Smoke cleared in less than 1 minute at all speeds.

Figure 6.1.3-2 Airflow visualisation for configuration 8

In configuration 9, complex mixing flows, visualised in Figure 6.1.3-3, were observed at all speeds including flow between windows C & D and E & F. All smoke lingered in the front of the taxi before dissipating in less than 2 minutes at all speeds.

Figure 6.1.3-3 Airflow visualisation for configuration 9

In configuration 10, a clear central flow occurred from the front half of the taxi and out through the front windows A & B, as shown in Figure 6.1.3-4, however the rear half of the taxi had rapid mixed flows. Smoke cleared in 30 seconds at 40 km/h, 10 seconds at 80 km/h and in less than 5 seconds at 100 km/h.

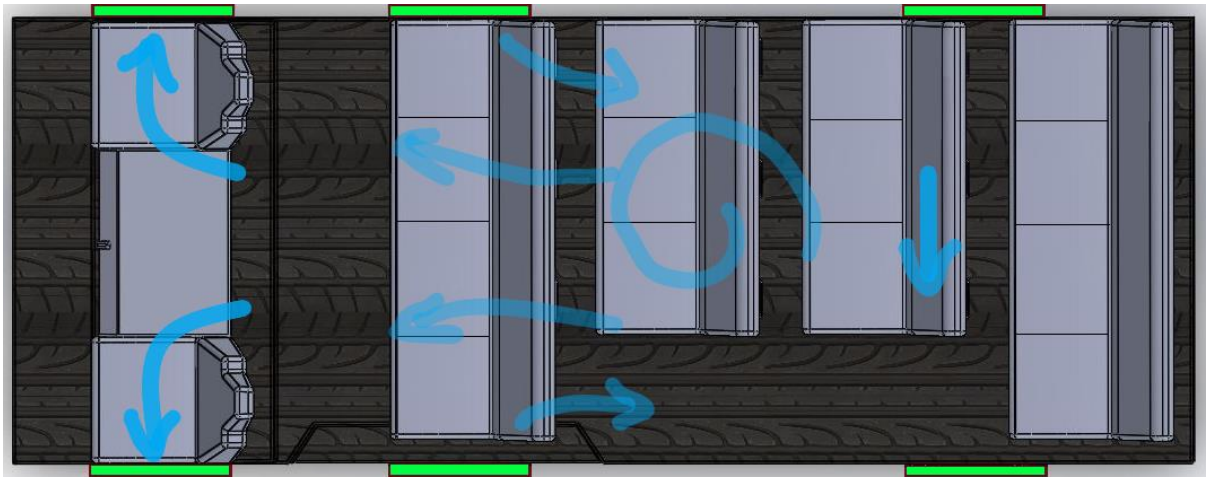

Figure 6.1.3-4 Airflow visualisation for configuration 10

6.2 Airflow Pattern Testing

On-road airflow characterisation was carried out at 80 km/h and 100 km/h for each of the 10 window configurations. At 80 km/h the experiments were carried out and repeated at all 3 sensor heights outlined in Chapter 4.3, whilst the 100 km/h the experiments were carried out at the bottom height. The data collected in the 80 km/h tests formed the bulk of the airflow characterisation analysis and the 100 km/h data were used mainly for comparative analysis. Table 6.2-1 below shows the variations in speeds achieved during the tests. The speeds achieved varied due to traffic conditions but remained within 10% of the set speed in most instances.

Table 6.2-1 Average taxi speeds achieved during tests

		Window Configuration									
Test Speed	Sensor Level	1	2	3	4	5	6	7	8	9	10
80 km/h	Lower	70.1	72.3	75.2	74.9	74.9	76.7	72.6	75.1	76	73.6
80 km/h	Middle	73.8	71.4	76.8	73.8	75.5	75.9	71.7	67.2	76	75.7
80 km/h	Upper	75.1	69.4	74.4	74.4	73	76	74.4	74.3	74.6	76.2
100 km/h	Lower	93.6	91.4	93	92.6	96.6	93	95.2	94.9	92.1	90.1

Each window configuration was tested for 5-minute intervals and the tests were repeated twice for the 80 km/h experiments and due to time restrictions the 100 km/h tests were not repeated. Each sensor placement test was carried out in the taxi on highways with normal off-peak traffic flow conditions and the results may have been influenced by traffic conditions.

The airflow direction was determined by assessing the distribution of data points as described in Chapter 5.2 during the 5-minute testing period.

At 80 km/h and 100 km/h the average airflow velocity differences across window configurations were more prominent. Configurations 3 and 4 had the highest average airflow velocities in their groupings however configuration 10 with all windows open produced the highest average airflow velocities consistently in all the tests. In each of the sensor placements, distinct airflow directions were measured at each of the test heights for several configurations.

When considering the overall airflow directions measured in the taxi, it was noted that sensor placement 2 (Figure 4.4.2-1) recorded more mixed and indistinct airflow than sensor placements 1 & 3 at the sides of the taxi. This trend was visible at both 80 and 100 km/h, as well as at the varying heights within the breathing zone (measured area). For the airflow velocities recorded, anemometers in sensor placement 2 consistently recorded lower averages than either placements 1 & 3.

The Table 6.2-2 below shows the average velocity and directions measured at the centre of the taxi at 80km/h, with changing sensor heights. Indistinct directions are labelled as n/a.

Table 6.2-2 80km/h average airflow velocity and direction summary at sensor placement 2

		Window Configuration									
Sensor Height		1	2	3	4	5	6	7	8	9	10
Lower	Velocity (m/s)	0.06	0.13	0.24	0.34	0.68	0.18	0.57	1.305	0.27	1.4
	Direction	n/a	SSW	SSE	SSE	WNW	SSW	N	n/a	SSW	W
Middle	Velocity (m/s)	0.11	0.19	0.82	1.12	0.58	0.38	1.46	2.88	0.81	2.5
	Direction	SE	S	SSW	S	WSW	W	SW	WNW	SW	NW
Upper	Velocity (m/s)	0.09	0.37	0.55	0.52	0.64	0.81	4.86	0.95	1.03	1.8
	Direction	E	WNW	SSW	SW	ENE	SSE	W	n/a	n/a	n/a

6.2.1 80 km/h Tests

Airflow velocity and direction were recorded for each of the sensor heights (lower, middle and upper) as outlined in Chapter 5.2 and illustrated in Figure 4.3-6. At each height, airflow data were recorded at each of the 12 sensor locations shown in Figure 4.4.2-1. Wind direction and velocity data graphs of sensor placement 2 for all 10 window configurations are shown in Figures 6.1.3.1-8 and are discussed below. The remaining sensor placement graphs can be found in the Appendices. In all the airflow direction and velocity graphs in this chapter, the order of data starts with configuration 1 and ends with configuration 10.

Lower sensor level

Figure 6.2.1-1 shows the airflows measured for all the different configurations with the sensors placed at the lower level. Uneven distributions of the three types of airflow were recorded. Distinct airflow occurred least often (configuration 6 & 7) whereas mixed flows were most abundant (configurations 3, 4, 5, 8 & 10) followed by non-distinct flows. A wide range of airflow velocities were measured that, at the same taxi speed, changed not only with sensor position but changed according to the window configuration. In Figure 6.2.1-2 the window configurations 4-10 with more open windows led to increased average velocities throughout the tests, however, single window configuration 3 also resulted in airflow velocity measurements comparable with that of configuration 4.

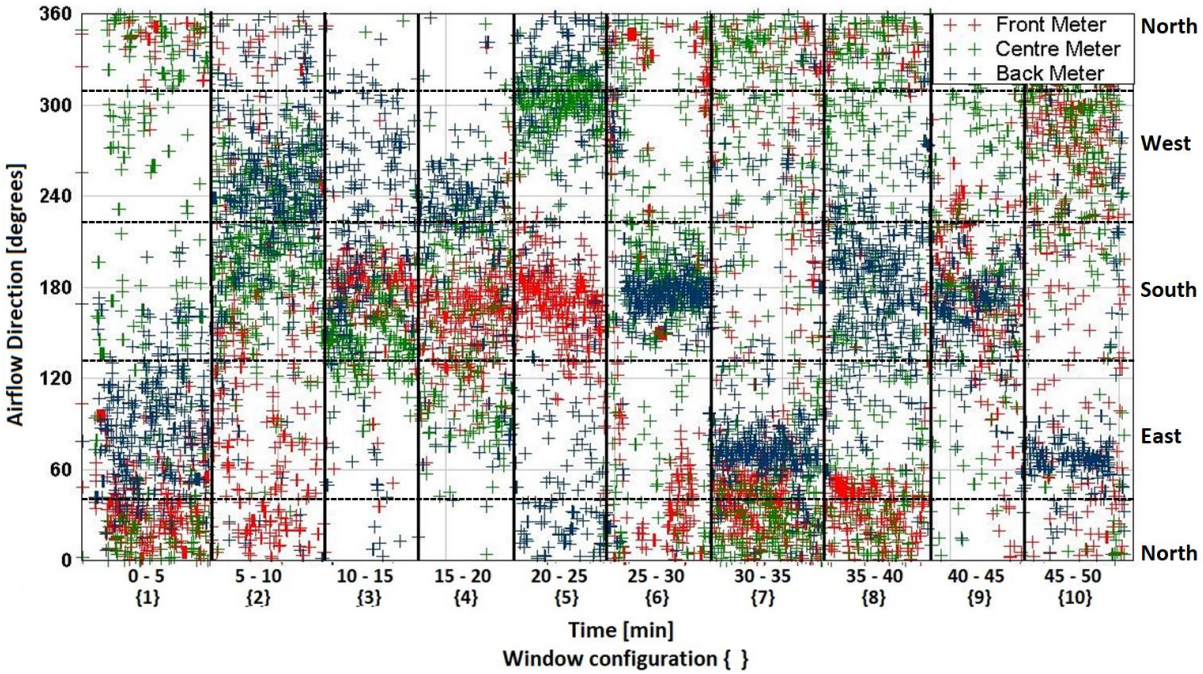

Figure 6.2.1-1 Airflow direction at lower sensor level for sensor placement 2

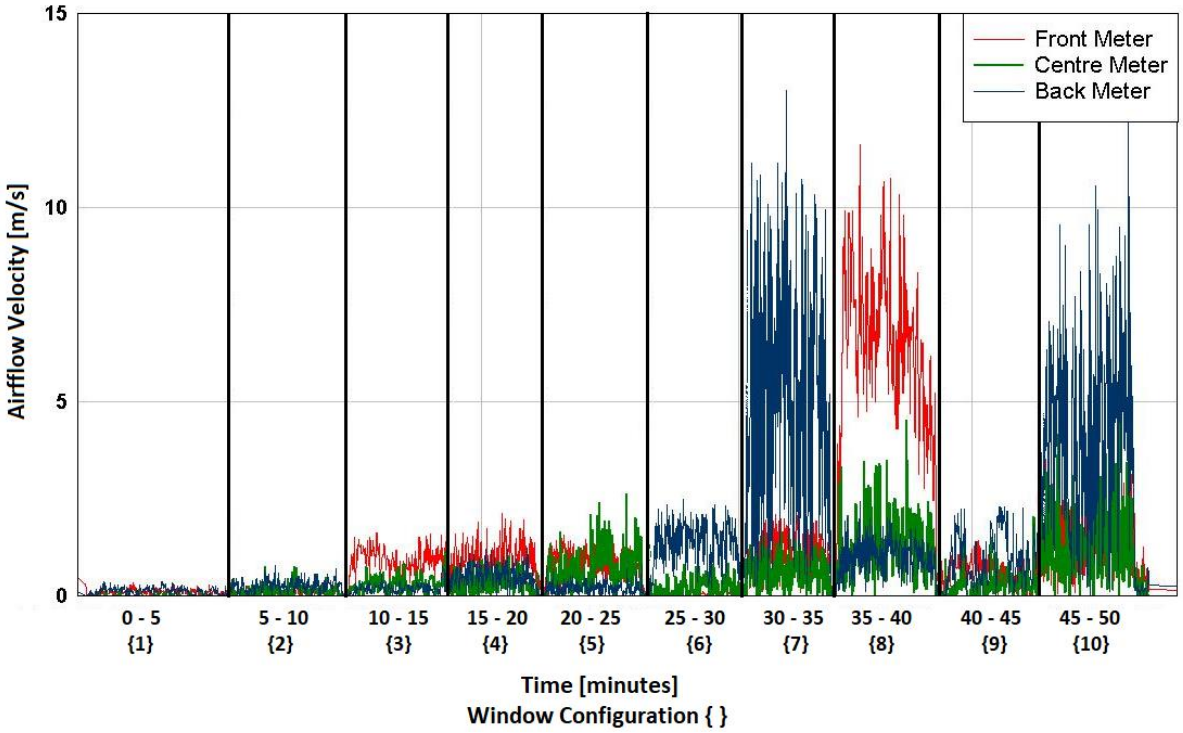

Figure 6.2.1-2 Airflow velocity at lower sensor level for sensor placement 2

Middle sensor level

Frequent fluctuating airflows were recorded at this level with a balance of indistinct and distinct airflows. In Figure 6.2.1-3 configuration 9 shows entirely indistinct airflows in all the sensors, whereas configuration 8 has a mixture of distinct in the front and middle sensors and fluctuating airflow in the back sensor. Figure 6.2.1-4 shows that higher airflow velocities occurred at this level, but echoed the patterns seen in the lower level measurements where peak average velocities occurred in configuration with more opened windows. It was noted that configuration 3 with a single open window resulted in greater airflow velocities than those in configurations 5,6 & 9 with multiple open windows.

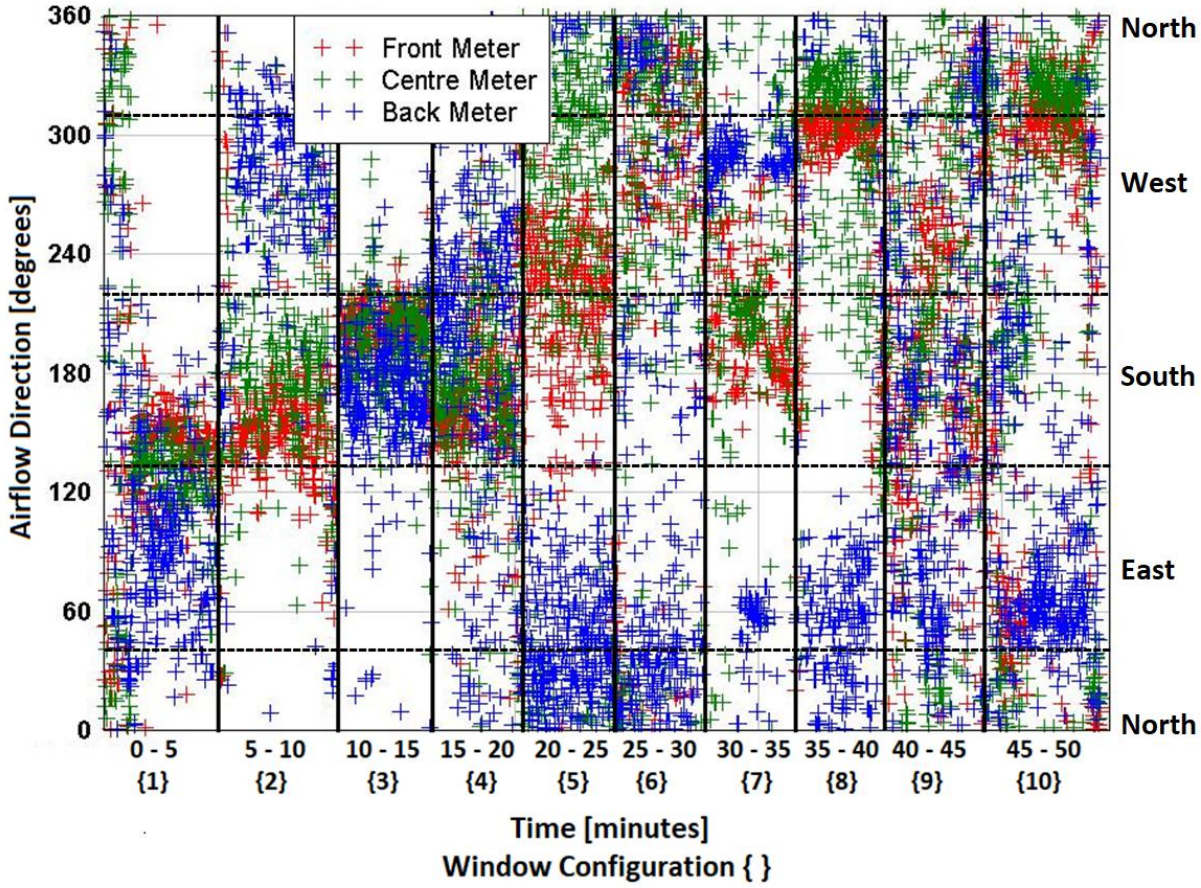

Figure 6.2.1-3 Airflow direction at middle sensor level for sensor placement 2

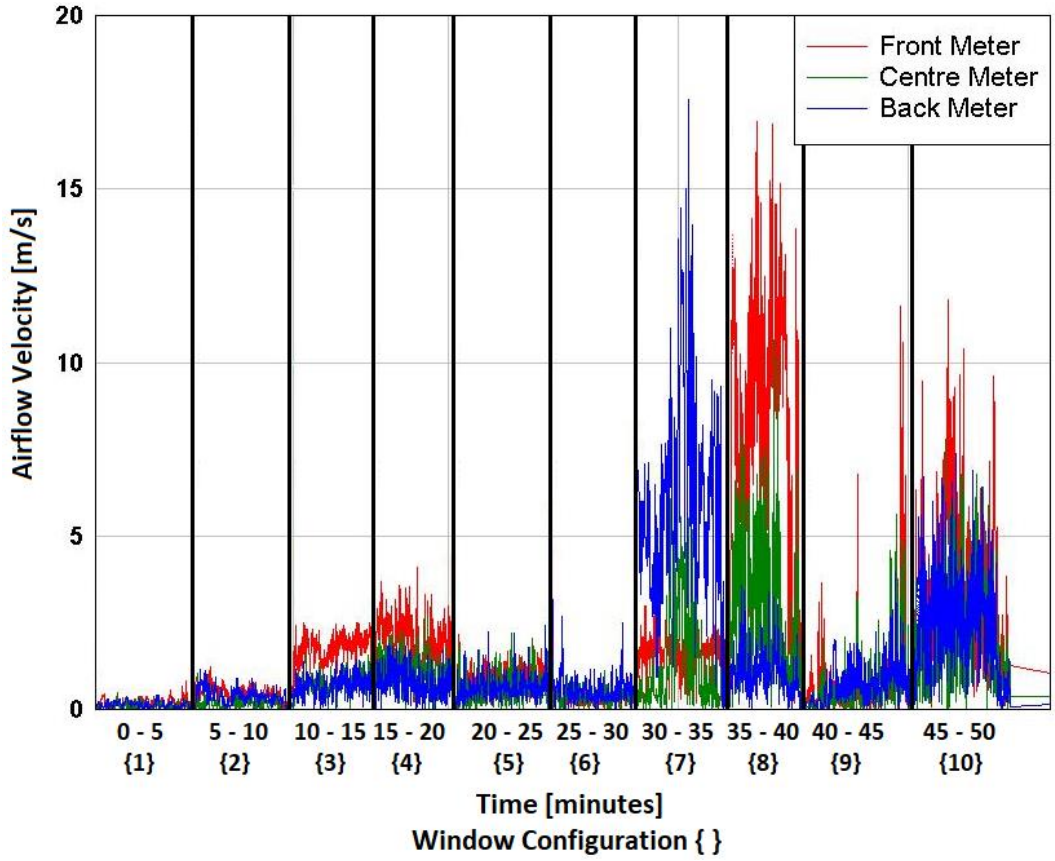

Figure 6.2.1-4 Airflow velocity at middle sensor level for sensor placement 2

Upper sensor level

The airflow patterns at the top level were similar to those in the middle level especially in configurations 3,4 & 10. Instances of all 3 airflow types can be seen in Figure 6.2.1-5. The airflow velocities at the upper level mirrored the values seen in the bottom and middle level tests. Configurations 7, 8 and 10 consistently resulted in the highest average wind velocities.

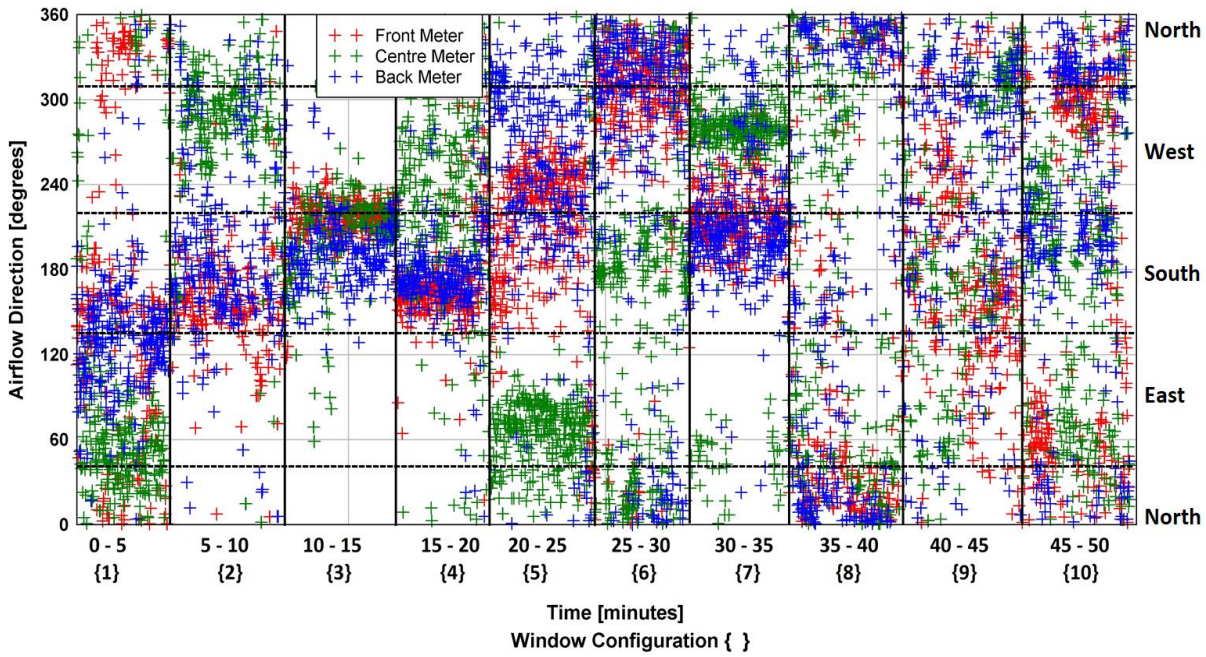

Figure 6.2.1-5 Airflow direction at upper sensor level for sensor placement 2

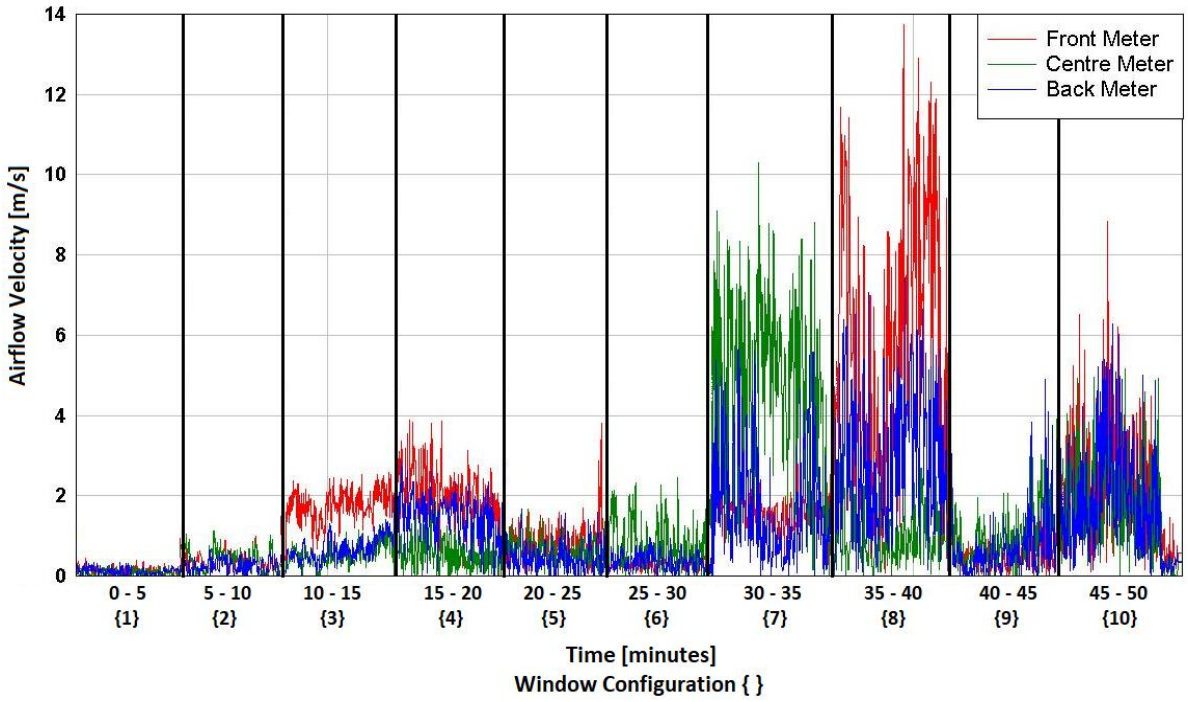

Figure 6.2.1-6 Airflow velocity at upper sensor level for sensor placement 2

Recurring airflow patterns and velocity distributions were observed at all the varying measurement heights. It was noted that increasing the open windows did not always result in increased airflow velocities but could lead to indistinct airflows instead as was seen for configuration 9.

6.2.2 100 km/h Tests

The 100 km/h test was only conducted at the lower level. It was noted that for half the configurations at 100 km/h the average airflow velocity could reach more than double those seen in the 80 km/h

tests, as shown in the peak velocities in Figure 6.2.2-2, yet the remaining configurations showed similar airflow velocities. As observed in the 80 km/h tests, the average airflow velocity generally increased when more windows were opened. The 100 km/h airflow types measured were primarily mixed and more instances of distinct airflows occurred than indistinct for all the sensor configurations. In Figure 6.2.2-2 distinct airflow can be seen in configurations 8, 9 & 10 for the front and back sensors, while the centre sensors recorded fluctuating and indistinct flows.

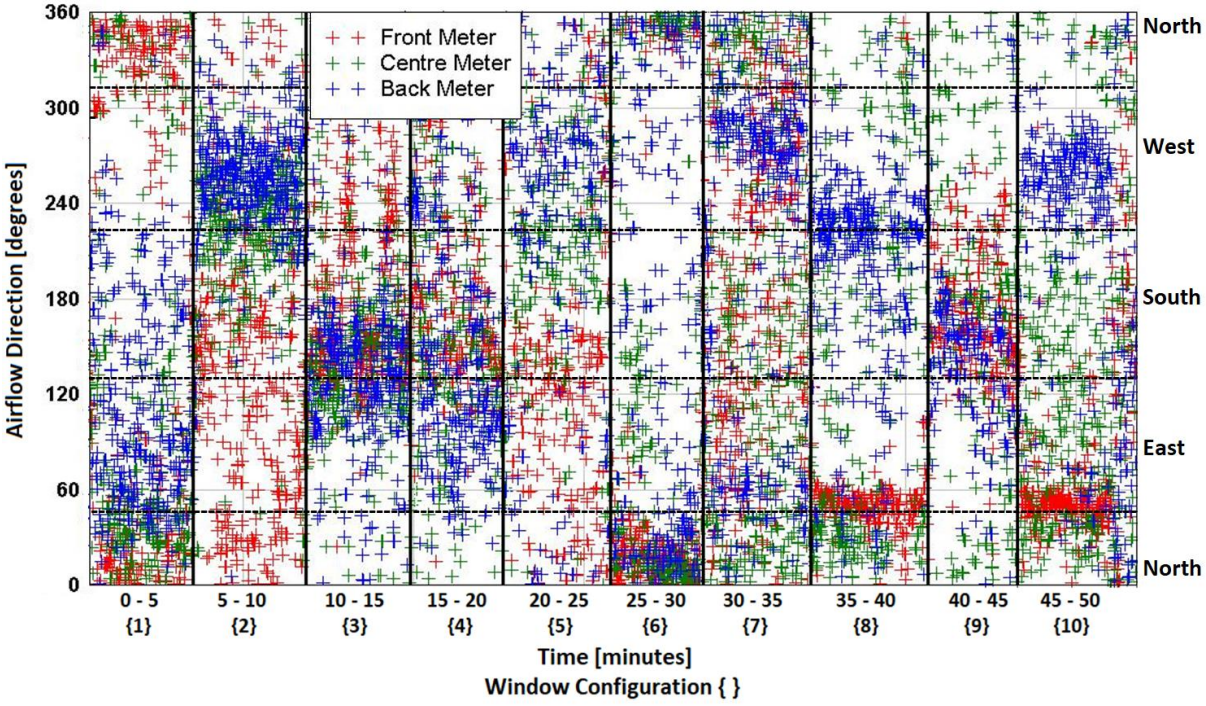

Figure 6.2.2-1 Airflow direction at lower sensor level for sensor placement 2

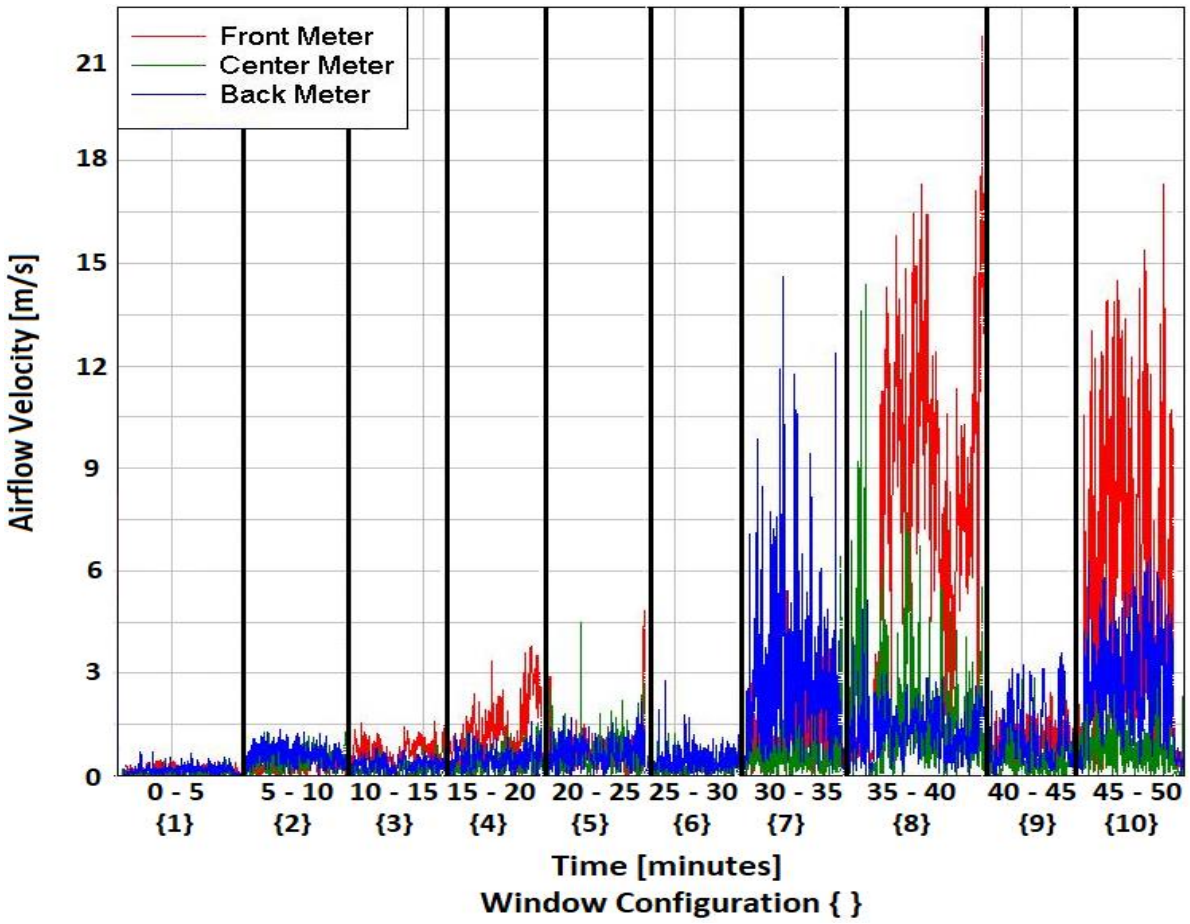

Figure 6.2.2-2 Airflow velocity at lower sensor level for sensor placement 2

6.3 Stationary Concentration Decay and Ventilation Rates

Data collected in a stationary taxi tests (Chapter 5.3.2) were used to produce CO_2 concentration decay curves along with the natural logarithm curves of the CO_2 shown in Figure 6.3-1, 2 & 3. The straight-line slope of the natural log (ln) curve was used to calculate the ventilation rate in the taxi using Equation 2.5.1-1. The initial concentration decay shown for configuration 0 was with all known openings in the taxi (doors, windows and air vents) closed. The decay is attributed to leakage and natural diffusion of air through minor openings in the taxi. The baseline concentration of 500ppm was not reached within 2 hours and the test was suspended.

The slopes of concentration decay curves of configurations 1-10 became steeper with increased window openings. In each of the curves below, the peak to stable minimum values of the CO_2 decay are shown.

Figure 6.3-1 shows the concentration decay curve when all windows were closed. The decay was steady and took over 2 hours to reach the stable minimum value

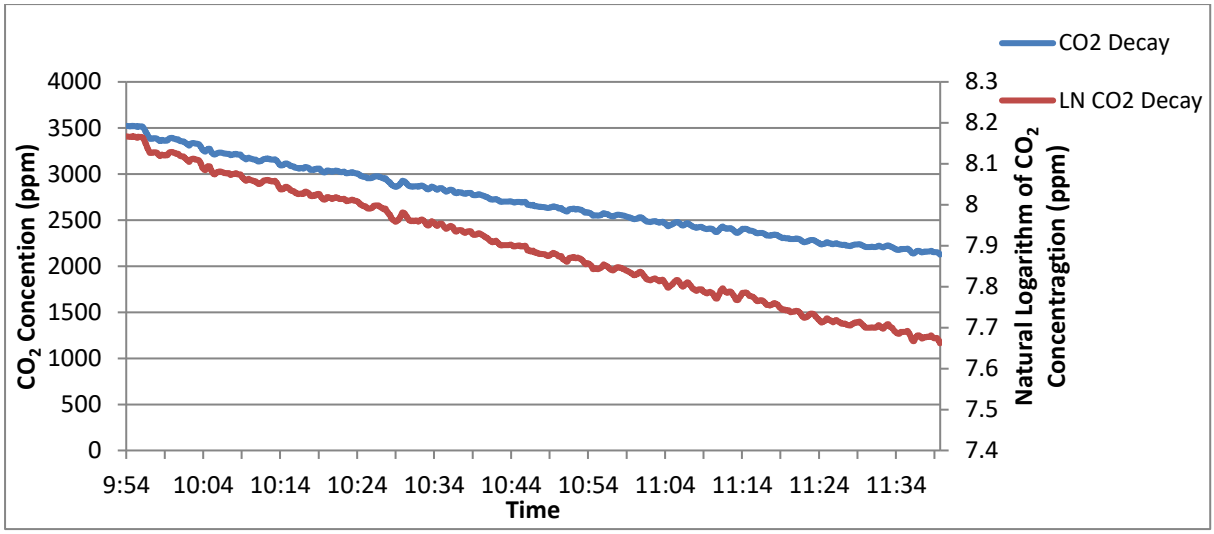

Figure 6.3-1 Static CO_2 decay configuration 0

Figure 6.3-2 shows the combined concentration decay curves of configurations 1,2 and 3. Appendix 1 shows the remaining concentration decay curves for configurations 4-10. In Figure 6.3-2 the slopes of configurations 1 and 3 are both steeper than that of configuration 2, indicating that there are differences in ventilation in single open window configurations. For configurations 4- 10, the concentration decay curves became steeper as more windows were opened. This indicated that the average ventilation rate was increasing as the number of open windows increased.

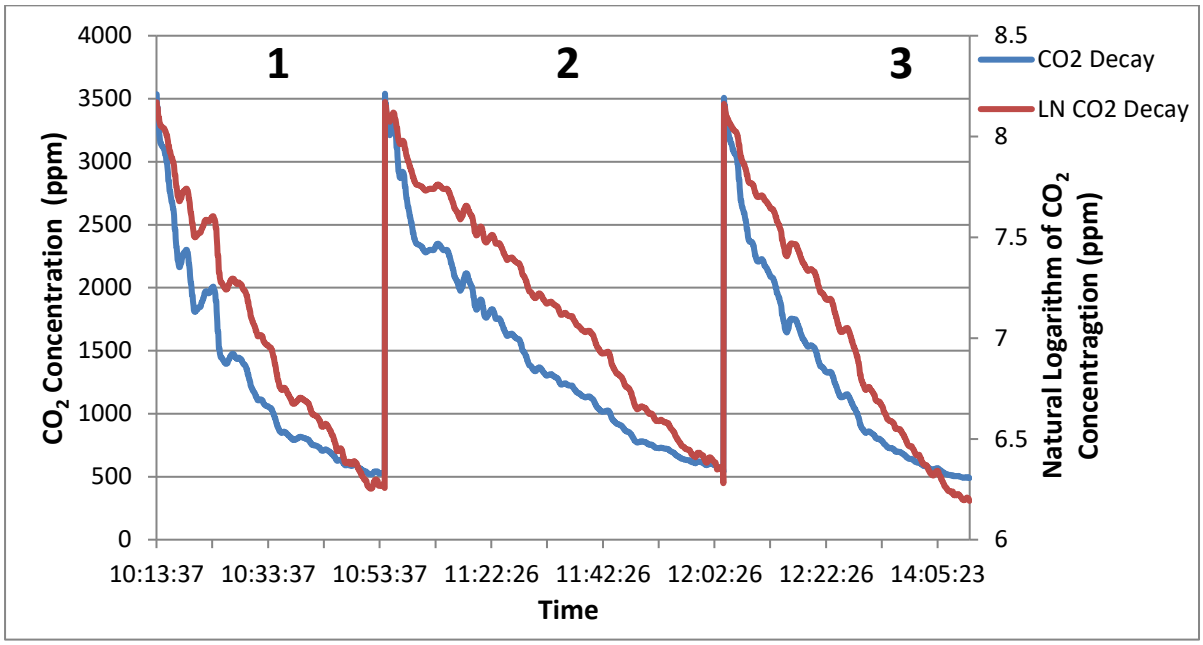

Figure 6.3-2 Static CO_2 peak to minimum decay of configurations 1-3

6.3.1 Ventilation Flow Rates

Measurements were taken of the CO_2 in an unoccupied taxi to assess base level ventilation rates for the varying window configurations chosen for the main experiments. Table 6.3.1-1 shows the ventilation data collected over 5 test days in a stationary taxi. With all windows and doors closed, configuration 0, the ventilation rate was 1.27 L/s. Single-side window configurations 1-3 shown in the table led to ventilation rates below 12 L/s. Double-sided window configurations 4-7 had ventilation rates that were almost double that of the single-sided configurations. With the highest number of windows open, configurations 7-10 resulted in the highest ventilation rates in the stationery taxi, 41-70 L/s, approaching and exceeding levels required in general wards in healthcare facilities of 60 L/s (Chapter 2.3.1). In was noted however that window configuration 10 with all 6 windows opened resulted in lower ventilation rates than those produced by configuration 9.

Table 6.3.1-1 Average stationary ventilation rates (L/s)

Configuration	Ventilation Rate (L/s)
0	1.27
1	10.50
2	4.23
3	7.86
4	14.80
5	24.37
6	21.45
7	45.27
8	44.96
9	61.28
10	57.26

6.4 Mobile Ventilation Rates

Mobile ventilation data were recorded for window configurations 4-9 in a fully occupied taxi over 7 days. Configurations 4 – 9 were chosen as they could be configured within the 1-hour testing period described in Chapter 5.3.3 and were most likely to provide the greatest range of ventilation rates. The temperature recordings taken during the mobile tests can be found in Appendix 1, these show temperature drops of up to 4°C resulting from opening windows when the taxi was at speed. The CO_2 concentration decay data were collected and processed (using Equation 2.5.1-1) into the ventilation flow rate results shown in Table 6.4-1. The table also shows the average speeds achieved by the taxi during the ventilation tests. The 40 km/h and 80 km/h tests were within 10% of the set speed, however, the 100 km achieved an average below 90 km/h. For all following ventilation flow rate information, the units used were L/s.

Table 6.4-1 Average mobile ventilation rates at average achieved speeds (L/s)

Configuration	Set speed (average speed) and average ventilation rate at each configuration		
	40 km/h (39.2 km/h)	80 km/h (75.6 km/h)	100kph (88.6 km/h)
4	61.58	106.93	108.46
5	34.85	43.24	50.72
6	44.39	43.42	41.16
7	218.36	227.74	286.41
8	131.62	191.75	255.66
9	49.68	110.83	115.33

As observed in the stationary ventilation tests, a general trend emerged that as the number of windows opened increased, the average ventilation rate increased as well. It was expected that as the number of window openings increased, as is the case with the transition from the two open window configurations 4, 5 & 6 to the four open window configurations 7, 8 & 9, the ventilation would also increase, but the collected data suggested otherwise. On average, configurations 4, 7 & 8 achieved the highest ventilation flow rates. In Section 6.2.1 the configurations 4, 7 & 8 were noted as producing the highest airflow velocities; the ventilation rates results closely matched the airflow velocity patterns.

The ventilation rates varied with changes in open window configurations as shown in Figure 6.4-1. Among two-open-window configurations 4, 5 & 6, configuration 4 alone resulted in nearly double the ventilation rates seen in both configurations 5 and 6 at all test speeds. Configurations 5 & 6 produced similar ventilation rates at all speeds. For four-open-window configurations 7, 8 & 9, configuration 7 resulted in nearly double the rates produced by configuration 9 at all speeds. In each individual configuration, apart from configuration 6, as the speed increased, the average ventilation rate increased. Configuration 4 with 2 open windows, resulted in ventilation rates like those of configuration 9 (with 4 windows open) implying that the ventilation flow rates could depend as much on interior flow resulting from window configuration as on numbers of open windows. Configurations 7 & 8 produced the highest ventilation rates ranging from 108 to 316 L/s, far exceeding the WHO recommendation for new healthcare facilities and airborne precaution rooms (Chapter 2.3.1).

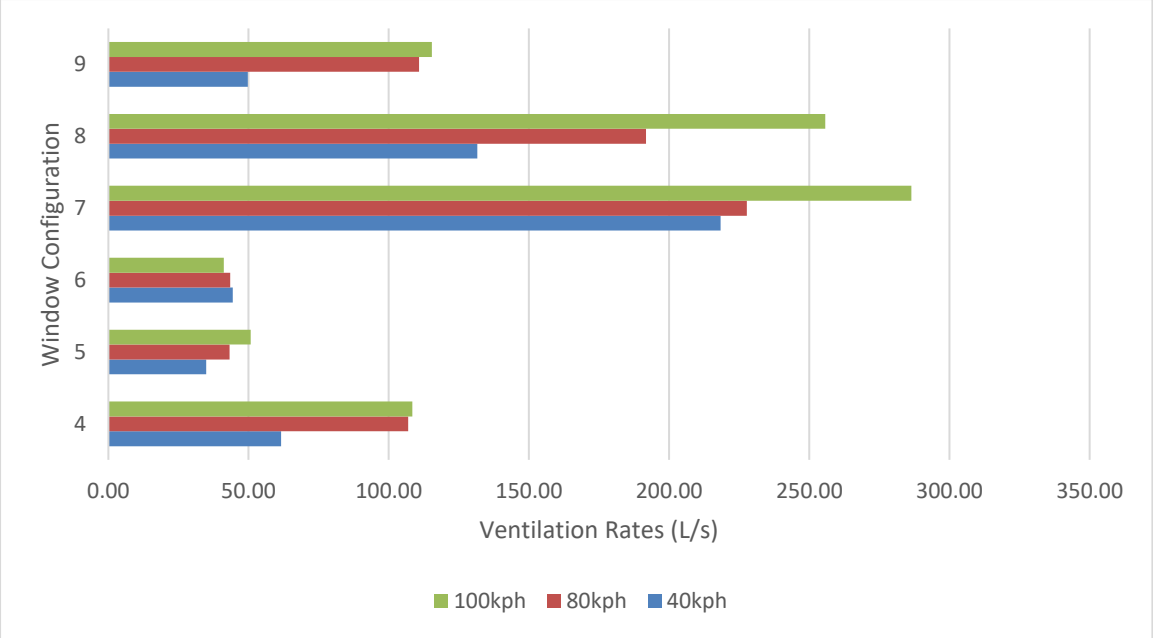

Figure 6.4-1 Effect of taxi speed on average ventilation rates at different window configurations

6.4.1 Ventilation Flow Rate Performance

In Chapter 2.3.1, ventilation rates for different kinds of healthcare facilities were discussed, ranging from general wards to airborne disease prevention rooms. The per person ventilation rates recommended in healthcare facilities are compared to the taxi interior ventilation rates achieved during the test periods in Table 6.4.1-1 where '<', '=' and '>' represent values below, matching and exceeding recommendations respectively.

Table 6.4.1-1 Performance of window configurations against healthcare guidelines; '<', '=' and '>' represent values below, matching and exceeding WHO recommendations respectively

		40 km/h				80 km/h				100 km/h			
		Configurations				Configurations				Configurations			
		4	7	8	9	4	7	8	9	4	7	8	9
Recommended rates (L/s)	General wards and outpatient departments (60)	=	>	>	<	>	>	>	>	>	>	>	>
	New health-care facilities (80)	<	>	>	<	>	>	>	>	>	>	>	>
	Airborne disease precaution rooms (160)	<	>	<	<	<	>	>	<	<	>	>	<

Configuration 4 produced ventilation rates that matched and exceeded ventilation rates suggested for general wards and outpatient departments (60L/s) at all three test speeds whereas configuration 9

produced results similar to configuration 4 at 80 km/h and 100 km/h. Configuration 7 matched and exceeded the ventilation rates suggested for new airborne infections prevention rooms (160L/s) at all three test speeds with a minimum ventilation rate of 218 L/s measured at 40 km/h. Configuration 8 similarly exceeded recommended ventilation rates with 190L/s at 80 km/h and 255L/s at 100km/h, whilst also exceeding the new healthcare facility ventilation rate (80L/s) at 40 km/h with a ventilation rate over 130L/s. Configurations 7 and 8 would be the recommended for minibus taxis to provide high ventilation rates at the tested speeds.

6.5 Linear Regression Model

A linear regression model was fit to the data set to examine how well the ventilation rate can be estimated in response to changing taxi speed and window configurations and to examine the relationship between these variables. A detailed explanation of the model and its parameters are provided in

Appendix 3. The model fit was assessed using residual plots depicting the differences between observed responses and model fitted responses using dependent scaling factors.

6.5.1 Fitted Model

The model-fitted mean ventilation values with estimation bands are shown in Figure 6.5.1-1 below, together with the data points. The window configuration groups are shown by the different plotting markers and colours. The light dashed line for each configuration group shows empirical means; and the bolder solid line shows the model-fitted means. The bands capture 95% confidence intervals (CI) for the mean ventilation value for different combinations of speed and configuration group.

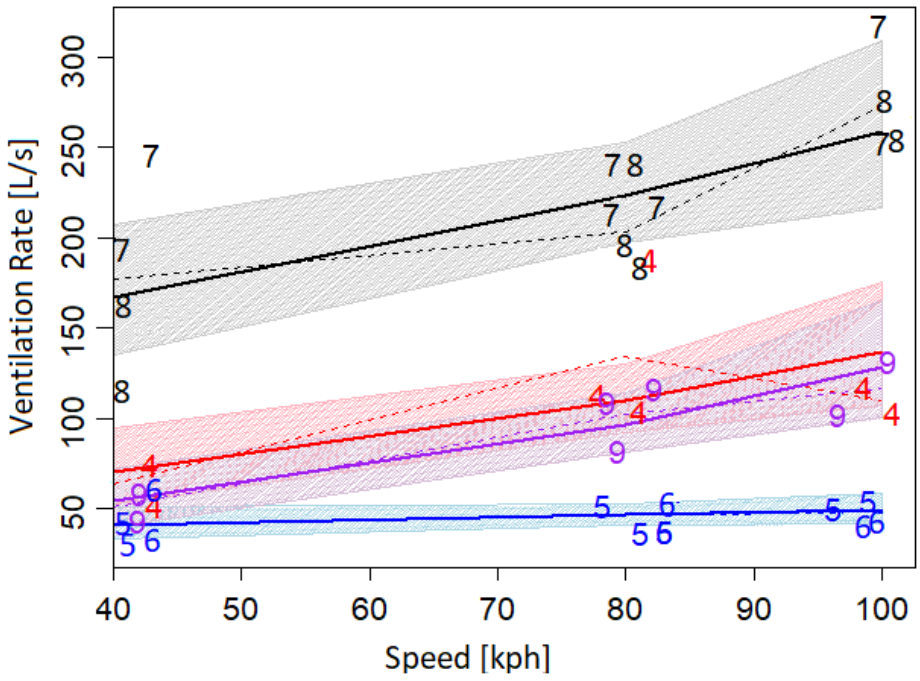

Figure 6.5.1-1 Model-fitted mean ventilation values

The ventilation rate model and data follow each other closely, however a single outlying point for configuration 4 is seen at 80 km/h in Figure 6.5.1-1. The ventilation model-fitted and empirical means of configurations 5 & 6 rise at a slower rate, evidenced by the less steep slope, while the model-fitted means of the remaining configurations closely resemble each other with comparatively steeper slopes. The ventilation rates in configurations 4, 7, 8 & 9 increased steadily with increasing taxi speed. The effect of configuration on ventilation at a speed of 40km/h, and the effect of speed on ventilation per given configuration is shown below in Table 6.5.1-1. Using configuration 4 as the comparative base, a mean multiplicative increase was seen only in the ventilation rate estimate for configurations 7 & 8. The changes for remaining configurations 5, 6 & 9 were fractional except for configuration 9 In the upper limit CI.

Table 6.5.1-1 Effect of configuration on ventilation rates at 40 km/h

		Ventilation Rate Estimate	95% CI lower limit	95% CI upper limit
Reference: Mean response for Configuration 4.		69.53	50.76	93.13
Mean multiplicative change in response when moving to another configuration group	Configurations 5&6	0.62	0.42	0.88
	Configurations 7&8	2.59	1.76	3.69
	Configuration 9	0.82	0.52	1.25

The effect of speed on the ventilation is shown in Table 6.5.1-2, where when the taxi speed is increased by 20 km/h from a starting speed of 40 km/h, the estimated change in ventilation rate is given for each specific configuration group. Configuration 9 and 4 have the highest mean multiplicative responses to increased speed.

Table 6.5.1-2 Effect of speed on ventilation

		Estimate	95% CI lower limit	95% CI upper limit
Mean multiplicative change in ventilation when speed increases by 20 km/h, for a specified configuration group.	Configuration 4	1.32	1.14	1.53
	Configurations 5&6	1.12	1.01	1.25
	Configurations 7&8	1.22	1.1	1.36
	Configuration 9	1.42	1.22	1.64

6.6 Transmission Risk Analysis

The transmission of airborne diseases in a closed environment is closely related to the number of occupants and the concentration of contaminants in the air likely to be breathed in. As the number of occupants in the taxi increases, rebreathed fraction of air within a taxi interior increases. This also increases the chances that the contagions in the air are breathed in by the occupants. CO^2 is used as a marker to estimate the fraction of air that is rebreathed. Ventilation replaces the old (rebreathed air) with clean (external) air and thus reduces the rebreathed air and airborne contagions.

In this section both the CO_2 decay and the ventilation rate data shown previously in Chapter 6.4 were used to illustrate the TB transmission probability against the key parameters (ventilation rate, passenger occupancy and number of infectious people) shown in the Issarow Equation 2.5.2-4.

As the number of infectious individuals in a taxi increase, the expected result is a substantial increase in the risk of transmission of TB due to the increase in airborne TB in the environment. Figure 6.6-1 shows this effect at a set ventilation rate of 20 L/s, where *I = 0* denotes the absence of TB transmission risk when there are no infectious passengers.

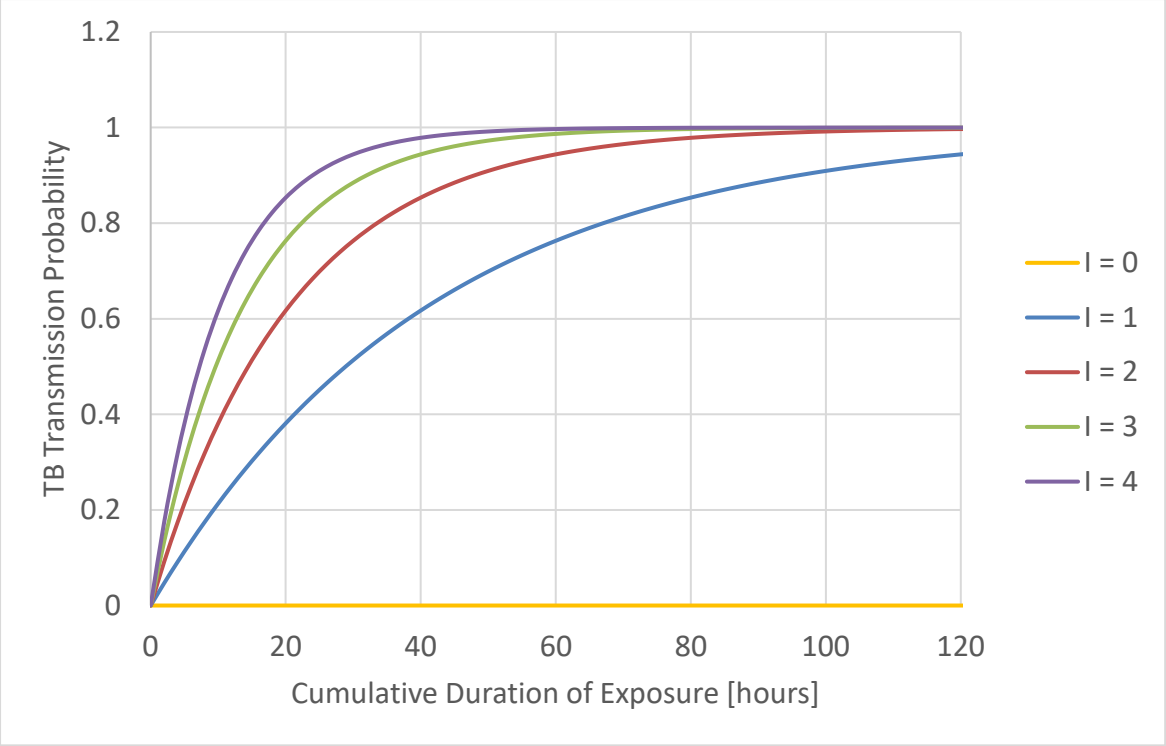

Figure 6.6-1 Effect of number of infectious individuals (*I*) on TB transmission probability for ventilation rate *Q = 20* L/s

In Figure 6.6-2 and Figure 6.6-3 the effect of ventilation on TB transmission probability is shown. The transmission probability is substantially reduced as the ventilation is increased as seen in Figure 6.6-2 where at 20 hours of exposure to a single infectious passenger, the risk of transmission drops from 0.85 to 0.62 when the ventilation rate is raised from 10 L/s to 20 L/s.

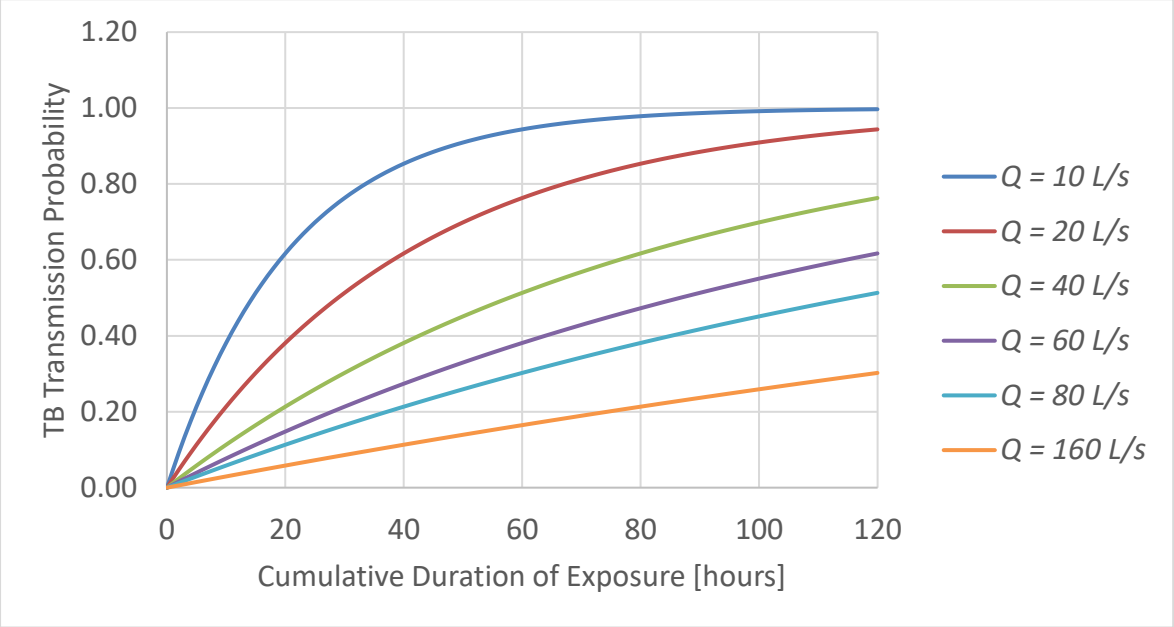

Figure 6.6-2 Effect of ventilation rate (*Q*) on TB transmission probability TB for one infected individual (*I = 1*)

In Figure 6.6-3 the effect of continuously increasing the ventilation rate becomes less pronounced, by 160 L/s (the recommended level in airborne disease precaution rooms as indicated in Chapter 2.3.1) the probability of transmission is below 0.012 when 4 infectors are within the taxi. Conversely as the ventilation rate decreases below 50 L/s the transmission probability rises exponentially even within the 1-hour exposure to any infectious occupant (passengers and drivers included).

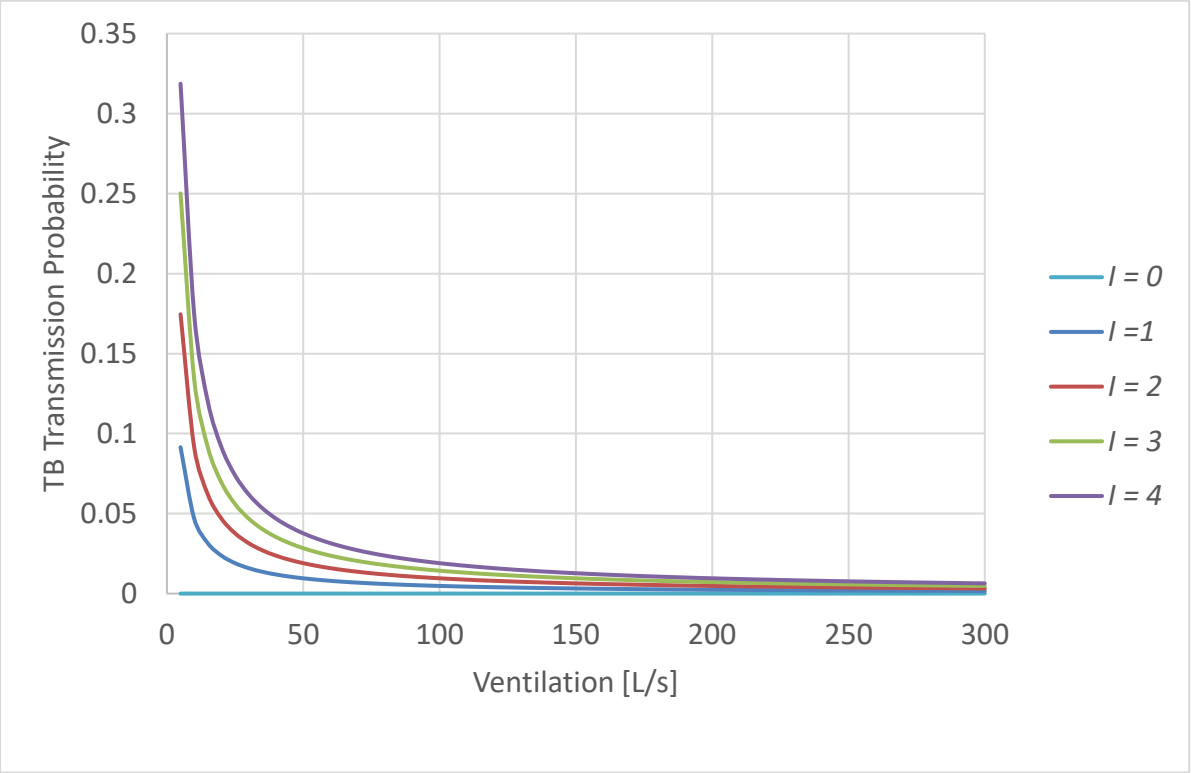

Figure 6.6-3 Effect of ventilation rate and number of infectious individuals (*I*) on TB transmission probability for 1 hour exposure

In Figure 6.6-4 with a set ventilation rate of 20 L/s, 'n' represents the total occupancy within the taxi. As the occupancy increases the average volume of rebreathed air increases and in the presence of an infectious occupant '*I=1*' the probability of TB transmission rises from 0.26 to 0.45 when the occupancy increases from 4 to 8 individuals. Figure 6.6-4 shows that for normal operating conditions in a taxi, where the occupancy is at capacity (as was discussed in Chapter 3.2.2), the probability of transmission is substantially higher than for 8 occupants.

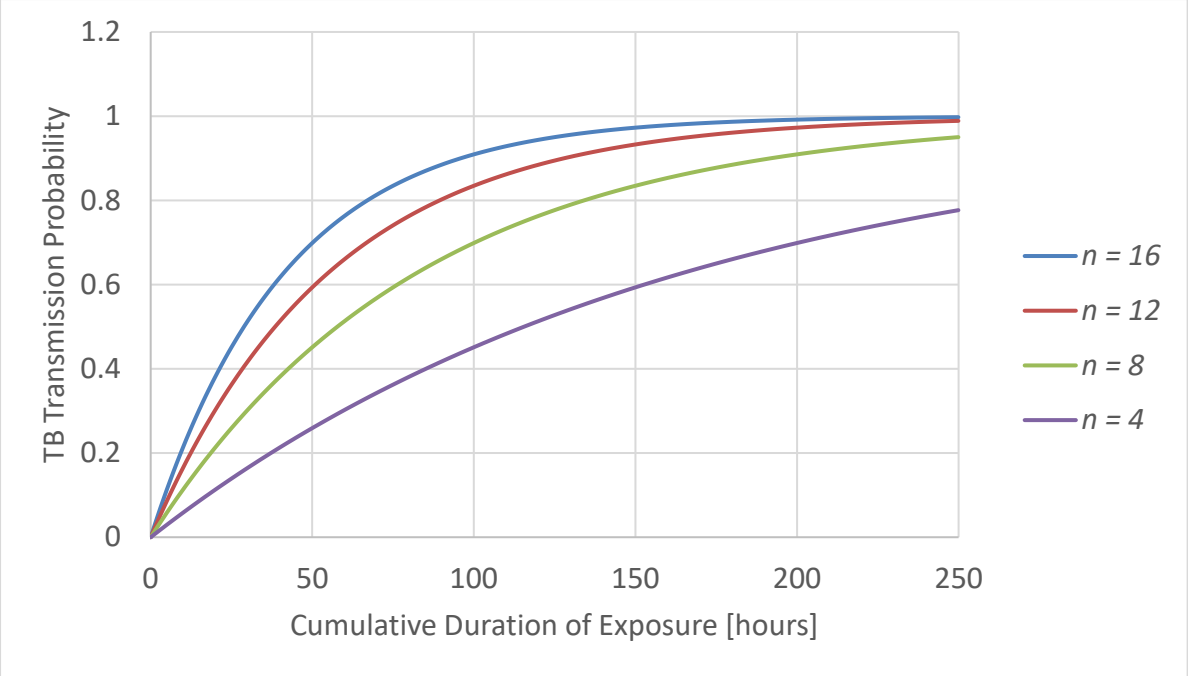

Figure 6.6-4 Effect of passenger occupancy on transmission probability for one infectious individual (*I = 1*) and ventilation rate *Q = 20* L/s

6.7 Summary

This chapter has shown the results of the three main experiments, namely i) the airflow visualisation, ii) the airflow pattern, iii) the ventilation rate assessment with added analyses on the ventilation rate through a linear regression model and the transmission risk using a dose-response probabilistic model.

Airflow patterns were visualised in the taxi at different speeds for all 10 window configurations. Configurations 4, 7, and 8 produced the most instances of distinct airflows, whilst configurations 3, 9 and 10 displayed more mixed flows than distinct flows. Visualisation tests produced results comparable to those seen in the bus study (Kale, et al., 2007). The bus study was limited to a single configuration with all windows opened and displayed complex flows, whereas in this study 10 configurations were used resulted in repeated instances of distinct, mixed and indistinct airflows.

Airflow was then characterised by measuring both velocity and direction at 36 points in the breathing zone of the passenger cabin. Patterns of airflow direction were noted for several configurations at different measurement heights, where distinct airflow directions were shown in Figure 6.2.1-1, Figure 6.2.1-3, Figure 6.2.1-5 and Figure 6.2.2-1. Patterns were revealed in the airflow velocities where configurations 3 & 4, 7 & 8 and 10 produced the highest averages throughout the tests as shown in Figure 6.2.1-2, Figure 6.2.1-4, Figure 6.2.1-6 and Figure 6.2.2-2 These results resembled those shown

in the airflow visualisation where the same configurations resulted in full smoke clearance during the test periods.

In the ventilation tests configurations 4, 7 & 8 produced the highest ventilation rates which matched the airflow characterisation results. Ventilation rates exceeding healthcare facility guidelines were recorded in configurations 4, 7, 8 & 9, whilst configurations 5 & 6 resulted in much lower ventilation rates as shown in Table 6.4-1. In the Johnstone-Robertson study on TB transmission reviewed in Chapter 2.6.1 (2012), 4 ventilation scenarios with three 3 window configurations were explored and produced ventilation rates ranging from 1.31 L/s and 25.09 L/s. These ventilation rates were produced in a stationary taxi. In the present study however, for all ventilation rates produced, multiple window configurations and taxi speeds were used.

As the taxi speeds were increased from 40 km/h to 100 km/h, a trend of increasing ventilation rate was shown in the linear regression model Figure 6.5.1-1. The effect of increasing ventilation was also shown to reduce the probability of transmission in Figure 6.6-2, however above a certain threshold the returns were diminishing as shown in Figure 6.6-3 where beyond 160 L/s the transmission risk was below 0.01 for multiple infectious occupants. This reduced effect on infection risk of increasing ventilation at high rates agrees with the logarithm-curve relationship stated in the ventilation study by (Nardell , et al., 1991).

The results have shown that in a fully occupied taxi, configurations 4, 7, 8 and 10 are optimal for producing ventilation rates that match and surpass the recommended guidelines in healthcare facilities. Configurations 9 could also produce ventilation rates similar to configuration 4 at the higher tested taxi speeds. The single open window configuration 3 produced airflow velocities like configuration 9 in the airflow pattern tests and could potentially result in similar ventilation rates (configuration 3 was not tested in the ventilation tests). At low taxi speeds, configuration 7 would produce the highest ventilation rates and result in the largest reduction of transmission risk, whilst at higher taxi speeds, configurations 8 and 10 would similarly result in substantially reduced transmission risk in the taxi.

Transmission models used in the studies (Johnstone-Robertson, 2012) (Hella, et al., 2017) were based on the Wells-Riley equation using the quanta of infection assuming stable interior conditions. In this study, the dose-response model (Issarow, et al., 2015) (accommodating the non-steady state conditions in a taxi) was used and achieved similar results to (Johnstone-Robertson, 2012) (Hella, et

al., 2017) showing that with increased airborne contagions (due to combinations of infectious people, low ventilation or high occupancy) the risk posed to susceptible individuals would be high with cumulative exposure.

7 CONCLUSION

In this study, experiments on airflow visualisation, airflow velocity and direction, ventilation rates and transmission probability risks in minibus taxi were carried out to augment the limited data available on the role taxis play as a contributor to the TB epidemic in South Africa. Compared to the Johnstone (2012) study reviewed in Chapter 2.6, this study included airflow visualisation and pattern tests in the methodology. This study expanded on the examination of ventilation rates in a minibus taxi by using more window configurations and testing the ventilation in both stationary unoccupied and mobile occupied taxis. This study used a different numerical model to estimate the risk of transmission in minibus taxis, and a wider range of parameters contributing to the risk of transmission were explored than noted in other studies (Johnstone-Robertson, 2012) (Andrews, et al., 2013) (Hella, et al., 2017). The conclusions made in this chapter are based on the specific conditions used in the study.

To the author's knowledge, this study shows the first use of ultrasonic anemometers in a moving minibus taxi for experimental airflow pattern characterisation. Studies in the literature performed similar airflow pattern tests only on scale models, fixed cabins with air distributors and CFD models (Kale, et al., 2007) (Zhang, et al., 2009). This study used a unique combination of sensors to simulate conditions seen in normal operating taxis. To the author's knowledge, this is also the first study to use the Issarow equation (2015) to perform transmission risk analysis in minibus taxis.

The study found the following:

i) Patterns exist in the passenger occupancy rates in operating taxis. Observable passenger behaviours create conditions within minibus taxis that can be simulated in experiments.

ii) Distinct airflows are created by different window configurations. Window configuration-specific airflow patterns can be created. These patterns are near-consistent at different heights within the breathing zone and at different taxi speeds. Ventilation rates are dependent on both taxi speed and window configuration, and not simply the number of open windows.

iii) The effect of ventilation in an occupied taxi on the risk of TB cross-infection was verified using a numerical transmission model. Ventilation rates produced by specific window configurations at the three test speeds were shown to meet guideline recommendations and reduce the risk of TB transmission.

Despite the ventilation capabilities achieved in the study, passengers might not tolerate the fully open window configurations whilst travelling at speed, due to the discomfort caused by temperature changes (Taylor, et al., 2016), or during inclement weather (rain and/or cold). Given that taxis are often congested or overloaded during peak hour commuting journeys (Statistics South Africa, 2014), the potential role of implementing AIC device measures such as ultraviolet germicidal irradiation (UVGI) devices, filtration devices or mechanical ventilation to address the suboptimal ventilation scenarios must be considered.

7.1 Limitations

Limitations of this study are:

i) A single taxi model was used to perform the tests and any conclusions drawn relate mainly to that model.

ii) External parameters such as temperature and wind velocity were not accounted for, and these could have had a large impact on the interior airflows recorded in the taxi. For example, high velocity winds on a test day could alter the expected ventilation rates from single window configurations, resulting in high average velocities and changed airflow patterns.

iii) The routes used during experiments were altered according to traffic conditions to maintain the set taxi speeds. These route changes could have affected the repeatability of the tests given that changing the taxi orientation could create anomalous data.

iv) Measurements of inflow air velocities at the windows were not taken as the necessary equipment was not available; these would give a clearer indication of the overall interior airflow.

v) CO_2 concentration decay experiments were not carried out for all 10 window configurations, therefore conclusions made in this study lack the full spectrum of ventilation rates achievable in the taxi. These could however be included in future work.

vi) This study did not consider the effects of passenger movement within the taxi as a factor in spreading airborne contaminants. It also did not consider the effect of door opening on ventilation rate within the taxi.

vii) The transmission risk simulated in this study did not consider the risk for individuals in their specific seating positions within the taxi, either based on proximity to infectious individuals or due to exposure to particles facilitated by airflow patterns.

viii) This study did not consider the effect of comfort levels (affected by noise, contact air velocity and temperature changes) in determining whether passengers would continue to use the open window configurations to provide adequate ventilation.

7.2 Recommendations

Further work could be done to augment the study:

i) A full grid of 12 anemometers should be used to give a complete image of airflow patterns at a measurement height.

ii) Closed-window CO_2 decay experiments should be conducted in an occupied taxi. This would emulate the weather conditions discussed in Chapter 3.2.1. Air diffusers in the taxi should be used in closed window conditions to further test the ventilation capabilities of the minibus taxi.

iii) The effects of door opening on providing ventilation when all windows are closed should be investigated as this is a way of applying natural ventilation in closed window scenarios.

iv) Computational fluid dynamics modelling could be used to better simulate transmission risk specific to each individual within the taxi, taking into account the effect of airflows in distributing the infectious particles as well as the positions of susceptible individuals with regard to the infectious spreaders.

REFERENCES

Andrews, J. R., Morrow, C. & Wood, R., 2013. Modeling the Role of Public Transportation in Sustaining Tuberculosis Transmission in South Africa. *American Journal of Epidemiology,* 177(6), pp. 556-561.

ANSYS, 2014. *Computational Fluid Dynamics (CFD) Software.* [Online]
Available at: http://www.ansys.com/Products/Simulation+Technology/Fluid+Dynamics
[Accessed 05 October 2014].

ASHRAE, 2004. *Ventilation for Acceptible Indoor Quality,* 2004: American Society of Heating Refrigerating and Air-Conditioning Engineers.

Atkinson, J., Chartier, Y., Pessoa-Silva, C. L. & Otaiza, F., 2009. Natural Ventilation for Infection Control in Health-Care Settings. In: J. Atkinson, Y. Chartier & C. L. Pessoa-Silva, eds. *WHO Publications/Guidelines.* Geneva: WHO, pp. 7-35.

Benatar, S. R. & Upshur, R., 2010. Tuberculosis and poverty: what could (and should) be done?. *The International Journal of Tuberculosis and Lung Disease,* 14(10), pp. 1215-1221.

Bock, N. et al., 2007. *Tuberculosis Infection Control in the Era of Expanding HIV Care and Treatment: Addendum to WHO Guidelines for the Prevention of Tuberculosis in Health Care Facilities in Resource-Limited Settings,* Geneva: WHO.

Cao, X., Liu, J., Jiang, N. & Chen, Q., 2014. Particle image velocimetry measurement of indoor airflow field: A review of the technologies and applications. *Energy and Buildings,* Volume 69, pp. Pages 367-380.

Cardo, D. et al., 2010. Moving toward Elimination of Healthcare-Associated Infections: A Call to Action. *Infection Control And Hospital Epidemiology,* 31(11), pp. 1101-1105.

CDC, 2005. *Guidelines for Preventing the Transimssion of Mycobacterium Tuberculosis in Health-Care Settings,* Atlanta: MMWR.

Chihota, V. N. et al., 2012. The population structure of multi- and extensively drug-resistant tuberculosis in South Africa. *Journal of Clinical Microbiology,* 50(3), pp. 995-1002.

Cobelens, F. G. et al., 2000. Risk of infection with Mycobacterium tuberculosis in travellers to areas of high tuberculosis endemicity. *The Lancet,* 356(9228), pp. 461-465.

Coker, I. et al., 2007. *Guidelines for the Utilisation of Ultraviolet Germicidal Irradiation (UVGI) Technology in Controlling Transmission of Tuberculosis in Health Care Facilities in South Africa,* s.l.: MRC National Tuberculosis Research Programme/South African Centre for Essential Community Services.

Cox, H. S. et al., 2010. Epidemic levels of drug resistant tuberculosis (MDR and XDR-TB) in a high HIV prevalence setting in Khayelitsha, South Africa.. *PLoS ONE,* 5(11: e13901), pp. 1-8.

Department of Transport, 2003. *Technical Report: The First South African National Household Travel Survey,* Pretoria: Department of Transport.

Dharmadhikari, A. S. et al., 2012. Surgical Face Masks Worn by Patients with Multidrug-Resistant Tuberculosis: Impact on Infectivity of Air on a Hospital Ward. *American Journal of Respiratory and Critical Care Medicine,* 185(10), pp. 1104-1109.

Eames, I., Shoaib, D., Kletter, C. A. & Taban, V., 2009. Movement of airborne contaminants in a hospital isolation room. *Journal of the Royal Society Interface,* Volume 6, p. S757–S766.

Gammaitoni, L. & Nucci, M. C., 1997. Using a Mathematical Model to Evaluate the Efficacy of TB Control Measures. *Emerging Infectious Diseases,* 3(3).

Golden, M. P. & Vikram, H. R., 2005. Extrapulmonary Tuberculosis: An Overview. *American Family Physician,* 72(9), pp. 1761-1768.

Granich, R., Binkin, N. J., Jarvis, W. R. & Simone, P. M., 1999. *Guidelines for the Prevention of Tuberculosis in Health-Care Facilities in Resource Limited Settings.* Geneva: WHO.

Grossman, P., 1983. Respiration, Stress, and Cardiovascular Function. *Psychophysiology,* 20(3), pp. 284 - 300.

Hathway, E. A., Noakes, C. J., Sleigh, P. A. & Fletcher, L. A., 2011. CFD Simulation of Airborne Pathogen Transport due to Human Activities. *Building and Environment,* Volume 46, pp. 2500-2511.

Hella, J. et al., 2017. Tuberculosis transmission in public locations in Tanzania: A novel approach to studying airborne disease transmission. *Journal of Infection,* 75(3), pp. 191-197.

Hewlett, A. L. et al., 2013. Mathematical Modeling of Pathogen Trajectory in a Patient Care Environment. *Infection Control and Hospital Epidemiology,* 34(11), pp. 1181-1188.

Issarow, C. M., Robin, W. & Nicola , M., 2015. Modelling the Risk of Airborne Infectious Disease Using Exhaled Air. *Journal of Thoeretical Biology,* pp. 100 - 106.

Johnstone-Robertson, 2012. *Masters Thesis: Calculating the Risk if Infection of Mycobacterium Tuberculosis in Endemic Settings,* Stellenbosch: Stellenbosch University.

Johnstone-Robertson, S. et al., 2011. Tuberculosis in a South African prison – a transmission modelling analysis. *The South African Medical Journal,* 101(11).

Kale, S. R., Veeravalli, S. V., Punekar, H. D. & Yelmule, M. M., 2007. Air Flow Through a Non-Airconditioned Bus With Open Windows. *Sadhana,* 32(4), pp. 347-363.

Ko, G., First, M. W. & Burge, H. A., 2002. The Characterization of Upper-Room Ultraviolet Germicidal Radiation in Inactivating Airborne Microorganisms. *Environmental Health Perspectives,* January, 110(1), pp. 95-101.

Kujundzic, E. et al., 2007. UV Air Cleaners and Upper-Room Air Ultraviolet Germicidal Irradiation for Controlling Airborne Bacteria and Fungal Spores. *Journal of Occupational and Environmental Hygiene,* Volume 3, pp. 536-546.

Lombard, M., Cameron, B., Mokonyama, M. & Andrew, S., 2007. *Report on Trends in Passenger Transport in South Africa,* Midrand: Development Bank of Southern Africa.

Majid, H., Hofmann, W. & Winkler-Heil, R., 2011. Comparison of Stochastic Lung Deposition Fractions with Experimental Data. *The Annals of Occupational Hygiene,* pp. 278-291.

Meadow, J. F. et al., 2014. Indoor airborne bacterial communities are influenced by ventilation occupancy and outdoor air source. *INDOOR AIR: International Journal of Indoor Environment and Health,* 24(1), p. 41–48.

Miller, F. J. et al., 2012. Development of a Rhesus Monkey Lung Geometry Model and Application to Particle Deposition in Comparison to Humans. *Inhal Toxicol,* pp. 869-899.

MSF, 2011. *DR-TB Drugs Under the Microscope,* s.l.: Médecins Sans Frontières/International Union Against Tubercilosis and Lung Disease.

Nardell , E. A., Keegan, J., Cheney, S. A. & Etkind, S. C., 1991. Airborne infection. Theoretical limits of protection achievable by building ventilation. *The American Review of Respiratory Disease,* 144(2), pp. 302-306.

Nardell, E. et al., 2008. Safety of Upper-Room Ultraviolet Germicidal Air Disinfection for Room Occupants: Results from the Tuberculosis Ultraviolet Shelter Study. *Public Health Reports,* Volume 125, pp. 52-60.

Nguyen, J. L., Schwartz, J. & Dockery, D. W., 2014. The relationship between indoor and outdoor temperature, apparent temperature, relative humidity, and absolute humidity. *INDOOR AIR: International Journal of Indoor Environment and Health,* 24(1), p. 103–112.

Noakes, C. J. & Sleigh, P. A., 2008. Applying the Wells-Riley equation to the risk of airborne infection in hospital environment: The importance of stochastic and proximity effects. *Indoor Air,* pp. 17-22.

NTCP, 2007. *South African National Tuberculosis Guidelines,* s.l.: s.n.

Persily, A. K., 1997. Evaluating Building IAQ and Ventilation with Indoor Carbon Dioxide. *ASHRAE Transactions,* 103(2), p. 12.

Pooran, A. et al., 2013. What is the Cost of Diagnosis and Management of Drug Resistant Tuberculosis in South Africa?. *Plos One,* 8(1), pp. 1-11.

Raza, M. W., Kazi, B. M., Mustafa, M. & Gould, F. K., 2004. Developing Countries Have Their Own Characteristic Problems With Infection Control. *Journal of Hospital Infection: Elsevier,* Volume 57, pp. 294-299.

Reed, N. J., 2010. The History of Ultraviolet Germicidal Irradiation for Air Disinfection. *Public Health Reports,* Volume 125, pp. 15-27.

REHVA, 2004. *Ventilation Effectiveness,* Brussels: REHVA.

Richardson, E. T. et al., 2014. Shared Air: A Renewed Focus on Ventilation for the Prevention of Tuberculosis Transmission. *PLos ONE,* 9(5).

Rudnick, S. N. & Milton, D. K., 2003. Risk of indoor airborne infection transmision estimated from carbon dioxide concentration. *INDOOR AIR: International Journal of Indoor Environment and Health,* 13(3), p. 237–245.

Shah, N. S. et al., 2017. Transmission of Extensively Drug-Resistant Tuberculosis in South Africa. *N Engl J Med,* Volume 376, pp. 243 - 253.

Statistics South Africa, 2014. *National Household Travel Survey 2013,* Pretoria: Statistics South Africa.

Sze To, G. N. & Chao, C. Y. H., 2009. Review and comparison between the Wells–Riley and dose-response approaches to risk assessment of infectious respiratory diseases. *Indoor Air,* 20(1), pp. 2-16.

Tan, P.-N., Steinbach, M. & Kumar, V., 2005. *Introduction to Data Mining.* Boston: Pearson Addison-Wesley.

Taylor, J. G. et al., 2016. Measuring ventilation and modelling M. tuberculosis transmission in indoor congregate settings, rural KwaZulu-Natal. *INT J TUBERC LUNG DIS,* 20(9), pp. 1155 - 1161.

Verver, S. et al., 2004. Proportion of tuberculosis transimssion that takes place in households in a high-incidence area. *The Lancet,* Volume 363, pp. 212-214.

WHO, 2009. *Natural Ventilation for Infection Control in Health-Care Settings,* Geneva: WHO.

WHO, 2011. *Methods for monitoring indoor air quality in schools.* Bonn, WHO.

WHO, 2013. *Global Tuberculosis Report,* Geneva: WHO.

Wood, R. et al., 2012. Indoor Social Networks in a South African Township: Potential Contribution of Location to Tuberculosis Transmission. *Plos One,* 7(6), pp. 1-5.

Yan, Y., Li, X., Shang, Y. & Tu, J., 2017. Evaluation of airborne disease infection risks in an airliner cabin using the Lagrangian-based Wells-Riley approach. *Building and Environment,* Volume 121, pp. 79-92.

Zamudio, C. et al., 2015. Public Transportation and Tuberculosis Transmission in a High Incidence Setting. *PLos ONE,* 10(2).

Zhang , Z., Zhang, W., Zhai, J. Z. & Chen, Q., 2007. Evaluation of Various Turbulence Models in Predicting Airflow and Turbulence in Enclosed Environments by CFD: Part-2: Comparison With Experimental Data From Literature. *HVAC&R Research,* 13(6), pp. 871-886.

Zhang, Z. et al., 2009. Experimental and Numerical Investigation of Airflow and Contaminant Transport in an Airliner Cabin Mockup. *Building and Environment,* 44(1), pp. 85-94.

APPENDICES

Appendix 1

Static CO_2 Concentration Decay Data

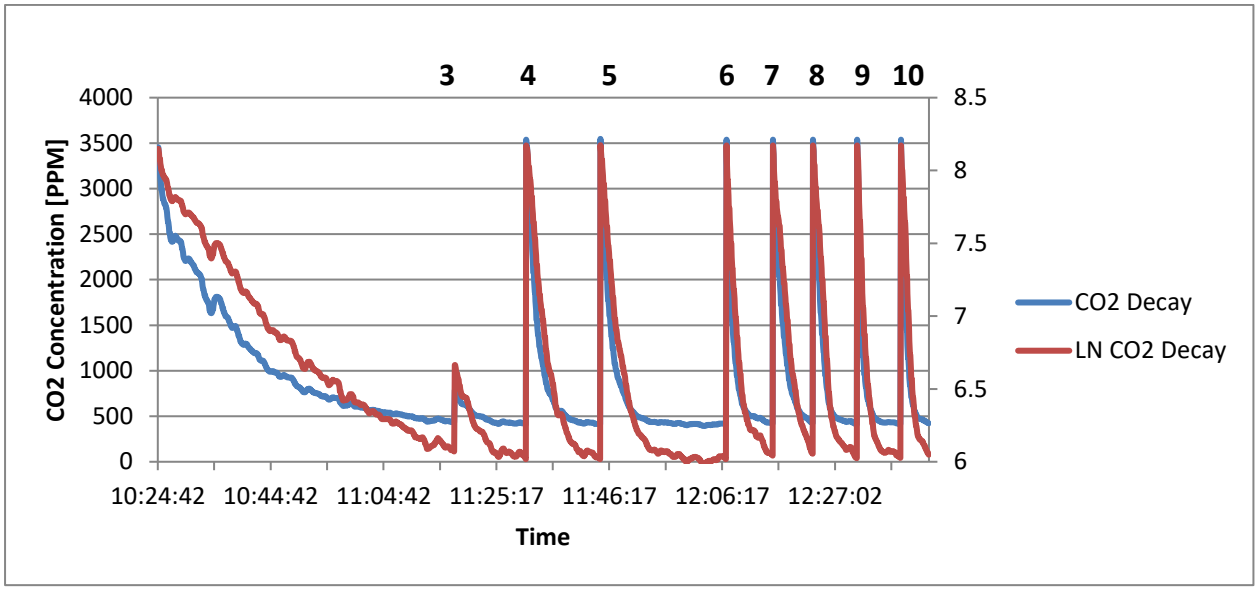

Figure 1 CO2 Decay Graphs of Configurations 3-10

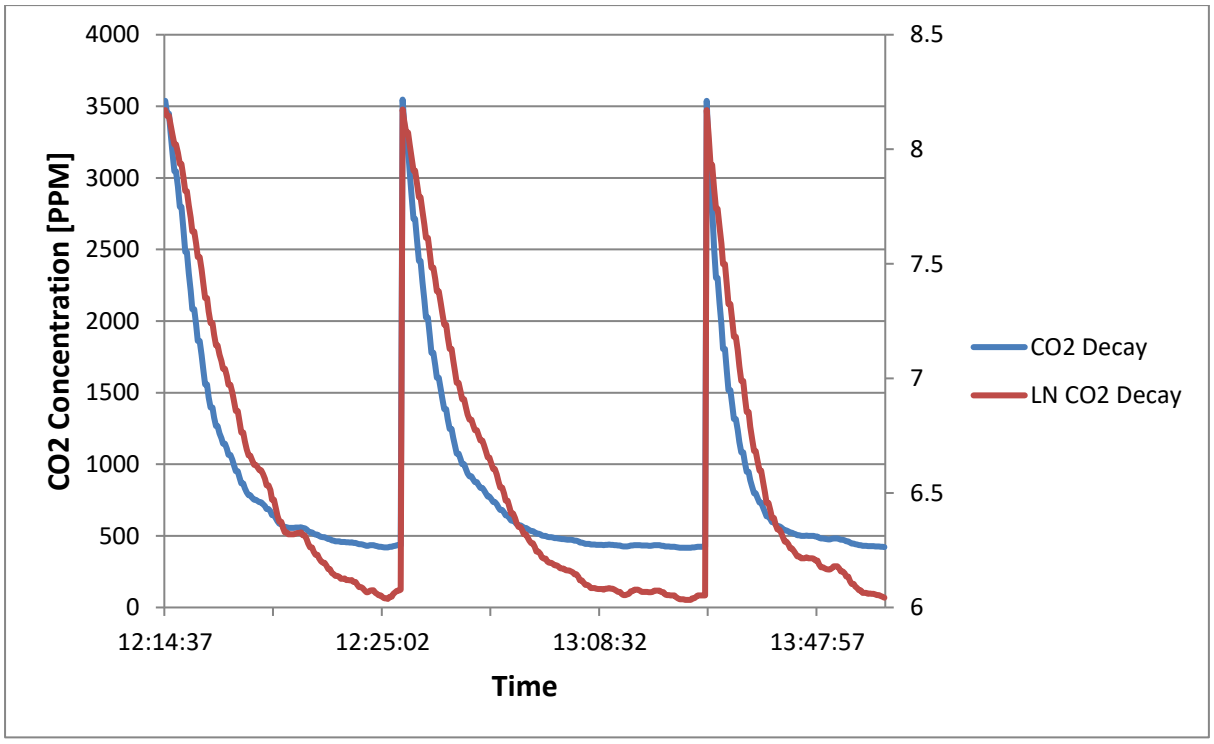

Figure 2 Static CO2 Peak to Minimum Decay of Respective Configurations 4-6

The figure above shows the combined concentration decay curves of configurations 4-6 with an average time of 21mins.

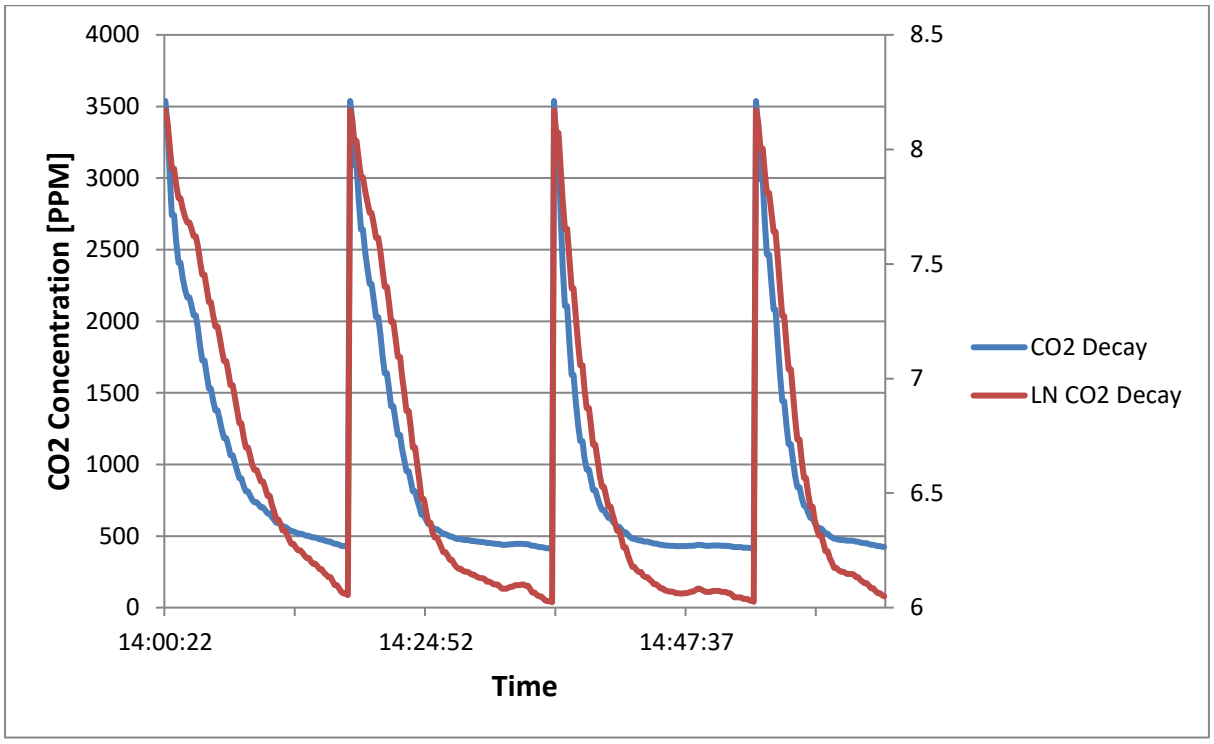

Figure 3 Static CO2 Peak to Minimum Decay of Respective Configurations 7 - 10

The figure above shows the combined concentration decay curves of configurations 7 - 10. The average decay time for configurations 7 - 9 was 9 minutes and that of configuration 10 was 8minutes.

Temperature changes in mobile ventilation tests

Below are the figures showing the temperature fluctuations directly caused by the window opening procedures in the ventilation tests. These could provide insight to the reluctance to using windows for ventilation despite their effectiveness, as a result of the discomfort.

The 80 km/h tests showed the largest temperature drops, exceeding 4°C. The 100 km/h tests showed the smallest fluctuations, this was due to the nature of the tests; CO_2 was dissipated faster than the temperature in the taxi could drop, reaching the near baseline levels in a short time.
The 40km/h tests showed temperature fluctuations that mirrored the 80 km/h tests.

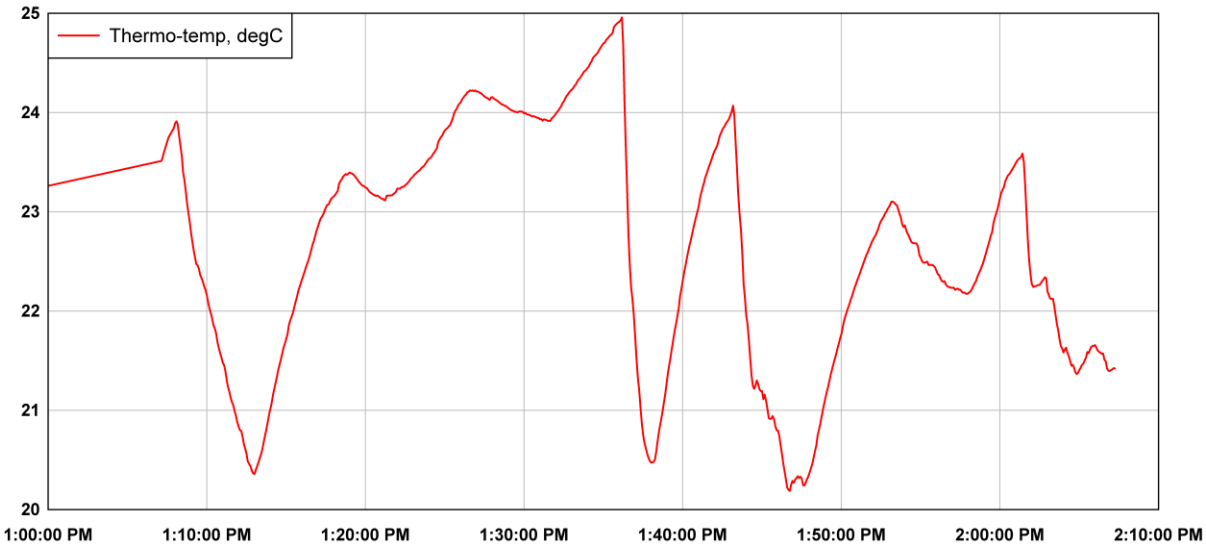

Figure 4 Temperature changes during 80 km/h test 1

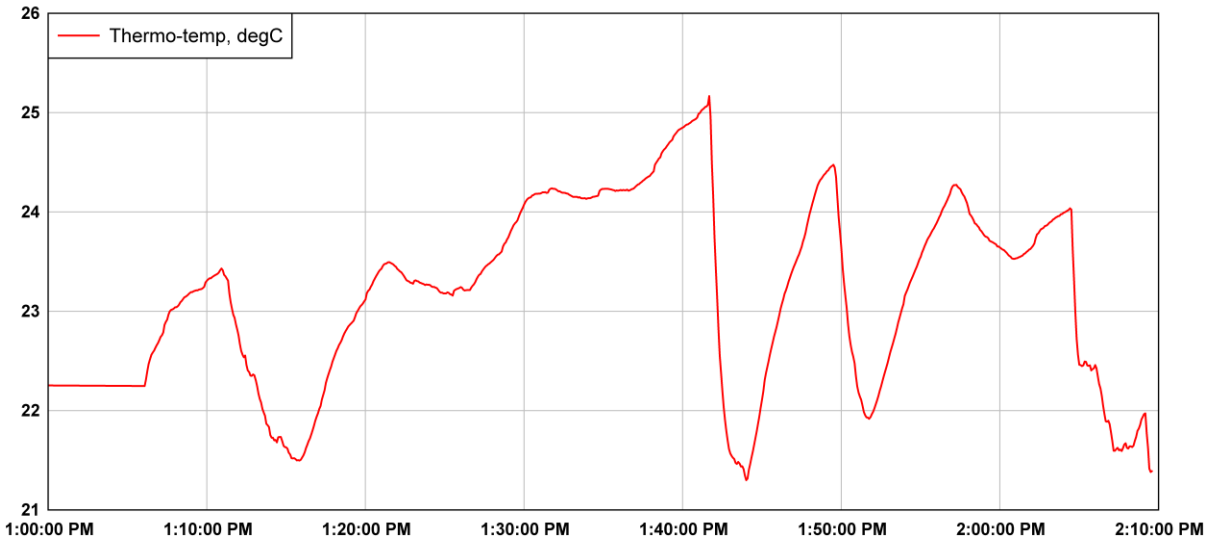

Figure 5 Temperature changes during 80km/h test 2

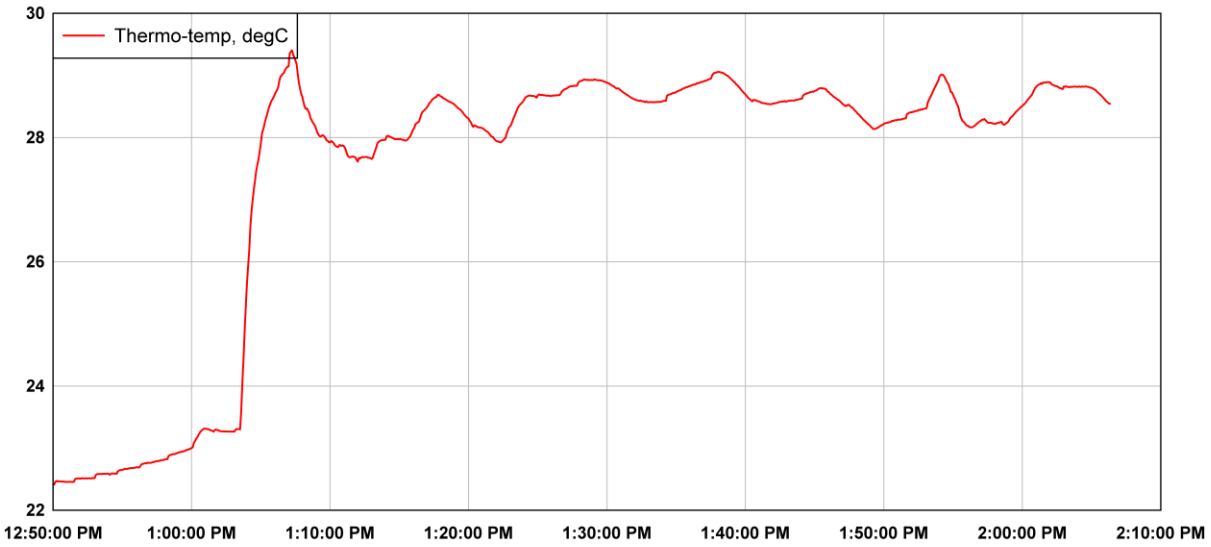

Figure 6 Temperature changes during 100 km/h test 1

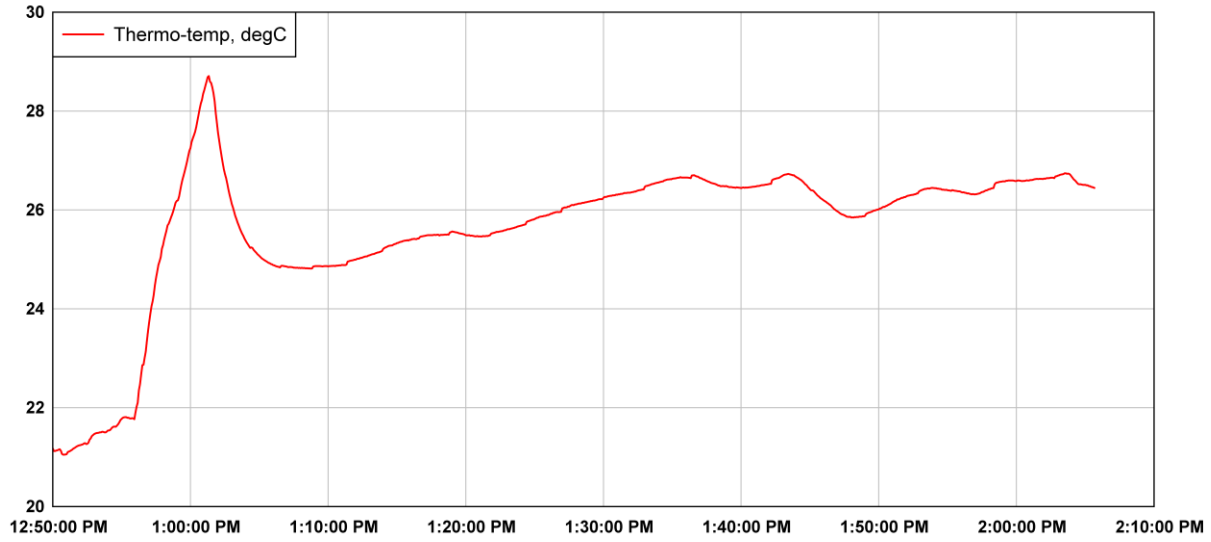

Figure 7 Temperature changes during 100 km/h test 2

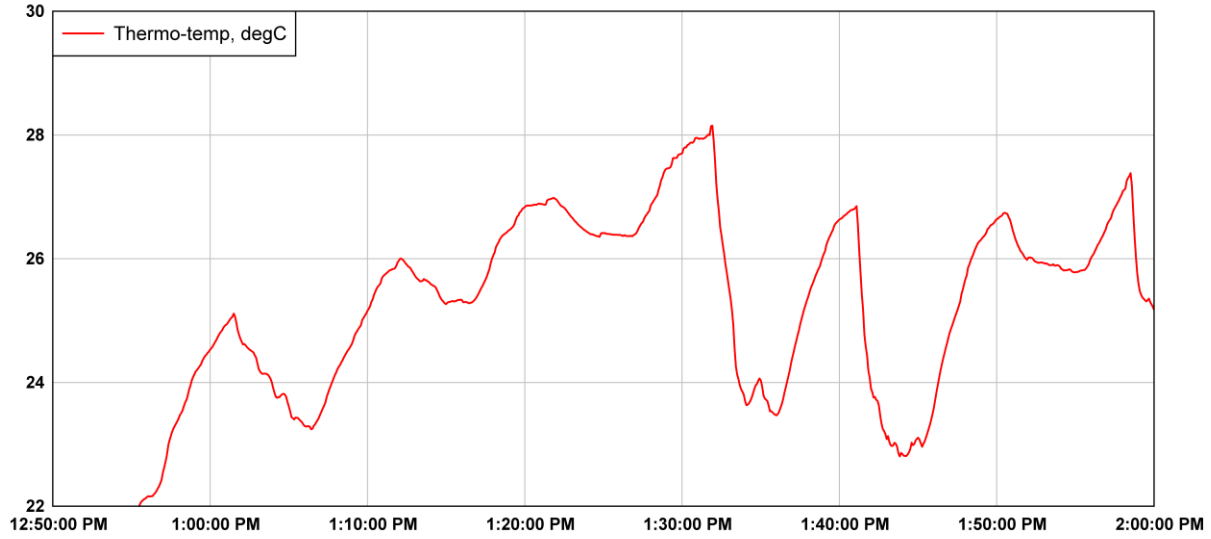

Figure 8 Temperature changes during 40 km/h test 1

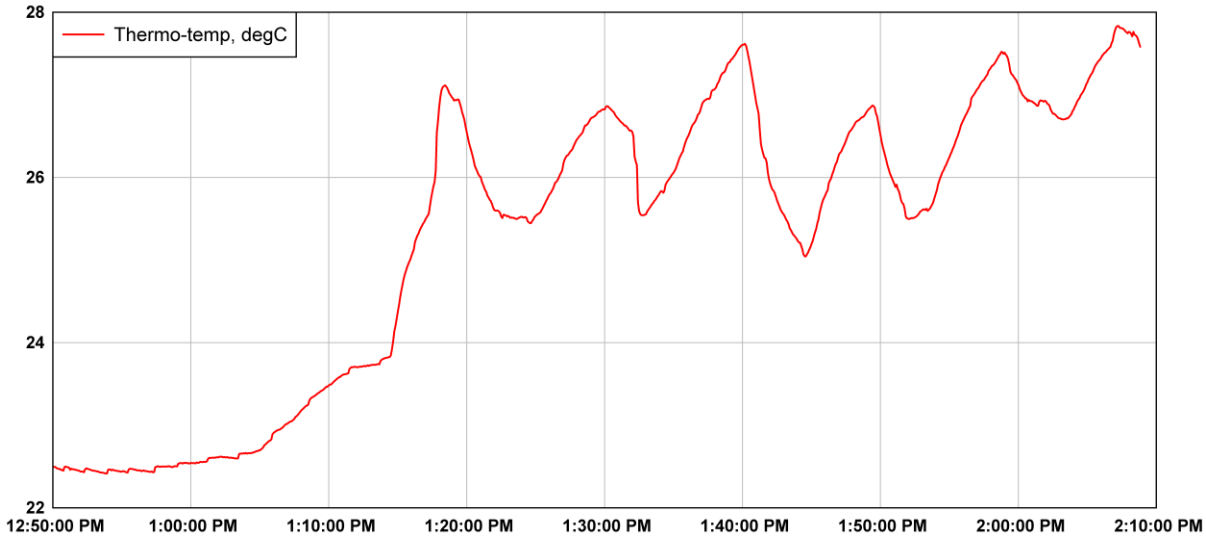

Figure 9 Temperature changes during 40 km/h test 2

Appendix 2

Wind direction and velocity graphs for 80 km/h tests

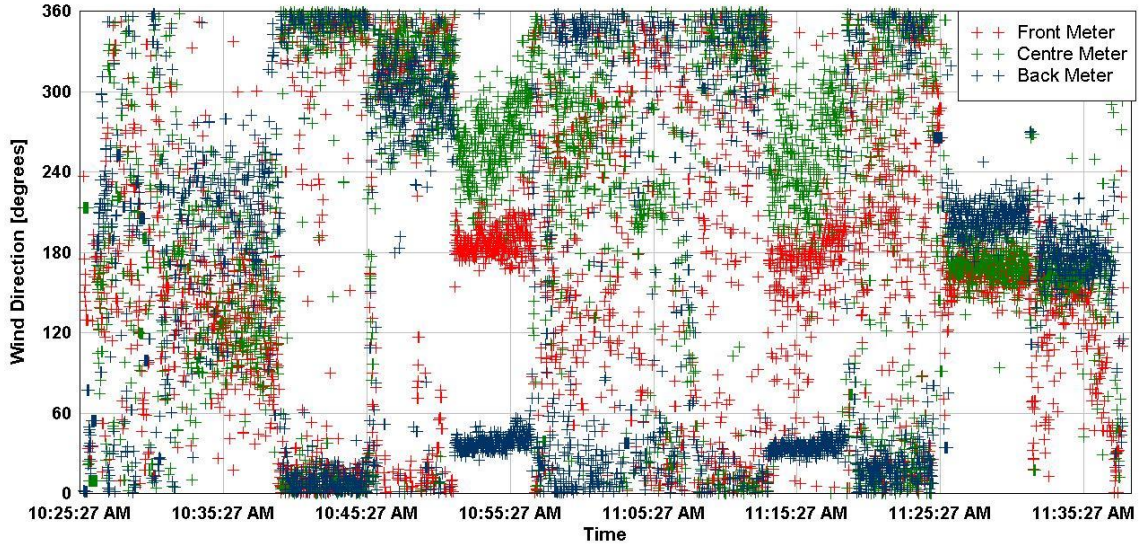

Figure 10 Wind Direction at Lower Meter Level for Sensor Placement 1

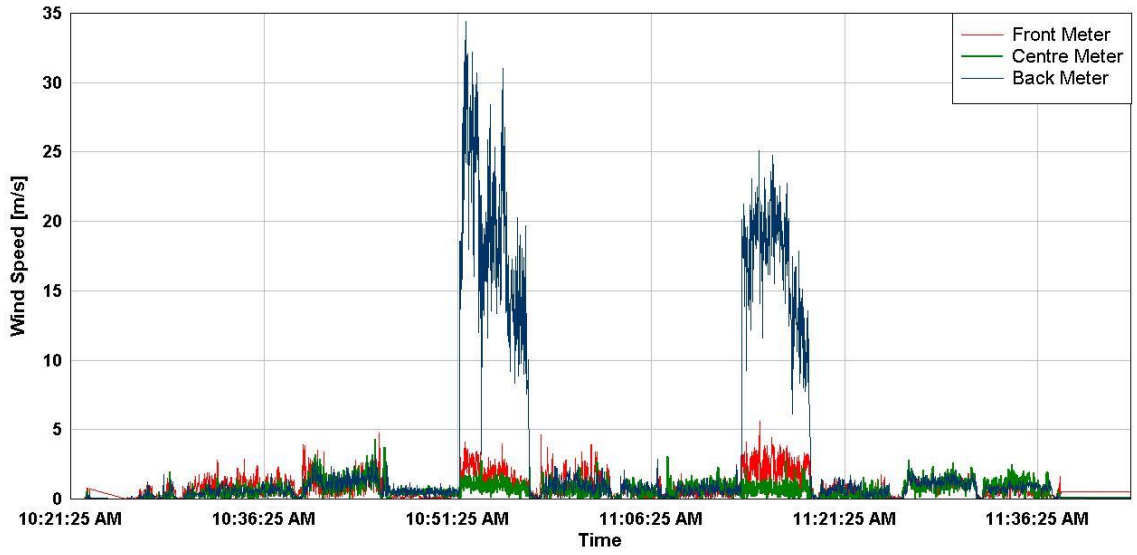

Figure 11 Wind Speed at Lower Meter Level for Sensor Placement 1

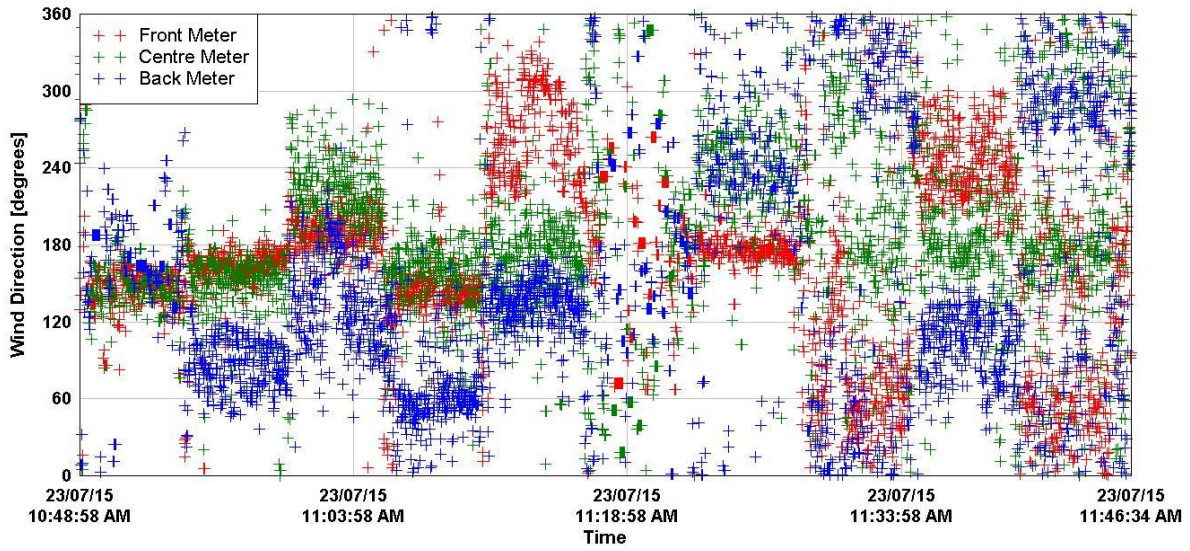

Figure 12 Wind Direction at Lower Meter Level for Sensor Placement 4

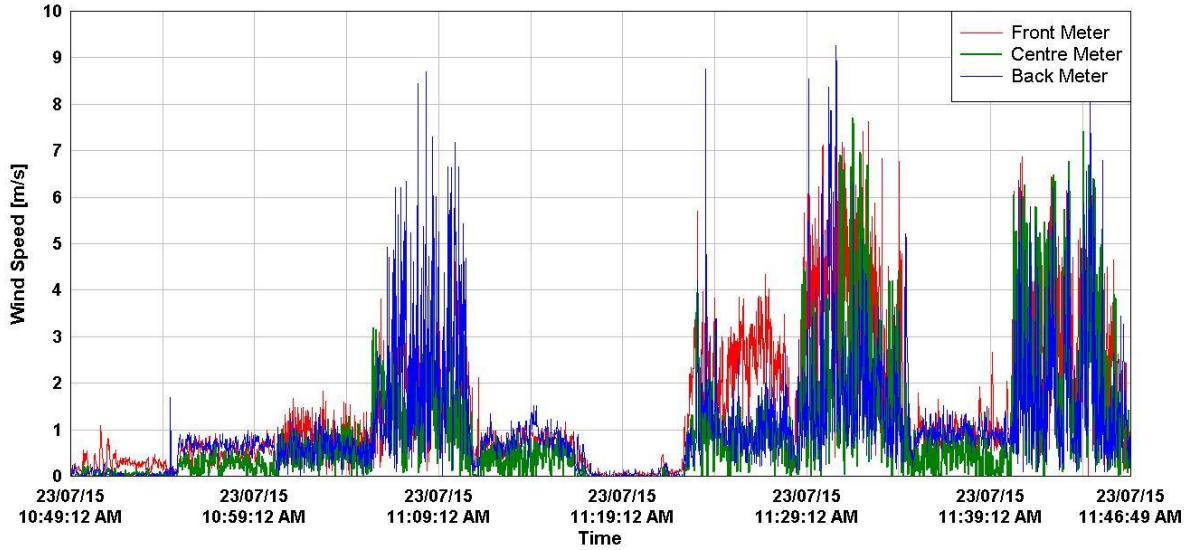

Figure 13 Wind Speed at Lower Meter Level for Sensor Placement 4

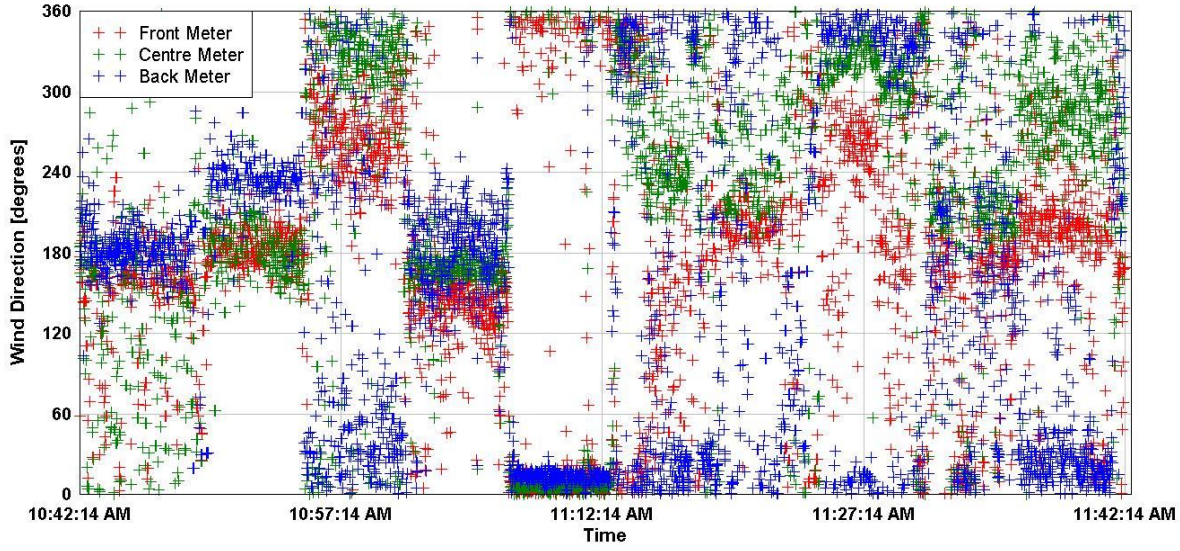

Figure 14 Wind Direction at Middle Meter Level for Sensor Placement 1

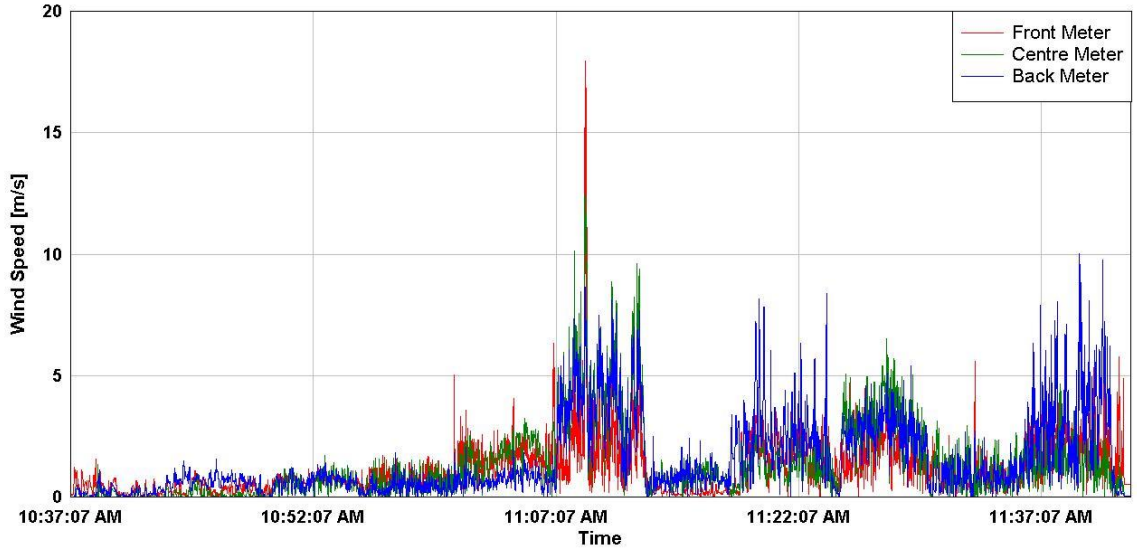

Figure 15 Wind Speed at Middle Meter Level for Sensor Placement 1

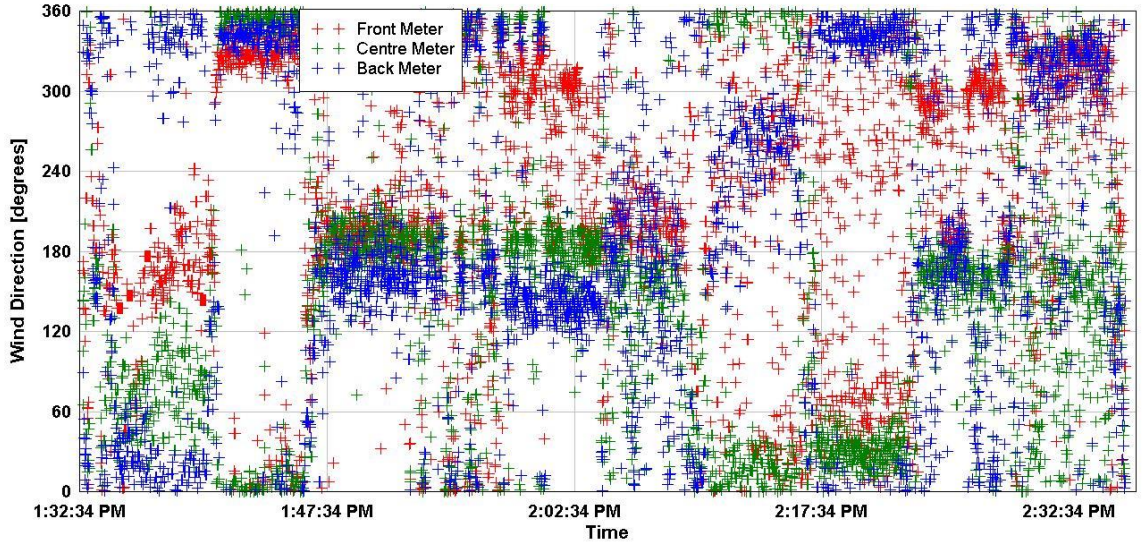

Figure 16 Wind Direction at Middle Meter Level for Sensor Placement 3

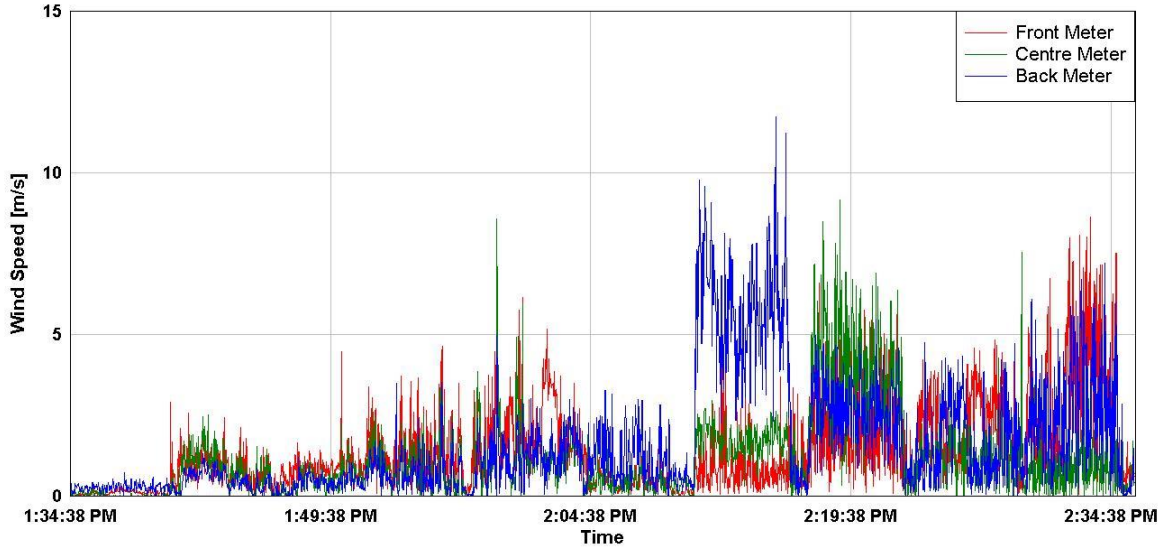

Figure 17 Wind Speed at Middle Meter Level for Sensor Placement 3

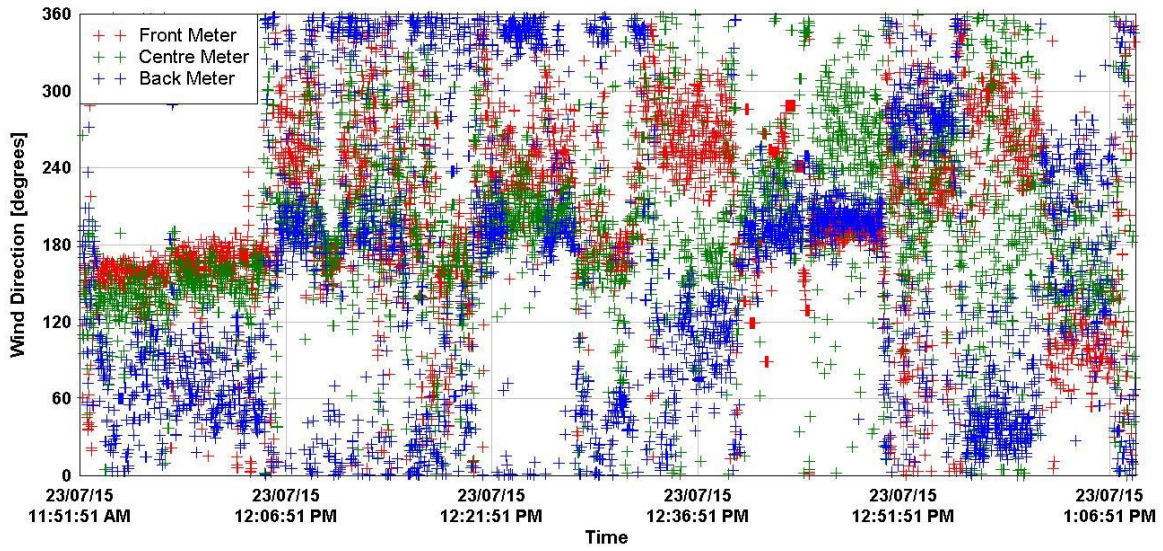

Figure 18 Wind Direction at Middle Meter Level for Sensor Placement 4

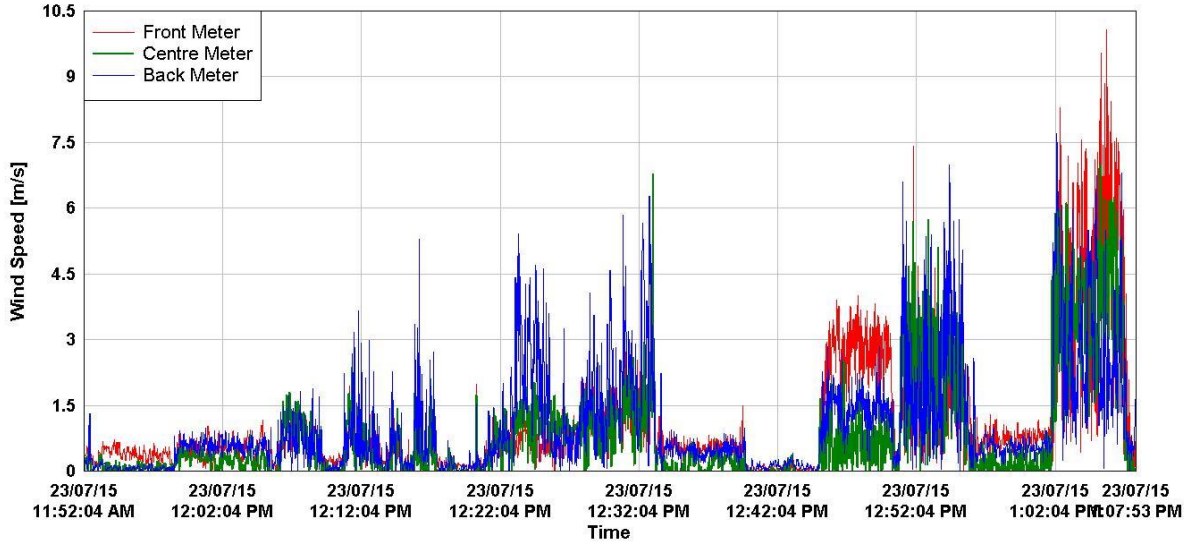

Figure 19 Wind Speed at Middle Meter Level for Sensor Placement 4

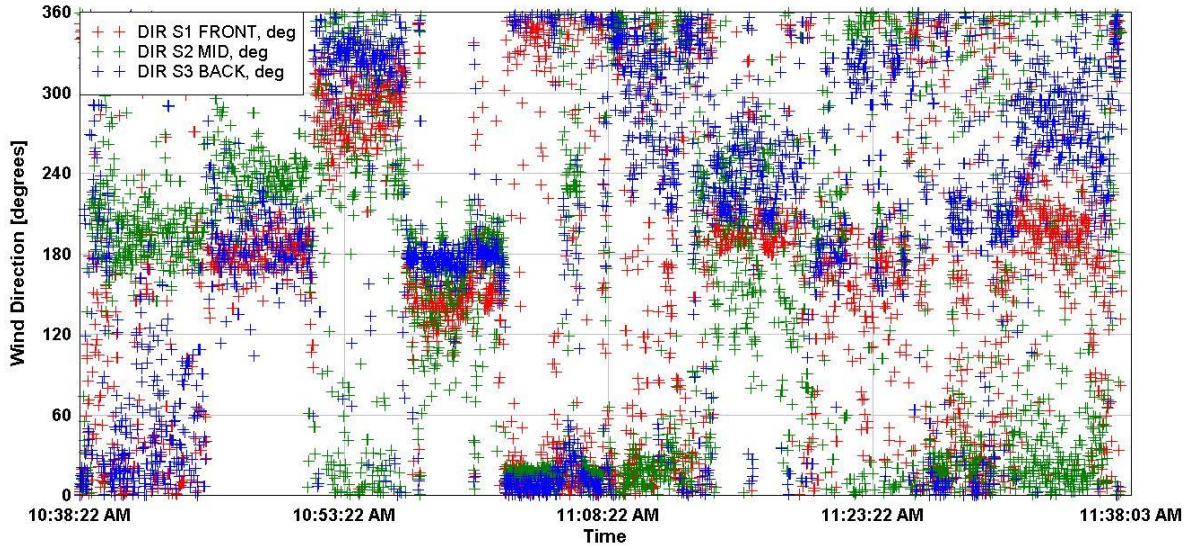

Figure 20 Wind Direction at Upper Meter Level for Sensor Placement 1

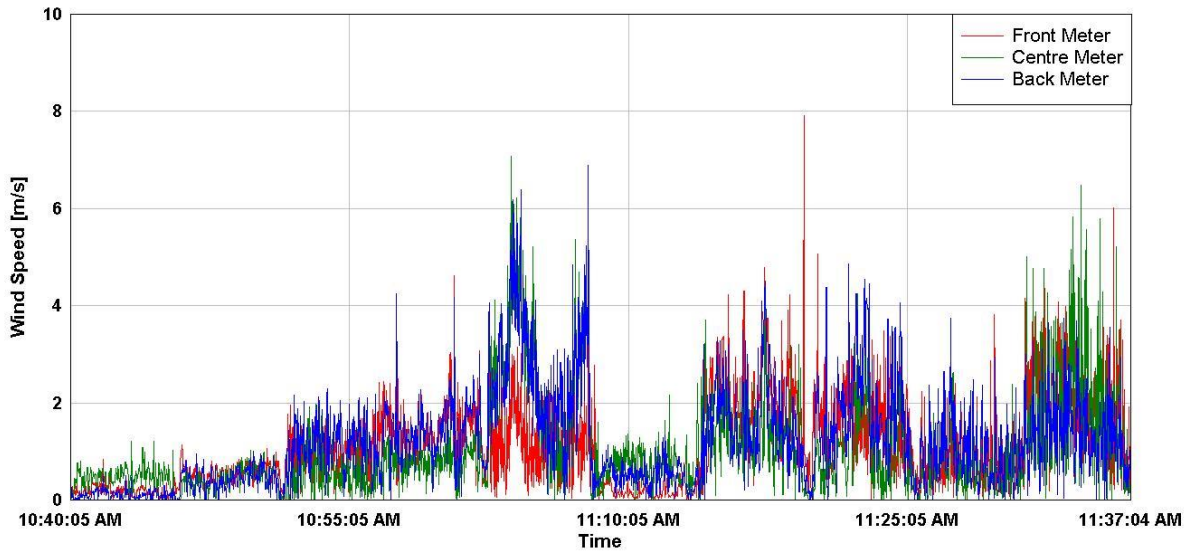

Figure 21 Wind Speed at Upper Meter Level for Sensor Placement 1

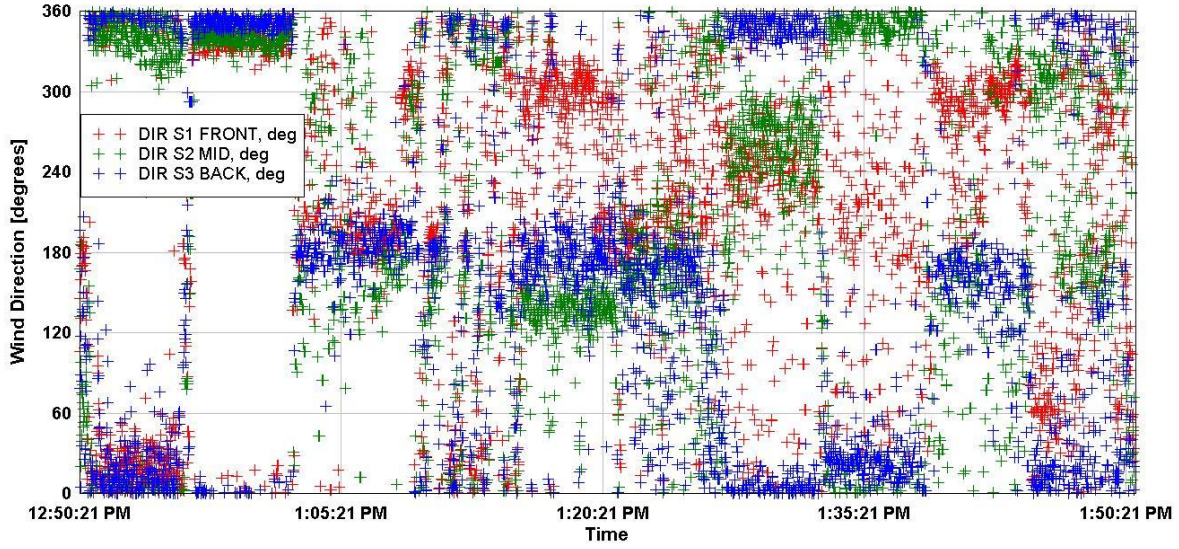

Figure 22 Wind Direction at Upper Meter Level for Sensor Placement 3

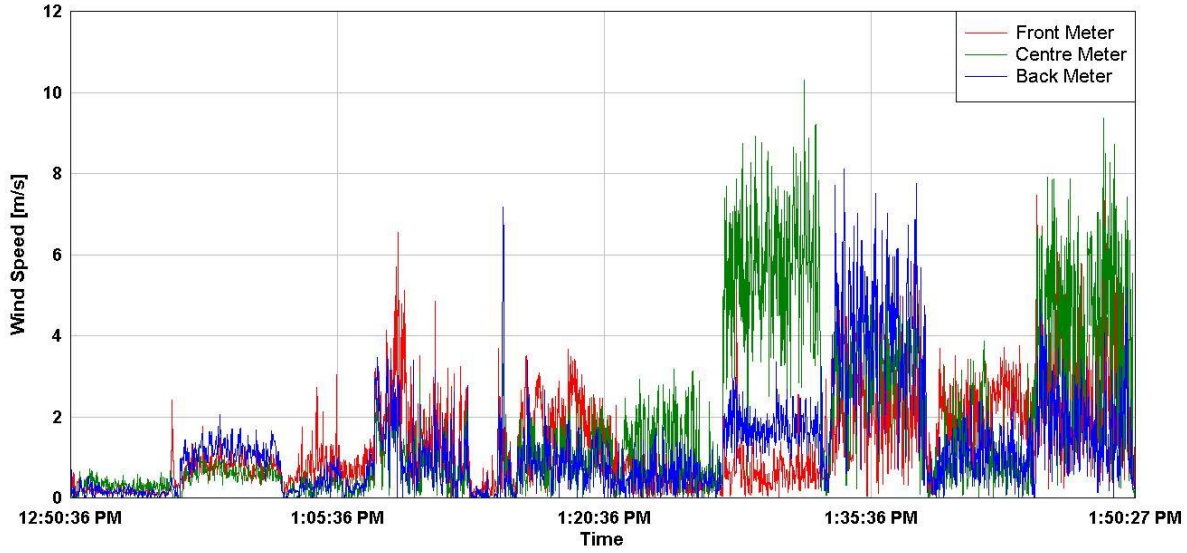

Figure 23 Wind Speed at Upper Meter Level for Sensor Placement 3

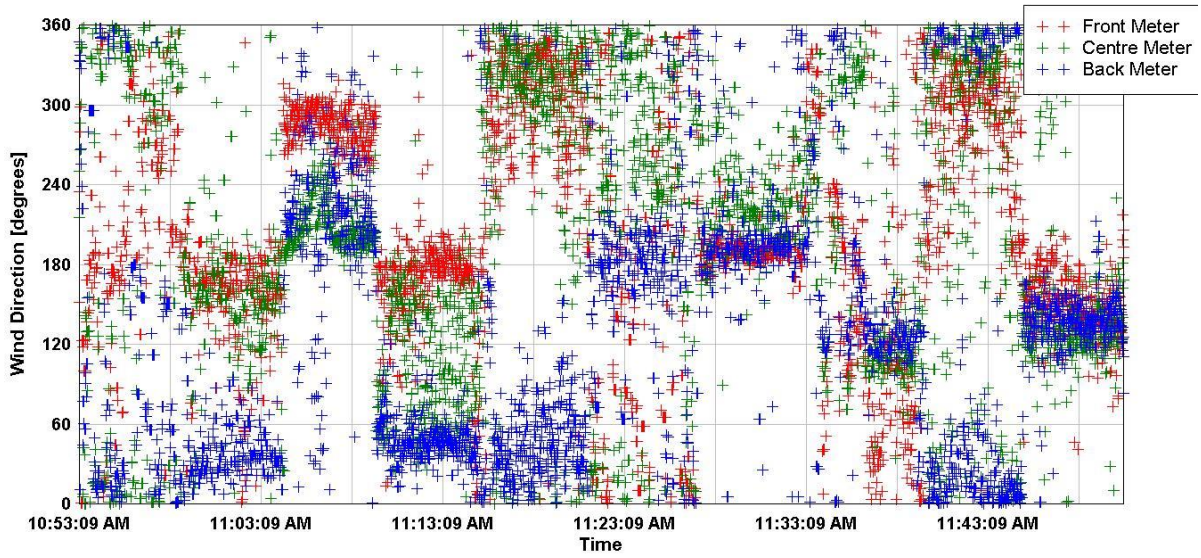

Figure 24 Wind Direction at Upper Meter Level for Sensor Placement 4

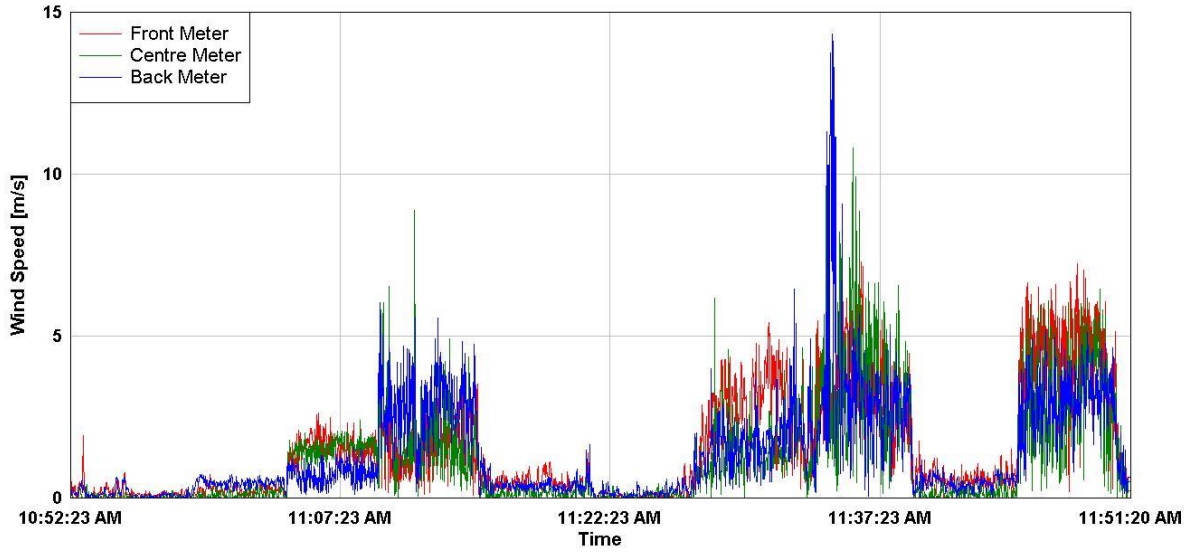

Figure 25 Wind Speed at Upper Meter Level for Sensor Placement 4

Appendix 3

Linear Regression Model

The linear regression analysis was conducted by a consultant from the Cape Town Department of Statistics.

Methodology

The response was always the log transformed ventilation value.

The response was first transformed using a log (base 10) transformation because the original response exhibited heteroscedasticity (changing variance). After a log transformation, an assumption of homoscedasticity seemed reasonable (the same σ^2 for all noise, once configuration group and speed were fixed).

- The R function 'lm' was used to fit a linear regression model to the data.
- The model specified that log 10 of the ventilation reading i, y_i, equaled

$$y_i = \alpha_0 + \alpha_s \cdot s_i + \alpha_{5\&6} \cdot \delta_{5\&6,i} + \alpha_{s,5\&6} \cdot s_i \cdot \delta_{5\&6,i} + \alpha_{7\&8} \cdot \delta_{7\&8,i} + \alpha_{s,7\&8} \cdot s_i \cdot \delta_{7\&8,i} + \alpha_9 \cdot \delta_{9,i} + \alpha_{s,9} \cdot s_i \cdot \delta_{9,i} + \varepsilon_i$$

  Where
  - ε_i is noise and is normally distributed (mean 0 and variance σ^2)
  - All the α terms or coefficients are model parameters to be estimated, together with σ^2 – these are estimated by a method of maximum likelihood
  - s_i is the speed for observation i (transformed to range 0 to 3, as explained above); $\delta_{5\&6,i}$ = 1 if observation i has configuration 5&6, 0 otherwise; $\delta_{7\&8,i}$ = 1 if observation i has configuration 7&8, 0 otherwise; $\delta_{9,i}$ = 1 if observation i has configuration 9, 0 otherwise (Configuration 4 is the reference category).

- Essentially, the linear regression model above was fitting a straight line between speed and the mean response, and the intercept and slope of the line could be different for each configuration group.

- A likelihood ratio test was used to assess whether a simpler model, in which the slope of the line was the same for each configuration group, appeared to be adequate. A small p-value would've lead to rejection of the simpler model (in favour of the model above).
- The overall significance of the model was assessed by comparing it to a model in which there were no predictors (the null model). A small p-value would lead to rejection of the simpler model (in favour of the model above).

Model Diagnostics

All showed reasonable model fit and assumptions. Figure 26 below shows the approximate bell-shaped curve of Histogram of standardised Pearson residuals which is approximately normally distributed with a mean of 0 and variance of 1.

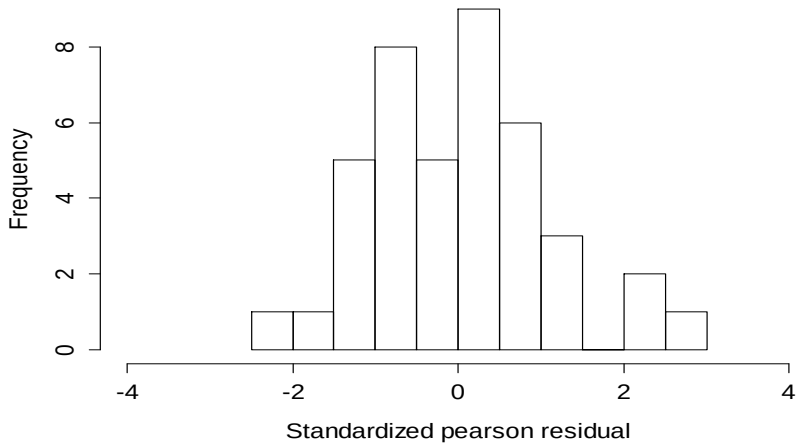

Figure 26 Histogram of Standardised Pearson Residual

In Figure 27 a plot of standardised Pearson residuals to fitted values, with each predictor is shown. The residuals must lie parallel to the mean reference value 0. As the fitted values were altered, the perpendicular distribution of the residual points was comparable. In Figure 27 the Pearson residuals for each fitted value were expected to be densely packed near the mean but to spread further away from the mean; as shown in Figure 26, less than 5% of the Pearson residuals were beyond the band value 2.

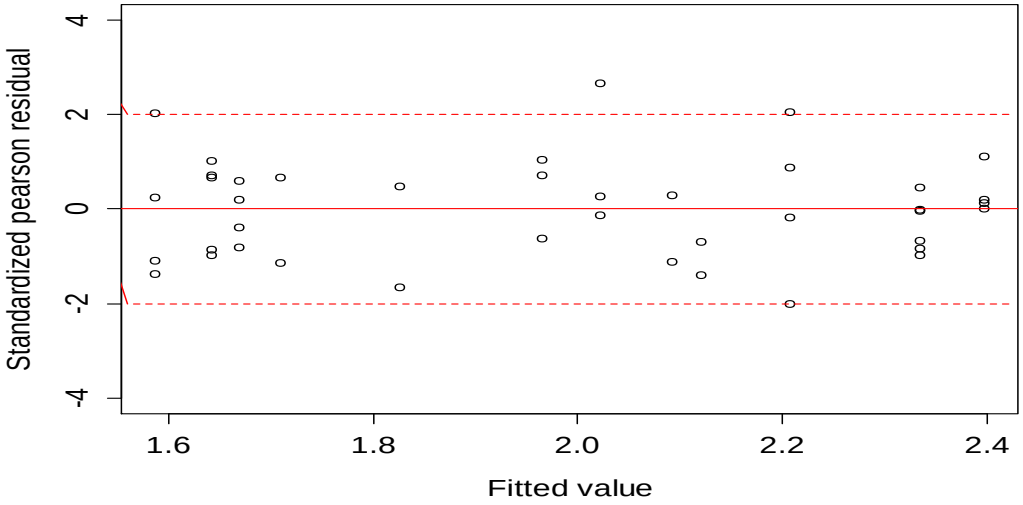

Figure 27 Standardised Pearson Residuals Scatter Plot

Presentation of Results

For each α parameter (coefficient), the estimated parameter had both the 95% CI and p-value given, where the likelihood of having a true α value was 95%. The α coefficients asymptotic normality was used to individually evaluate significance of the parameters. A null-hypothesis for $\alpha = 0$ was used, where small p-values signal $\alpha \neq 0$; this would've showed that the parameters had noticeable effects on the interaction of the variables.

- Also serving as a diagnostic tool, to summarise the fitted model less technically, a plot was produced showing the data points together with the mean response based on the fitted model.
- The effect sizes (effect of configuration on ventilation at a speed of 0, and effect of speed on ventilation per configuration), on the original scale of the response, were also shown.

When presenting results in terms of the original untransformed ventilation values, the response followed a log-normal distribution – both when considering either the ventilation value for a specific combination of speed and configuration group or the ratio of two ventilation values as there were specified changes in speed/configuration group. The mean of this response was a function of the model parameters specified above (the α terms and σ). A point estimate of the mean was obtained by substituting estimates of the model parameters into the function, and a confidence interval (CI) for the mean was obtained through bootstrapping – a dataset was simulated each of 10000 times from the fitted model, and the 2.5th and 97.5th percentiles of the resulting distribution of estimates of the mean provided lower and upper CI limits.

Table 1 Estimates of the α terms

		Effect size	95% CI lower limit	95% CI upper limit	P-value
(Intercept)	α_0	1.8254	1.6889	1.9619	<0.001
Speed40	α_s	0.0982	0.0323	0.1642	0.005(1)
Configuration 5&6	$\alpha_{5\&6}$	-0.2396	-0.4070	-0.0721	0.006(2)
Configurations 7&8	$\alpha_{7\&8}$	0.3823	0.2151	0.5495	<0.001(2)
Configuration 9	α_9	-0.1172	-0.3103	0.0758	0.225
Speed40: Configs 5&6	$\alpha_{s,5\&6}$	-0.0707	-0.1515	0.0101	0.084(3)
Speed40: Configs 7&8	$\alpha_{s,7\&8}$	-0.0346	-0.1154	0.0461	0.389
Speed40: Config 9	$\alpha_{s,9}$	0.0298	-0.0635	0.1230	0.520

Estimate of sigma: 0.0995

Likelihood ratio test comparing model above to a simpler one with no interaction between speed and configuration: p-value = 0.07819. The small p-value suggested there might have needed to be allowance for different slopes by configuration group.

Likelihood ratio test comparing model above to simpler one with no predictors: p-value = <0.001. The small p-value suggested that the model's predictors were contributing towards explaining the response.

Increased speed increased ventilation, for reference category configuration 4. Each unit increase in speed increased the mean response by 0.10.